

THESIS

LIBRARY Michigan State University

This is to certify that the

thesis entitled

ENCODERLESS STATOR FIELD-ORIENTATED CONTROL OF INDUCTION MACHINES

presented by

MOHAMMAD BILAL MALIK

has been accepted towards fulfillment of the requirements for

M.S. degree in Electrical & Computer Engineering

Date April 23, 2001

MSU is an Affirmative Action/Equal Opportunity Institution

Hassan Khalil
Major professor

O-7639

PLACE IN RETURN BOX to remove this checkout from your record.

TO AVOID FINES return on or before date due.

MAY BE RECALLED with earlier due date if requested.

DATE DUE	DATE DUE	DATE DUE
MAR 0 4 2002		
SEP 1 8 2006		
•		

6/01 c:/CIRC/DateDue.p65-p.15

ENCODERLESS STATOR FIELD-ORIENTATED CONTROL OF INDUCTION MACHINES

Ву

MOHAMMAD BILAL MALIK

A THESIS

Submitted to

Michigan State University
in partial fulfillment of the requirements
for the degree of

MASTER OF SCIENCE

Department of Electrical and Computer Engineering 2001

ABSTRACT

ENCODERLESS STATOR FIELD-ORIENTATED CONTROL OF INDUCTION MACHINES

By

MOHAMMAD BILAL MALIK

Control of induction machines without using speed or position sensors is an attractive and challenging problem. Stator flux-orientated control is one of the schemes proposed in this context, which has its advantages and limitations. Our work concentrates on the same and includes all the necessary ingredients, namely, analysis, simulation and experiments. Our emphasis is on the speed control problem, which naturally includes the torque control.

The analysis begins with a discussion on pure integrators, which play a vital role in stator-based techniques. Next comes the analysis of steady-state errors. This analysis is valuable in the sense that it not only gives quantitative error estimates but also is useful in evaluating the limitations of the control scheme. There is a handy discussion on noninteracting control i.e. the ability to control speed (or torque) and flux independent of each other.

A series of simulations have been provided to verify and illustrate the analysis. This kind of approach gives a better perspective and understanding of the profound details of a problem. We have used some new and novel ideas to develop an experimental setup. This includes the use of a personal computer as an embedded processor. The flexibility, power and convenience to perform new experiments produced results that closely match analysis and simulations.

In the name of Allah, the most Merciful and the most Beneficent

То

My parents

ACKNOWLEDGEMENTS

I am grateful and indebted to my advisor Dr. Hassan Khalil for his kind guidance, assistance, encouragement and valuable time. Working with him has been a great learning experience in the field of nonlinear controls.

I also enjoyed working with Dr. Elias Strangas. His keen interest, support and useful advice helped a lot in improving my understanding of machines and constructing the experimental setup.

I appreciate and thank to all others who helped directly or indirectly in the completion of this thesis.

I am also thankful to National University of Science and Technology, Pakistan for supporting my study for the degree of Master of Science.

TABLE OF CONTENTS

LIST OF FIG	GURES	IX
LIST OF TA	\BLES)	CIII
1 INTRODU	JCTION	1
1.1. Co	ontrol of Induction Machine; A Historical Perspective	1
1.1.1.	Control of Induction Machine using Position/Speed Measurement	s3
1.1.2.	Control of Induction Machine without Position/Spe	ed
Measur	rements	4
1.2. Fie	eld-Orientated Control and its Variants	5
1.3. Ou	ur Contribution	6
1.3.1.	Analysis	7
1.3.2.	Experimental Setup	8
2 MATHEM	IATICAL MODELING AND ANALYSIS	10
2.1. Th	ree-Phase Symmetrical Induction Machine	10
2.1.1.	Stator Based Machine Model	14
2.1.2.	Second Order Effects	16
2.2. Sta	ator Flux Estimation	17
2.2.1.	Pure Integrators	17
2.2.2.	Current Components	19
2.2.3.	Open Loop and Closed Loop Integrators	21
2.2.4.	Approximation of an Integrator	23
2.2.5.	Equivalent Errors in Polar Coordinates	28

2.2	2.6.	Remarks on Flux Estimation	33
2.3.	Cor	ntrol of Induction Machine Using Speed Measurements	34
2.3	3.1.	The Control Variables	35
2.3	3.2.	Coupled Nature of Direct and Quadrature Current Components	36
2.3	3.3.	Flux Controller and Decoupling Through Feed Forward	36
2.3	3.4.	Torque and Speed Controller	41
2.3	3.5.	Position Measurement	41
2.3	3.6.	High Gain Observers	42
2.4.	Spe	eed Estimation and Error Bounds	44
2.5.	Cor	ntrol of Induction Machine Using Speed Estimation	47
2.	5.1.	Low and High Speed Operation	49
2.	5.2.	Starting of the induction machine	50
2.	5.3.	Speed Reversal	50
2.6.	Low	vest Possible Speeds	51
2.7.	Disc	crete-Time Implementation	53
2.7	7.1.	Discrete-Time Control of Continuous-Time Nonlinear Systems	53
2.7	7.2.	Difficulties Associated with High Sampling Rates	54
2.7	7.3.	Suggested Solutions	57
3 COM	IPUTE	ER SIMULATIONS	58
3.1.	Imp	ortance of Simulations in Design	58
3.2.	Pur	e Integration	61
3.2	2.1.	Equivalence of Open and Closed Loop Integration	61
3.5	2.2.	Unknown Initial Conditions	66

	3.2.3.	Transient Behavior	68
	3.3. S	tator Flux and Speed Estimation	70
	3.3.1.	Integrator Approximation	72
	Observa	tions	72
	3.3.2.	Uncertainty in Stator and Rotor Resistances	77
	Observa	tions	77
	3.4. C	losed Loop System with Feedback from Measured Speed	84
	3.4.1.	Controller Performance in Presence of Errors	86
	3.4.2.	Operation at different speeds and loads	91
	3.4.3.	The Role of Decoupler	94
	3.5. C	losed Loop System with Feedback from Estimated Speed	96
	3.5.1.	Controller Performance in Presence of Errors	98
	Observa	utions	98
	3.5.2.	Operation at Different Speeds and Loads	104
4	EXPERI	MENTAL SETUP AND RESULTS	108
	4.1. Ir	ntroduction	108
	4.2. T	he Experimental Setup	109
	4.3. P	ersonal Computer as Embedded Processor	111
	4.3.1.	Computational Power	111
	4.3.2.	Memory Resources	112
	4.3.3.	Available Data Types	112
	4.3.4.	Mass Data Storage	112
	435	Simulating Real Data	113

4.3	3.6.	Development Environment	113
4.3	3.7.	Flexibility	113
4.3	3.8.	Summary	114
4.4.	RT	Linux Philosophy	114
4.5.	Sof	tware Planning	115
4.	5.1.	Hierarchy of the real time task	116
4.6.	Dig	ital IO Card	118
4.7.	Ма	chine Control Card	118
4.	7.1.	Analog to Digital Conversion	119
4.	7.2.	4-Channel Digital to Analog Converter	121
4.	7.3.	PWM Generation	122
4.	7.4.	Shaft Encoder Interface	122
4.8.	Ор	en Loop Experiment	123
4.9.	End	coderless Speed Control of Induction Machine	126
Obs	ervatio	ons	127
5 CON	CLUS	SIONS AND RECOMMENDATIONS	130
5.1.	Co	nclusions	130
5.2.	Red	commendations	132
BIBLIC	OGRA	PHY	134

LIST OF FIGURES

Figure 1-1. Block diagram of control of induction machines using speed/position
measurements4
Figure 1-2. Block diagram of encoderless control of induction machines5
Figure 2-1. Stator Flux Estimation in Polar Coordinates
Figure 2-2. Frequency domain representation of disturbance with integrator
approximated by first order filter25
Figure 2-3. Frequency domain representation of disturbance with integrator
approximated by second order filter27
Figure 2-4. Error propagation from rectangular to polar coordinates31
Figure 2-5. Stator field-orientated control of induction machines using speed
measurements40
Figure 2-6. Transfer functions of different high gain observers43
Figure 2-7. Encoderless stator field-orientated control of induction machines48
Figure 2-8. A possible scheme to handle high sampling rates57
Figure 3-1. Comparison of open and closed loop estimators62
Figure 3-2. Closed loop stator flux estimation62
Figure 3-3. Open loop stator flux estimation63
Figure 3-4. Equivalence of closed and open loop integrators for DC disturbances
64
Figure 3-5. Equivalence of closed and open loop integrators for low frequency
disturbances65

Figure 3-6. Stator flux estimation with pure integrator and false initial conditions
66
Figure 3-7. Response of a pure integrator with false initial conditions67
Figure 3-8. Investigation of transient behavior of stator flux estimator using pure
integrators in presence of parameter uncertainty68
Figure 3-9. Sensitivity of pure integrators to transient offsets69
Figure 3-10. Block diagram of stator flux and speed estimation in open loop70
Figure 3-11. Errors due to integrator approximation at high speeds (Part I)73
Figure 3-12. Errors due to integrator approximation at high speeds (Part II)74
Figure 3-13. Errors due to integrator approximation at low speeds (Part I)75
Figure 3-14. Errors due to integrator approximation at low speeds (Part II)76
Figure 3-15. Errors due to integrator approximation and uncertainty in stator
resistance at high speeds (Part I)78
Figure 3-16. Errors due to integrator approximation and uncertainty in stator
resistance at high speeds (Part II)79
Figure 3-17. Errors due to integrator approximation and uncertainty in stator
resistance at low speeds (Part I)80
Figure 3-18. Errors due to integrator approximation and uncertainty in stator
resistance at low speeds (Part II)81
Figure 3-19. Errors due to integrator approximation and uncertainty in rotor
resistance at high speeds82
Figure 3-20. Errors due to integrator approximation and uncertainty in rotor
resistance at low speeds83

Figure 3-21. Controller performance under ideal conditions using measured
speed85
Figure 3-22. Controller performance with integrator approximation ($\omega_c = 1 \text{ rads/s}$)
using measured speed87
Figure 3-23. Controller performance with integrator approximation ($\omega_c = 1 \text{ rads/s}$)
and $R_{so} = 1.05R_s$ as an uncertainty using measured speed88
Figure 3-24. Controller performance with integrator approximation (ω_c = 1 rads/s)
and $R_{ro} = 1.25R_{r}$ as an uncertainty using measured speed89
Figure 3-25. Controller performance with integrator approximation
($\omega_c=1\mathrm{rads/s}$), $R_{so}=1.05R_s$ and $R_{ro}=1.1R_r$ as uncertainties using measured
speed90
Figure 3-26. Controller performance at various speeds using speed
measurements92
Figure 3-27. Controller Performance for different loads using measured speed.93
Figure 3-28. Controller performance without a decoupler95
Figure 3-29. Controller performance under ideal conditions97
Figure 3-30. Controller performance with integrator approximation ($\omega_c = 1 \text{ rads/s}$)
99
Figure 3-31. Controller performance with integrator approximation ($\omega_c = 1 \text{ rads/s}$)
and $R_{so} = 1.05R_s$ as an uncertainty100
Figure 3-32. Controller performance with integrator approximation ($\omega_c = 1 \text{ rads/s}$)
and $R_{ro} = 1.25R_r$ as an uncertainty101

Figure 3-33. Controller performance with error due to HGO102
Figure 3-34. Controller performance with integrator approximation
($\omega_c = 1 \text{ rads/s}$), $R_{so} = 1.05 R_s$ and $R_{ro} = 1.1 R_r$ as uncertainties and error due to
HGO103
Figure 3-35. Controller performance at various speeds (Encoderless Case)106
Figure 3-36. Controller performance at various loads (Encoderless Case)107
Figure 4-1. Block diagram of the experimental setup110
Figure 4-2. Software plan116
Figure 4-3. Hierarchy of real-time task117
Figure 4-4. Block diagram of machine control card119
Figure 4-5. Analog to digital conversion120
Figure 4-6. Anti-aliasing filter (3 rd order low pass Butterworth)121
Figure 4-7. Block diagram of digital to analog conversion121
Figure 4-8. Block diagram of PWM generation122
Figure 4-9. Open Loop Estimation (Part I)124
Figure 4-10. Open Loop Estimation (Part II)125
Figure 4-11. Experimental results of closed loop system without using
speed/position sensors129

LIST OF TABLES

Table 3-1. Machine parameters used in simulations		
Table 4-1. Parameters of machine used in actual experiment	126	

CHAPTER 1

INTRODUCTION

1.1. Control of Induction Machine; A Historical Perspective

The induction machine is called the 'workhorse' of industry. This term carries a deep historical background of over a century. Induction machines are known for their simplicity, ruggedness and reliability. There are no magnets and hence no chance of demagnetization. Their construction is suitable for volume manufacturing. They give good efficiency whilst being compact. Besides all these advantages, they have a lower cost. Amongst the variants of induction machine, squirrel-cage induction machine is the most popular. One of the possible methods to manufacture squirrel-cage induction machines is to die-cast the aluminum rotor. Laminated steel is used as the insulator owing to its much higher resistivity. This type of rotors can work under very harsh environments and up to temperatures below the melting point of aluminum. We have used an induction machine of the same construction. These features make induction machines an attractive choice over other options.

The most common application of induction machines is in the fixed-speed drives. A fixed voltage and fixed frequency signal is applied. Although induction machine is not a synchronous machine, within wide operating range the slip is small and the machine runs near synchronism. This behavior is independent of the load within permissible limits.

Running the machine at fixed speed naturally limits its applications and scope. Development in the field of variable-speed drives and power electronics helped extending the use of induction machine at variable speeds. One common example is the use of variable frequency variable voltage 3-phase inverters as the power source for induction machine. This method is still popular in variable speed drives using induction machine.

The earlier variable-speed drive techniques only provided a good steady-state solution. The idea of replacing DC machines with induction machines was not feasible in applications requiring high dynamic performance. Whereas, keeping in view the qualities of induction machine, it was highly desirable to use it in high performance applications such as servomechanisms. This desire of industrialists and design engineers did not come true until the concept of field orientation was first proposed by Blaschke [2].

The dynamic model of an induction machine can be represented by a sixth-order state space model. The non-linear dynamic structure with interactions requires sophisticated and complex control schemes. The cost of many of these schemes was initially prohibitive. The developments in the field of VLSI and micro computing alleviated these difficulties and now a days we have the capability to implement schemes of our choice. The contemporary development in power electronics also reduced the cost and improved the performance and reliability of inverters. These inverters are one of the basic ingredients of modern control schemes of induction machines.

1.1.1. Control of Induction Machine using Position/Speed Measurements

The first step to control the speed of induction motor is to use speed measurements in the feedback control loop. From the point of view of machine, we do not directly control the speed. Rather the torque is controlled whilst maintaining the flux at a desired level. In many applications the desired flux is constant and the problem is essentially a torque control problem. The concept of field-orientated control makes it possible to decouple the torque control from the flux. If we are successful in our goal, we achieve the same or at least comparable dynamic performance as in the case of DC machines. The overall concept is analogous to control of field and armature currents in DC machines.

Measuring flux faces some practical difficulties. It is therefore, advantageous to employ a flux estimation scheme based on terminal voltage and current measurements. The motor is either fed power either through a voltage source inverter or a current source inverter. Both the methods have their own prose and cons, but the objective remains the same. Our work concentrates on voltage-fed induction machines.

In summary the controller uses flux estimates and speed measurements for controlling the speed of the machine. In certain applications the requirement could actually be to control the torque rather than speed. However, our work concentrates on speed control problem. A simplified block diagram is illustrated in figure 1-1.

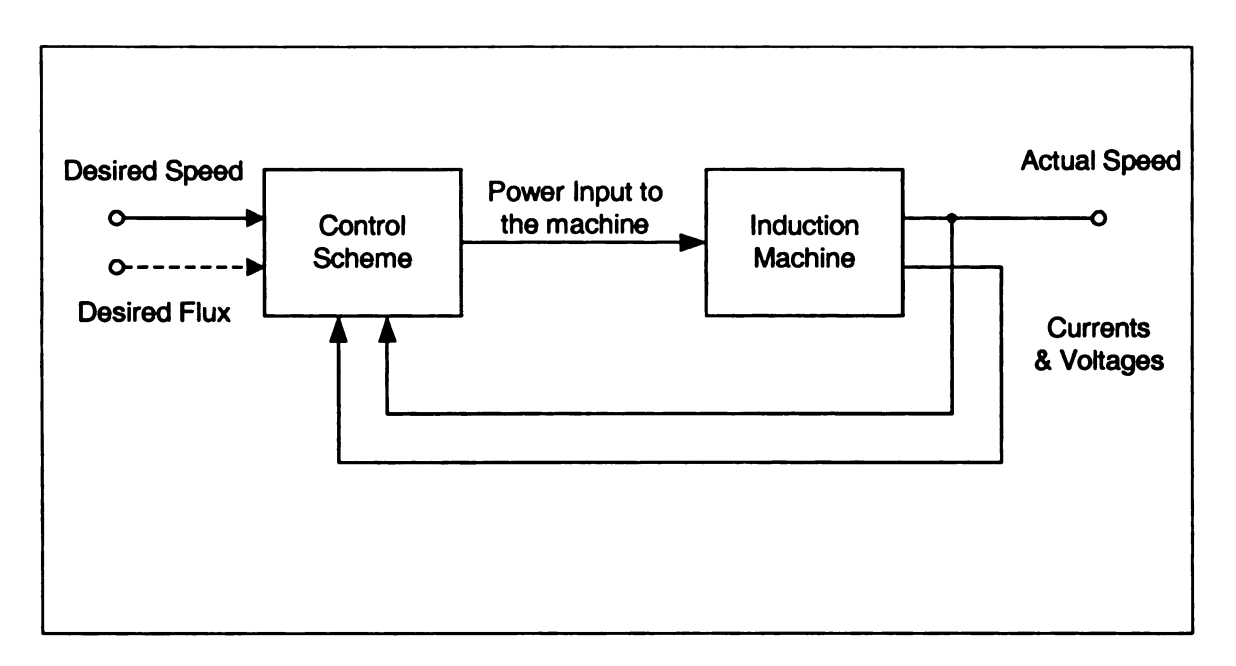


Figure 1-1. Block diagram of control of induction machines using speed/position measurements

1.1.2. Control of Induction Machine without Position/Speed Measurements

Once the basic problem of controlling induction machines was solved and many control schemes had evolved, the attention of the design engineers and researchers turned towards a more challenging problem. The idea is to omit the position/speed sensor and develop a method to estimate the speed from terminal voltages and currents. Mechanical sensors are often undesirable because of space and mounting restrictions. On one hand, the system becomes costly whereas ruggedness of the mechanical sensors is questionable as well. These factors have a greater importance for smaller machines.

Comparing with the previous scheme, now we have to estimate both the flux and speed. The actual speed is no longer a part of the feedback control loop. The obvious consequence is that we have to incorporate more sophisticated algorithms that are computationally extensive and require deeper analysis. Another factor that is not immediately apparent is the loss of some robustness

properties. In this context, many schemes are available but all of them face certain difficulties and none of them is functional in the complete operating range of induction machine. The hardest part is to control the machine at very low or zero speeds. A general solution of the problem is still unknown and the quest continues.

A simplified block diagram of the encoderless control of induction machines is illustrated in figure 1-2.

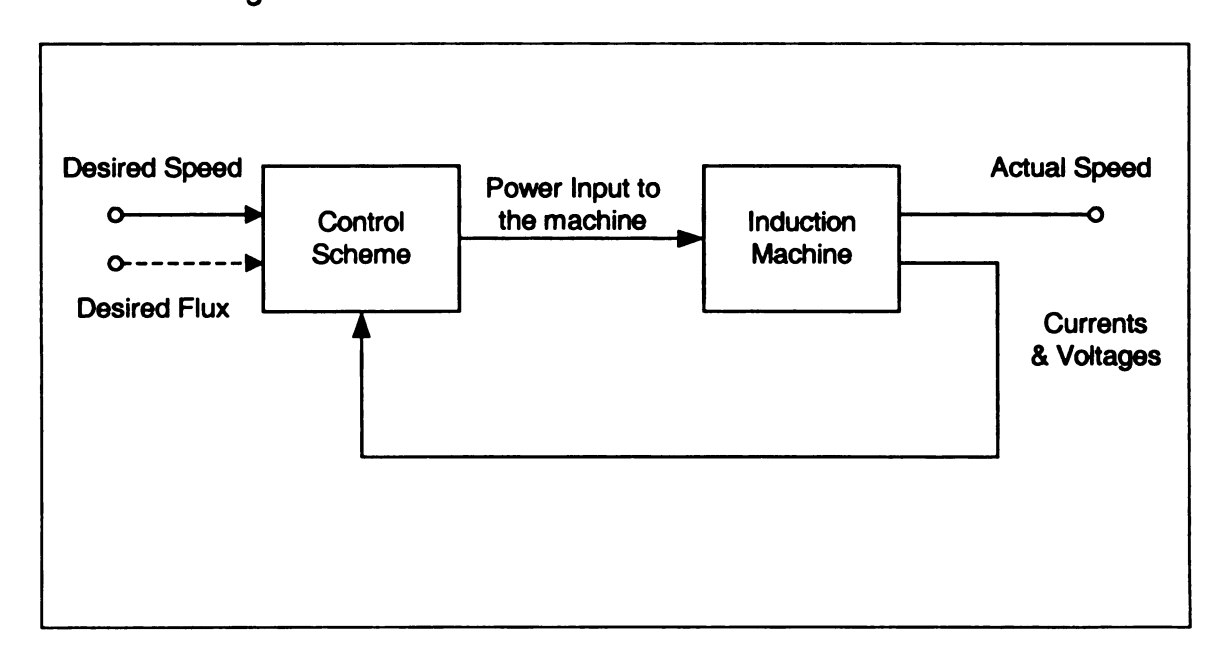


Figure 1-2. Block diagram of encoderless control of induction machines

1.2. Field-Orientated Control and its Variants

Torque producing capability of machines comes from the interaction of flux with currents. This phenomenon is governed by well-known laws of electromagnetism. In an induction machine there are no permanent magnets and the flux itself is produced by a component of current. Furthermore current is flowing in both the stator as well as rotor windings. The two currents are coupled through

the process of electromagnetic induction. In-between the stator and rotor is a small air-gap. In the simplest of divisions, we have three possible types of flux that co-exist in induction machine. These are the stator, rotor and air-gap fluxes. The concept of field orientation is to transform the state variables in such a way that all the new variables are defined with respect to any one of the fluxes. We are not redefining or altering the machine model. It is just represented with a different set of variables. Such transformations that do no change the inherent properties of a model are referred to as diffeomorphism in control theory. The advantage of this procedure is that it may give us additional knowledge and better understanding about the model. This helps in developing control schemes effectively. Since the measurements are from the physical quantities, field-orientated control schemes make use of both the actual and transformed variables.

Corresponding to three different fluxes, we can have stator-, rotor- or air-gap- flux orientated control. All of these methods have their advantages and demerits. Depending on the application and requirements one may be superior to the others. Details of these methods and other possible variations can be found in Leonhard [12], Novotony and Lipo [15] and Vas [21].

1.3. Our Contribution

We would be working on the stator based field-orientated encoderless control of induction machine. The main motivation comes from a scheme proposed by Leonhard [12]. We have modified the actual proposal to either gain certain benefits or for the convenience of implementation. The same or similar schemes

have been used for many years in the research area and industry. A lot of relevant literature is available both in textbooks as well as research papers. Our contribution to this important field comes in two forms.

1.3.1. Analysis

A number of control systems and techniques come into existence as a result of extensive experimentation. Some of these control schemes are actually employed for mass production without in-depth analysis. However, this approach prohibits getting the best out of a control scheme. Unfortunately, performing analysis is a difficult problem in the case of non-linear systems like induction machine. One can find many qualitative statements in the literature that are based on experience and skill of the design engineers. Whereas, this information is valuable, it becomes a great help if we can deduce quantitative results in the form of mathematical equations. Naturally it is not possible in a single effort to resolve or analyze all the details and problems related to an elaborate control scheme. We have tried to do analysis relating to many important issues.

To begin with some useful work has been done on pure integrators. Integration plays a vital role in stator-based techniques. Next comes the analysis of steady-state errors. These errors appear either due to parameter uncertainty or other limitations involved in the overall scheme. This analysis is valuable in the sense that it not only gives quantitative error estimates but also is very useful in evaluating the limitations of the control scheme. Prior information about the valid operating region of a control scheme is vital. There is a brief discussion on high-gain observers, which are becoming integral part of many estimation schemes.

Stator-based methods require some form of decoupler to fulfill the requirements of noninteracting control i.e. the ability to control speed (or torque) and flux independent of each other. There is a handy discussion on this topic. Some of the topics have been discussed without mathematical analysis but are based on common knowledge and logical reasoning.

A series of simulations have been provided to verify and illustrate the analysis. This kind of approach gives a better perspective and understanding of the profound details of a problem. Some of the results that are not obvious become conspicuous after the combination of simulations and analysis.

A final remark is that our work is a contribution and enhancement to a well-known control scheme. It is nothing radically new but should provide to be a useful tool in control of induction machines. We would say that a convenient base is ready for a design engineer to perform actual experiments.

1.3.2. Experimental Setup

Development of a control scheme for machines cannot be considered to be complete without actual implementation. Most of the work in this context has utilized power of today's micro controllers and advanced electronics. Very recent development in real time operating systems has added a new dimension to micro computing. A personal computer can now be used as an embedded processor. The computational power, system resources and flexibility of a personal computer can never be matched by an embedded technology. We availed this technological breakthrough and have developed a new experimental setup with a PC as its microcomputer. We have developed our own machine interface card

that has added to flexibility and convenience to perform new experiments. Practical limitations are reduced and we have freedom to do certain tasks that are not thought off in many other methods of implementation. We consider this setup to be an important contribution to the field of control of induction machines.

CHAPTER 2

MATHEMATICAL MODELING AND ANALYSIS

2.1. Three-Phase Symmetrical Induction Machine

The actual dynamical model of a three-phase symmetrical induction machine is quite complicated and nonlinear. It involves many effects that do not contribute significantly in the normal operation of the machine. If we try to develop a model incorporating all the effects, it would become too complicated. The task of designing a control would become tedious. It may actually obscure the part of the model that plays the major role in the operation of the machine. For these reasons we use a simplified model. The details of the derivations and basic assumptions can be found in Leonhard [12], Novotny [15], or Vas [21]. This model is kind of standard in dealing with control of induction machine. It has the added benefit that it is not particularly specific to a certain type of induction machines. Rather it relates to the operation of an induction machine in a way that is common to all types.

A three-phase symmetrical induction machine can be represented, without loss of generality, by an equivalent two-phase model. Whereas this development is a mathematical artifice, the physical machine does always have three phases. One of the three currents i_{s_1} , i_{s_2} , i_{s_3} in a three-phase machine is redundant because the

neutral is isolated and cannot act as a current source or sink. The same is true for the terminal voltages u_{s1}, u_{s2}, u_{s3} . Hence

$$i_{s1} + i_{s2} + i_{s3} = 0 u_{s1} + u_{s2} + u_{s3} = 0$$
 (2.1)

We define the two-phase equivalent current vector as

$$i_{sa} = \frac{3}{2}i_{s1}$$

$$i_{sb} = \frac{\sqrt{3}}{2}(i_{s2} - i_{s3})$$
(2.2)

which can be conveniently represented by a complex variable

$$i_s = \frac{3}{2}i_{s1} + j\frac{\sqrt{3}}{2}(i_{s2} - i_{s3})$$
 (2.3)

Similarly

$$u_s = \frac{3}{2}u_{s1} + j\frac{\sqrt{3}}{2}(u_{s2} - u_{s3})$$
 (2.4)

Note that we have a degree of freedom over the choice of the constants in the above equations as discussed by Vas [21]. Different authors follow different standards. We try to remain consistent with the above notation, which has been used by Leonhard. The inverse relation is given by

$$i_{s1} = \frac{2}{3}i_{sa} = \frac{2}{3}\operatorname{Re}[i_{s}]$$

$$i_{s2} = -\frac{1}{3}i_{sa} + \frac{1}{\sqrt{3}}i_{sb} = \frac{2}{3}\operatorname{Re}\left[i_{s}e^{-j\frac{2\pi}{3}}\right]$$

$$i_{s3} = -\frac{1}{3}i_{sa} - \frac{1}{\sqrt{3}}i_{sb} = \frac{2}{3}\operatorname{Re}\left[i_{s}e^{j\frac{2\pi}{3}}\right]$$
(2.5)

Similar equations hold for terminal voltages. We would like to emphasize that from now onwards the analysis and design of the control would be carried in two-phase variables. It will be only for the actual implementation where we will have to shift to or form the physical three phase terminal quantities.

A final remark about the transformations we are using is that the length of the quantities is not preserved. In fact if want to calculate the actual equivalent in terms of physical quantities, we have to multiply the two-phase quantities by 2/3. The result is apparent from first equation of (2.2). This may become important if we want to make use of the rated quantities of a machine in two-phase representation. A typical example would be to design a controller that regulates the flux to the rated flux of the machine.

The two-phase model of the machine is given by the following set of equations.

$$R_{s} \cdot \boldsymbol{i}_{s} + L_{s} \frac{d\boldsymbol{i}_{s}}{dt} + L_{m} \frac{d}{dt} \left(\boldsymbol{i}_{r} \cdot e^{j p \theta} \right) = \boldsymbol{u}_{s} \left(t \right)$$
 (2.6)

$$R_{r} \cdot \boldsymbol{i}_{r} + L_{r} \frac{d\boldsymbol{i}_{r}}{dt} + L_{m} \frac{d}{dt} \left(\boldsymbol{i}_{s} \cdot e^{-j p\theta} \right) = \boldsymbol{u}_{r} \left(t \right)$$
 (2.7)

$$J\frac{d\omega}{dt} = T_d - T_l = \frac{2}{3}L_m \operatorname{Im} \left[i_s \left(i_r e^{jp\theta} \right)^* \right] - T_l$$
 (2.8)

$$p\frac{d\theta}{dt} = \omega \tag{2.9}$$

Where

 R_s — Stator resistance

 R_r — Rotor resistance

 L_s — Stator inductance

 L_r — Rotor inductance

 L_m — Magnetizing inductance

is — Stator current vector

u_s — Stator terminal voltage vector

i_r — Rotor current vector

u_r — Rotor terminal voltage vector

p — Number of pole pairs

 θ — Rotor mechanical position

T_d — Electrical torque developed

 T_l — Load torque

J — Moment of Inertia of the load and the rotor shaft

 ω — Mechanical speed

Besides these quantities we would be using and referring to the following quantities

 τ_s — Stator time constant $\begin{pmatrix} L_s \\ R_s \end{pmatrix}$

 τ_r — Rotor time constant $\binom{L_r}{R_r}$

λ_s — Stator flux vector (rectangular coordinates)

 λ_s — Stator flux magnitude

 ρ — Stator flux angle with respect to stationary frame of reference

 i_{ms} — Stator based magnetizing current (rectangular coordinates)

 i_{ms} — Magnitude of i_{ms}

Note: We are using bold letters for vectors or complex quantities and regular letters for scalars. The symbol δ will be used as a difference operator.

We also have the following definitions, which will be used later

$$L_s = (1 + \sigma_s) L_m$$

$$L_r = (1 + \sigma_r) L_m$$
(2.10)

where σ_{s} and σ_{r} are the stator and rotor leakage factors respectively.

The following factors are helpful in simplifying equations and are referred to in the literature quite often.

$$\sigma = 1 - \frac{L_m^2}{L_s L_r} = 1 - \frac{1}{(1 + \sigma_s)(1 + \sigma_r)}$$

$$\alpha_s = \frac{1}{\tau_s}$$

$$\alpha_r = \frac{1}{\tau_r}$$

$$\beta = \frac{L_m}{\sigma L_s L_r}$$

$$\gamma = \frac{1}{\sigma}$$

$$\eta = \frac{1}{\sigma}$$
(2.11)

There would be some other definitions and terminology that we will be discussing as we proceed with our analysis.

2.1.1. Stator Based Machine Model

Our main emphasis in this work is on the stator flux orientated control of a voltage-fed Induction motor. To continue with this development we define certain

machine variables with respect to the stator, which is going to be our frame of reference.

The stator flux vector is defined as

$$\lambda_{s} = L_{m} \cdot i_{ms} \tag{2.12}$$

Where i_{ms} is the stator based magnetizing current and is given as

$$i_{ms} = (1 + \sigma_s)i_s + i_r e^{j\,p\theta} \tag{2.13}$$

Eliminating all the references to the inaccessible rotor currents and assuming $u_r = 0$ for a singly fed machine, the machine equations (2.6) to (2.9) take the form

$$\dot{\lambda}_{s} = u_{s} - R_{s}i_{s} \tag{2.14}$$

$$\sigma L_{s} \dot{i}_{s} + L_{s} \left(1/\tau_{r} - j\omega\sigma \right) i_{s} = \dot{\lambda}_{s} + \lambda_{s} \left(1/\tau_{r} - j\omega \right) \tag{2.15}$$

$$T = \frac{2}{3} L_m \operatorname{Im} \left[i_s i_{ms}^* \right]$$
 (2.16)

The inner voltage vector is defined as

$$v_s = \frac{R_r}{1 + \sigma_r} i_{ms} + j\omega \left(L_m i_{ms} - \sigma L_s i_s \right)$$
 (2.17)

Equations (2.14) and (2.15) assume the form

$$v_s = u_s - \left(R_s + \frac{L_s}{L_r}R_r\right)i_s - \sigma L_s i_s$$
 (2.18)

It is easily seen that the machine model is specified completely by stator-based quantities.

2.1.2. Second Order Effects

We will concentrate on the simplified model of the induction machine. However, it is important for the designer to always keep in mind the unmodeled part of the system. Under certain circumstances any of these unmodeled effects may have a significant role in the operation of the machine and would not be negligible any more. The impact of this factor could render a design restricted to a specific region of operation. Just to emphasize what we have mentioned, following is a list of unmodeled effects.

- Magnetic saturation
- Finite permeability of the stator and rotor iron
- Iron losses
- End windings
- Slot effects including non-ideally distributed sinusoidal winding
- Sensor dynamics
- Inverter nonlinearities include dead time
- Delays and latency less than one sampling period
- Non-ideal behavior of anti-aliasing filters
- Non-ideal behavior of power supplies
- Approximate behavior of discretization of continuous time systems

We will discuss some of the above points during various aspects of the control design. However, they would not be a formal part of the control schemes.

2.2. Stator Flux Estimation

Flux, being a physical quantity, can be measured. In fact many of the earlier field orientation schemes relied on measurements of the stator flux. The two most commonly employed methods were to either insert additional sensing coils or to make use of some sort of magnetic field sensors like Hall effect IC's. It was not long before it was realized that stator flux observers could be built using stator voltages u, and currents i, whilst achieving somewhat similar performance as would have been expected by inserting additional sensing coils. On the other hand the Hall effect IC's are not rugged and therefore not suitable for the harsh operating environments that exist inside a machine. In most case, there are going to be severe thermal and mechanical stresses on the sensors. Considering all these factors and limitations, the natural solution that appears to fit well into the industrial requirements is to estimate flux rather than to measure it.

We will assume that the stator voltage u_s and current i_s are available online. An open-loop stator flux estimator is obtained by integrating equation (2.14).

$$\lambda_{s} = \int (u_{s} - R_{s}i_{s})dt \tag{2.19}$$

The integrand in this equation is sometimes referred to as the voltage behind the stator resistances.

2.2.1. Pure Integrators

Pure Integrators always face difficulties due to the following factors

Low frequency drifts

There are many sources of error that contribute to low frequency drifts. The most significant are the DC offsets, higher internal noise inherent in semiconductors at low frequencies and aliasing errors in sampled data systems. The last one is very important, as it may eventually become a major factor in determining the lowest frequency at which the encoderless control could be employed. Small errors or spurious signals at the input of the integrator may result in undesirably large disturbance at the output of the integrator. The main reason is the very large gain of the integrator at low frequencies. This prohibits us to use the pure integrator in its true form.

Transient offsets

Major causes of this problem are the unmodeled effects and inaccurate parameters in the machine model and sensor/inverter dynamics.

Inappropriate initial conditions.

The lack of information about the exact conditions when the system is powered up, forces us to make certain assumptions about the initial conditions. These assumptions can almost never be exact.

Furthermore, we only know some nominal value of the stator resistance R_{so} . Hence we end up building an estimator of the form.

$$\hat{\lambda}_{s} = \int \left[\left(u_{s} - R_{so} i_{s} \right) + d \right] dt \tag{2.20}$$

Where d is the disturbance term. It is easy to note that if d has a DC component then after long time the estimator would become useless. To

investigate the effect of R_{so} we neglect d and define the error in estimator as follows

$$\delta \lambda_{s} = \lambda_{s} - \hat{\lambda}_{s} = -\int (R_{s} - R_{so}) i_{s} dt \qquad (2.21)$$

This expression is true for any i_s but does not give us much information. On the other hand, we are generally more interested in the steady state errors. Typical steady state currents when expressed as complex variables would be of the form given below.

$$\mathbf{i}_{s} = I_{s}e^{j(\omega_{s}t + \phi)} \tag{2.22}$$

Putting this expression in equation (2.21) gives us

$$\|\delta \lambda_{s}\| = |R_{s} - R_{so}| \frac{I_{s}}{\omega_{s}} \tag{2.23}$$

Although an idealization, this is an important result and tells us that the error in the flux estimator is directly proportional to the difference in actual and nominal stator resistances and the magnitude of the stator current. On the other hand it is inversely proportional to the frequency of the stator current. This observation is particularly important because it gives us a measure of how low we could go as far as the speed is concerned.

2.2.2. Current Components

Equation (2.13) gives a relation of the magnetizing current to stator and rotor currents in an induction machine. In this relation the magnetizing current i_{ms} is in rectangular coordinates. Transforming into polar coordinates we get

$$i_{ms} = i_{ms}e^{j\rho} \tag{2.24}$$

where ρ is the orientation of the stator flux with respect to a stationary frame of reference. As we will see, this angle would in fact form the basis of the stator field orientated control. In other words it is perhaps the most important parameter in the design of the control. Unfortunately in a realistic and physical situation we do not have an exact knowledge of this stator flux angle ρ . The stator flux estimator if transformed into polar coordinates gives us

$$\hat{i}_{ms} = \hat{i}_{ms} e^{j\hat{\rho}} \tag{2.25}$$

The principle of field orientation is primarily based on resolving the stator currents into the direct and quadrature axes. Consider the following equation

$$\mathbf{i}_s e^{-j\rho} = i_{sd} + j i_{sq} \tag{2.26}$$

where the direct component i_{sd} is along the direction of the moving frame of reference defining stator flux coordinates. The quadrature component i_{sq} is orthogonal to i_{sd} .

The torque from equation (2.16) can now be expressed as

$$T_{d} = \frac{2}{3} \operatorname{Im} \left[\lambda_{s} i_{sq} \right]$$

$$= \frac{2}{3} L_{m} \operatorname{Im} \left[i_{ms} i_{sq} \right]$$
(2.27)

The actual components are unavailable and we resort to using the estimate of the field orientation.

$$\mathbf{i}_{s}e^{-j\hat{\rho}} = \hat{\mathbf{i}}_{sd} + j\,\hat{\mathbf{i}}_{sa} \tag{2.28}$$

We will be extensively using these stator current components as well as the magnetizing current in both the analysis and design of the control schemes.

2.2.3. Open Loop and Closed Loop Integrators

There are two types of Integrators generally discussed in literature. The integrator we are using for the stator flux estimation is referred to as open loop integration. Another variation of the stator flux estimator is to implement it in polar coordinates instead of rectangular coordinates. This form is called closed loop integration. Differentiating equation (2.19) and transforming it into field coordinates we get

$$\dot{\lambda}_s + j\lambda_s\dot{\rho} = (\boldsymbol{u}_s - R_s\boldsymbol{i}_s)e^{-j\rho} = (u_{sd} - R_s\boldsymbol{i}_{sd}) + j(u_{sq} - R_s\boldsymbol{i}_{sq})$$
 (2.29)

The equations for stator flux in polar coordinates are

$$\dot{\lambda}_s = (u_{sd} - R_s i_{sd}) \tag{2.30}$$

$$\dot{\rho} = \frac{\left(u_{sq} - R_s i_{sq}\right)}{\lambda_s} \tag{2.31}$$

The measured quantities are u_s and i_s and we have to make use of equation (2.29) in order to obtain direct and quadrature quantities in equations (2.30) and (2.31). The transformation to field coordinates require the use of ρ which is in fact the output of the observer. There is a feedback involved in the estimator and hence the integration in the estimator is referred to as the closed loop integration. Following block diagram illustrates this fact.

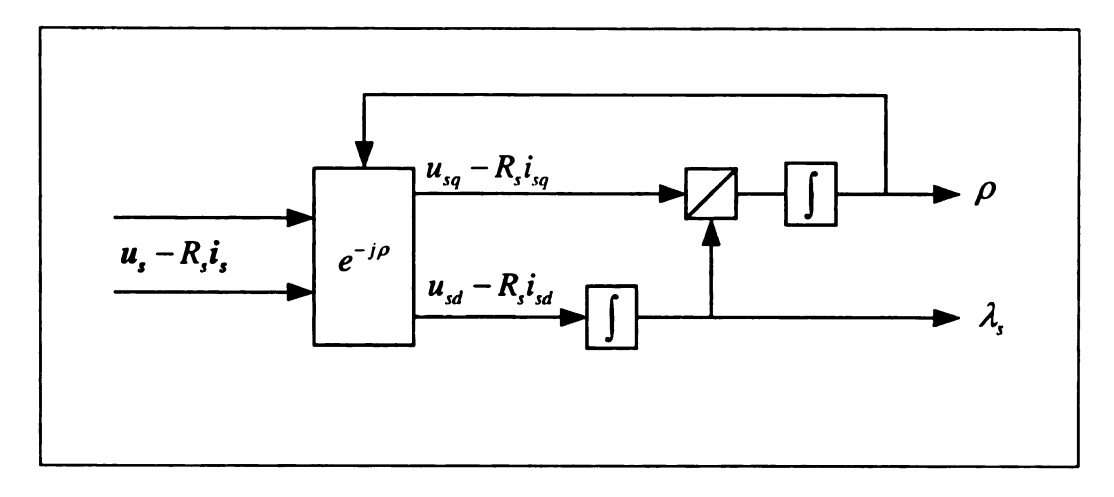


Figure 2-1. Stator Flux Estimation in Polar Coordinates

One might think that the integrator drifts would be reduced for this scheme. Leonhard [12] has said: "If the operation is performed inside a feedback loop, as in the case when being carried out in field coordinates, the effects of integrator drifts are reduced to normal offsets". However, theory and simulations do not support this reasoning. The transformation from one estimator to the other is just a change of variables. It is a well-known fact in Lyapunov analysis that the stability properties are not affected in such transformations. The only thing that may be achieved by a change of variables is that we may be able to isolate the unstable part of the system from the stable one. Both equations of the estimator in the rectangular coordinates are not asymptotically stable. The change of variable into polar coordinates doest not even partition the system such that one part is asymptotically stable. These issues will be illustrated through simulations in next chapter. According to our findings, we do not gain any benefit by transforming into polar coordinates. In fact it may be difficult to replace the pure integrator with a filter approximation in polar coordinates.

2.2.4. Approximation of an Integrator

The arguments we have gone through so far clearly imply that it is not possible to employ pure integrators in a physical control system estimating the stator flux. We have to resort to some approximation of the pure integrator. In this section we investigate the effects of approximating pure integrators with two different types of filters. We start with the following filter, which is in fact the most commonly used method in this regard.

$$\frac{1}{s} \approx \frac{1}{s + \omega_c} \tag{2.32}$$

The corresponding equation for the stator flux estimator is as follows.

$$\dot{\hat{\lambda}}_{s} = -\omega_{c}\hat{\lambda}_{s} + u_{s} - R_{so}i_{s} + d(t)$$
(2.33)

where d(t) is the disturbance vector. Equation (2.33) results in the following error dynamics with the definition of error the same as in equation (2.21).

$$\dot{\delta \lambda_s} = -\omega_c \delta \lambda_s + \omega_c \lambda_s - (R_s - R_{so}) i_s - d(t)$$
 (2.34)

To investigate the boundedness of error we use a Lyapnov function. In the following analysis we would assume only real variables and all the operations would be real. This is typical in Lyapnov analysis. The rest of development extensively uses complex variables for notational convenience.

$$V\left(\delta\lambda_{s}\right) = \frac{1}{2}\left(\delta\lambda_{s}^{T}\delta\lambda_{s}\right) \tag{2.35}$$

The magnetic saturation of the machine keeps λ_i bounded whereas any practical controller has saturation properties that help i_i to remain bounded. Hence in a

physical system λ_s , i_s and d are always bounded and we can define a bound of the following form.

$$\left|\omega_{c}\lambda_{s}-\left(R_{s}-R_{so}\right)\mathbf{i}_{s}-\mathbf{d}\left(t\right)\right|\leq\gamma\tag{2.36}$$

Hence

$$\dot{V} = \delta \lambda_{s}^{T} \delta \dot{\lambda}_{s}$$

$$\dot{V} \leq 0 \quad \text{for} \quad \|\delta \lambda_{s}\| \geq \frac{\|\gamma\|}{\omega_{s}}$$
(2.37)

The boundedness of error is proved for any waveforms of λ_s , i_s and d. This result is, therefore a conservative estimate for the error bounds. However, if we make use of the typical steady-state conditions given below, we get better estimates of the steady-state errors.

$$i_s = I_s e^{j(\omega_s t + \phi)}$$

$$\lambda_s = \Lambda_s e^{j(\omega_s t + \psi)}$$
(2.38)

Leaving out the disturbance term we can actually solve equation (2.33). The natural response of this stable system decays very slowly with time. We are only interested in the forced response.

$$\delta \lambda_{s} = \frac{1}{\omega_{c} + j\omega_{s}} \left[\omega_{c} \Lambda_{s} e^{j(\omega_{s}t + \psi)} - \delta R_{s} I_{s} e^{j(\omega_{s}t + \phi)} - \left(\omega_{c} \Lambda_{s} e^{j\psi} - \delta R_{s} I_{s} e^{j\phi} \right) e^{-j\omega_{c}t} \right] (2.39)$$

For $\omega_s^2 \gg \omega_c^2$ which is equivalent to $j\omega_s + \omega_c \approx j\omega_s$ equation (2.39) reduces to

$$\delta \lambda_s \approx \frac{\omega_c}{\omega_s} \Lambda_s e^{j\left(\omega_s t + \psi - \frac{\pi}{2}\right)} - \frac{\delta R_s}{\omega_s} I_s e^{j\left(\omega_s t + \phi - \frac{\pi}{2}\right)}$$
(2.40)

We have left out the last term of equation (2.39), which decays after long time.

As far as the disturbance is concerned we do not know the exact waveforms. It would be preferable to model it as a signal which is band limited to ω_d .

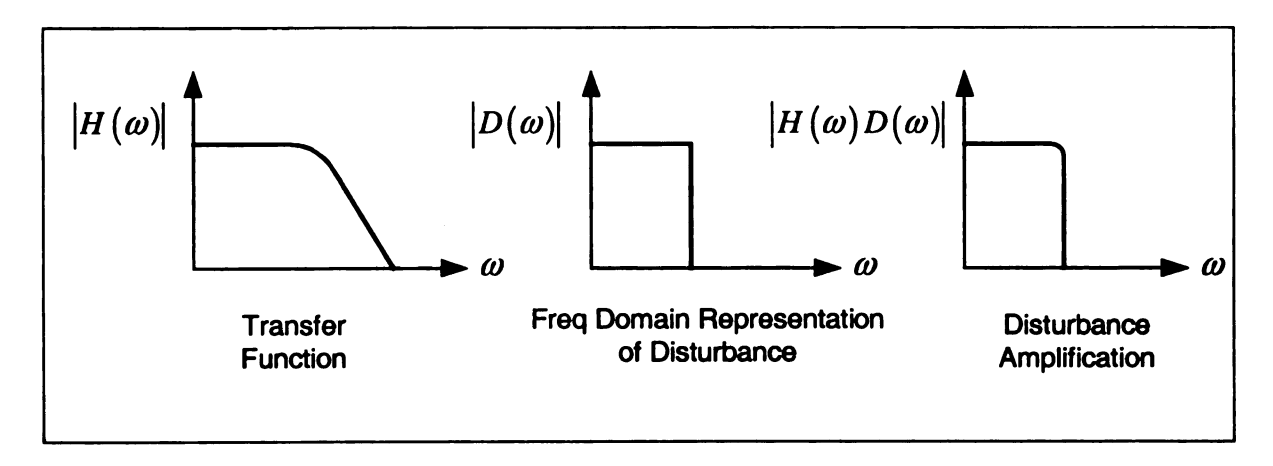


Figure 2-2. Frequency domain representation of disturbance with integrator approximated by first order filter

The figure illustrates that if $\omega_d \ll \omega_c$ then the low frequency disturbance would be amplified $1/\omega_c$ times. This could become a problem if ω_c is small. Combining equation (2.40) with the amplification of the disturbance term we get

$$\|\delta\lambda_{s}\| \leq \frac{\omega_{c}\Lambda_{s}}{\omega_{s}} + \frac{|R_{s} - R_{so}|I_{s}}{\omega_{s}} + \frac{1}{\omega_{c}} \sup |d(t)|$$

$$\approx \frac{|R_{s} - R_{so}|I_{s}}{\omega_{s}} + \frac{1}{\omega_{c}} \sup |d(t)|$$
(2.41)

It is instructive to note that we had introduced three sources of errors; namely the approximation of the integrator with a filter, the mismatch between nominal and exact stator resistances and the presence of the disturbance. The three terms of the first equation correspond to these sources of errors and interestingly are independent of each other. This is because the error dynamics equation is linear. The error due to first term is small and does not cause much of a difference.

To overcome the problem of amplification of the drift we may employ another form of the integrator approximation given by

$$\frac{1}{s} \approx \frac{s}{\left(s + \omega_c\right)^2} \tag{2.42}$$

We would be implementing the estimator as

$$\ddot{\hat{\lambda}}_{s} = -2\omega_{c}\dot{\hat{\lambda}}_{s} - \omega_{c}^{2}\hat{\lambda}_{s} + \dot{u}_{s} - R_{so}\dot{i}_{s} + \dot{d}(t)$$
(2.43)

The corresponding error dynamics are given as

$$\delta \ddot{\lambda}_{s} = -2\omega_{c}\delta \dot{\lambda}_{s} - \omega_{c}^{2}\delta \lambda_{s} + 2\omega_{c}\dot{\lambda}_{s} + \omega_{c}^{2}\lambda_{s} + \dot{u}_{s} - (R_{s} - R_{so})\dot{i}_{s} + \dot{d}(t)$$
 (2.44)

The boundedness of $\delta \lambda$, can be shown by Lyapnov analysis but as in the previous case these bounds would be conservative. We therefore, try to estimate the steady-state errors for the typical operating condition given in equation (2.38). The forced response of equation (2.44), neglecting the disturbance term, is

$$\delta\lambda_{s}(t) = \frac{1}{(\omega_{c} + j\omega_{s})^{2}} \left[\left(\omega_{c}^{2} + 2\omega_{c}\omega_{s} j \right) \Lambda_{s} e^{j(\omega_{s}t + \psi)} - j(R_{s} - R_{so}) \omega_{s} I_{s} e^{j(\omega_{s}t + \phi)} \right] - \frac{1}{(\omega_{c} + j\omega_{s})^{2}} \left[\left(1 + \omega_{c}t + j\omega_{s}t \right) \Lambda_{s} e^{-j\omega_{c}t} \right]$$
(2.45)

The last term decays though very slowly. We can carry out a similar approach to investigate the amplification of the disturbance term. Refer to the following figure where the disturbance is assumed to be band limited to ω_d .

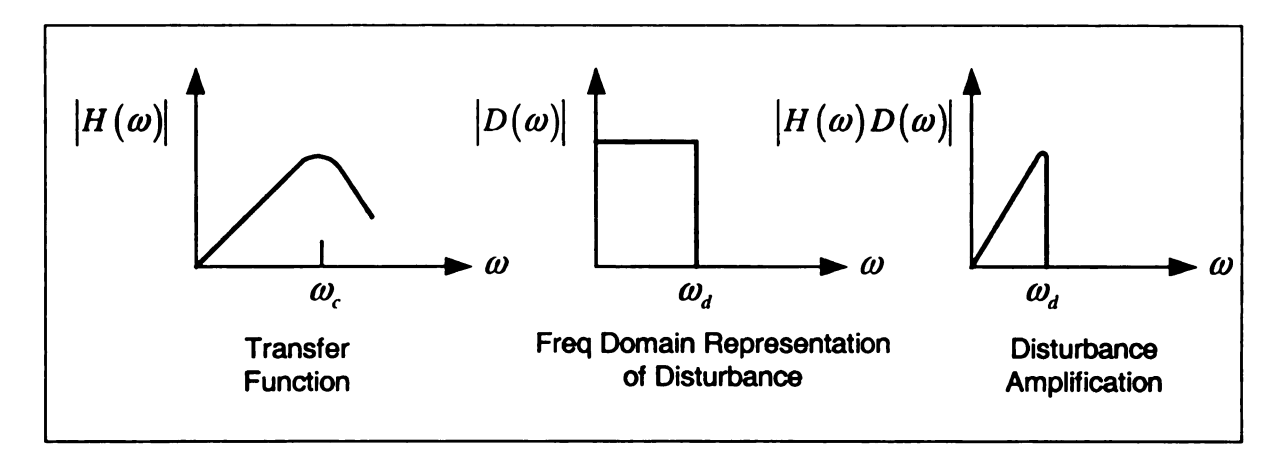


Figure 2-3. Frequency domain representation of disturbance with integrator approximated by second order filter

There are two possible ways to estimate the behavior of the filter to the disturbance term. If $\omega_c \gg \omega_d$ then the amplification of the disturbance term can be approximated by the following expression

$$h(t)*d(t) \approx \frac{\dot{d}(t)}{\omega_c^2}$$
 (2.46)

where h(t) is the impulse response of the filter. It is evident from the above expression that the DC component of the disturbance is completely blocked. Another approximation could be as follows

$$h(t)*d(t) \approx \frac{\omega_d}{\omega_c^2} d(t)$$
 (2.47)

Furthermore If $\omega_d < \omega_c^2$ then the amplification of the disturbance is O(d(t)). The disturbance is assumed to be small itself as compared to the actual signals. Now if $\omega_s \gg \omega_c$ then after bringing back the disturbance term into the solution (2.45) of equation (2.44) we get

$$\|\delta \lambda_{s}\| \leq \frac{2\omega_{c}\Lambda_{s}}{\omega_{s}} + \frac{|R_{s} - R_{so}|I_{s}}{\omega_{s}} + O(\boldsymbol{d}(t))$$

$$\approx \frac{|R_{s} - R_{so}|I_{s}}{\omega_{s}}$$
(2.48)

This is an interesting result when compared to equation (2.23). The conclusion is simply that the second-order approximation of the integrator not only takes care of the low frequency disturbances but also approximates the integrator pretty well. It is important to note that if the condition $\omega_s \gg \omega_c$ is not satisfied then equation (2.48) is not a good approximation of equation (2.45) and may cause some undesirable results and eventually lead to an error in the speed estimate. A slight improvement in the decaying term of equation (2.45) is possible if we use complex conjugate poles instead of a double pole. One possible scheme could be

$$\frac{1}{s} \approx \frac{s}{s^2 + s\omega_c + \omega_c^2} \tag{2.49}$$

The corresponding error term, omitting the decaying terms, is

$$\delta \lambda_{s}(t) = \frac{\omega_{c}}{\omega_{c} + j\omega_{s}} \Lambda_{s} e^{j(\omega_{s}t + \psi)} \frac{1}{(\omega_{c} + j\omega_{s})^{2}} \left[j(R_{s} - R_{so}) \omega_{s} I_{s} e^{j(\omega_{s}t + \phi)} \right]$$

$$\|\delta \lambda_{s}\| \approx \frac{\omega_{c} \Lambda_{s}}{\omega_{s}} + \frac{|R_{s} - R_{so}| I_{s}}{\omega_{s}} + O(d(t))$$
(2.50)

Another advantage of this form is that it resembles more to the first order filter.

The first two terms are identical to the corresponding terms in equation (2.41).

2.2.5. Equivalent Errors in Polar Coordinates

It is sometimes convenient to carry a part of analysis in polar coordinates. However, our stator flux estimator is in rectangular coordinates. It would be useful to calculate equivalent errors in the polar coordinates. This development is for a general case, which we would convert to our estimator later. If y is some complex quantity given as

$$y = \alpha + j\beta \tag{2.51}$$

with its estimate

$$\hat{y} = \hat{\alpha} + j\hat{\beta} = (\alpha - \delta\alpha) + j(\beta - \delta\beta)$$
 (2.52)

where $\delta \alpha$ and $\delta \beta$ are the errors in rectangular coordinates.

Assuming that the error is small as compared to the actual values, we can carry out the following derivations.

$$|y|^{2} - |\hat{y}|^{2} = \alpha^{2} + \beta^{2} - (\alpha - \delta\alpha)^{2} - (\beta - \delta\beta)^{2}$$

$$\approx 2\alpha\delta\alpha + 2\beta\delta\beta$$
(2.53)

As $|y| + |\hat{y}| \approx 2|y|$ for small errors, we get

$$\delta |y| \approx \frac{\alpha \delta \alpha + \beta \delta \beta}{|y|} \tag{2.54}$$

Representing the quantities under consideration in polar coordinates

$$y = |y|e^{j\theta}$$

$$\hat{y} = |\hat{y}|e^{j\hat{\theta}}$$
(2.55)

gives

$$y - \hat{y} = |y|e^{j\theta} - |\hat{y}|e^{j\hat{\theta}} \approx |y|\left(e^{j\theta} - e^{j\hat{\theta}}\right)$$
 (2.56)

The error in complex exponential is therefore

$$\delta e^{j\theta} = \frac{\delta \alpha + j\delta \beta}{|y|} \tag{2.57}$$

This equation can also be useful in finding equivalent error in rectangular coordinates provided we have knowledge of the error in polar coordinates.

Another useful variant of equation (2.57) is

$$\delta e^{-j\theta} = e^{-j\theta} - e^{-j\hat{\theta}} = -\frac{\delta e^{j\theta}}{e^{j(\theta + \hat{\theta})}} \approx -\frac{\delta e^{j\theta}}{e^{j2\theta}}$$
(2.58)

In most of the cases we would be interested in $\delta e^{i\theta}$ rather than $\delta \theta$ itself. However, a special case of equation (2.57) arises when θ and error in it are small. In that case

$$\cos(\theta) \approx 1$$

$$\cos(\hat{\theta}) = \cos(\theta - \delta\theta) \approx 1$$

$$\sin(\theta) \approx \theta$$

$$\sin(\hat{\theta}) = \sin(\theta - \delta\theta) \approx \theta - \delta\theta$$
(2.59)

resulting in

$$\delta e^{j\theta} = \left[\cos(\theta) - \cos(\hat{\theta})\right] + j\left[\sin(\theta) - \sin(\hat{\theta})\right] \approx j\delta\theta \tag{2.60}$$

We are now in a position to estimate the errors in magnitude and angle of the magnetizing current. Equations (2.54) and (2.57) show that bounded errors in rectangular coordinates result in bounded errors in polar coordinates. A word of caution is that the above derivations are based on relative errors being small. If this were not the case bounded error in rectangular coordinates may become unbounded in polar coordinates. The following figure illustrates that the small errors in rectangular coordinates result in bounded errors in magnitude as well as in angle. However, if the error in rectangular coordinates becomes too large the

angle may no longer be bounded. The right figure illustrates this situation where \hat{y} can be pointing in any direction. This is a matter of concern if the actual quantities are becoming small themselves. This important fact may become one of the factors that limit the slow speed operation of the machine where the currents and voltages are small. The sources of errors are the same or even worse as depicted in equation (2.48).

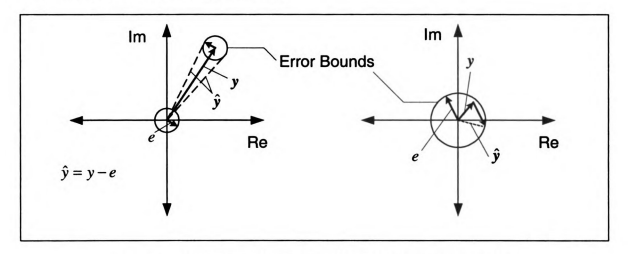


Figure 2-4. Error propagation from rectangular to polar coordinates

The striking observation is that the philosophy of field-orientated control becomes ineffective at the worst-case scenario of the above figure. To summarize, we say that estimated stator flux angle is the most critical parameter for the field-orientated control but is susceptible to extreme conditions.

Now we represent the error bounds for the steady-state condition. The errors will be assumed to be small as compared to the actual quantities. Putting equations (2.38) and (2.40) in equation (2.54) we get, after performing some trigonometric manipulations

$$\delta \lambda_s \approx \frac{\delta R_s I_s}{\omega_s} \sin(\psi - \phi)$$
 (2.61)

The first term of right hand side of equation (2.40) is cancelled out when put in equation (2.54). Since $\psi < \phi$ for the motoring mode, the error in magnitude has opposite sign as compared to δR_s . Furthermore, when the difference $\psi - \phi$ is small, the error should be small and can be expressed as

$$\delta \lambda_s \approx \frac{\delta R_s I_s}{\omega_s} (\psi - \varphi) \tag{2.62}$$

A similar approach leads us to

$$\delta e^{j\rho} = \frac{\omega_c}{\omega_s} e^{j\left(\omega_s t + \psi - \frac{\pi}{2}\right)} - \frac{\delta R_s I_s}{\omega_s \Lambda_s} e^{j\left(\omega_s t + \phi - \frac{\pi}{2}\right)}$$

$$\approx -\frac{\delta R_s I_s}{\omega_s \Lambda_s} e^{j\left(\omega_s t + \phi - \frac{\pi}{2}\right)}$$
(2.63)

From equation (2.13) $I_s < i_{ms}$, which gives us

$$\left|\delta e^{j\rho}\right| < \frac{\left|\delta R_{s}\right|}{\omega_{s}L_{m}} \tag{2.64}$$

From equations (2.26) and (2.28)

$$i_s \left(\delta e^{-j\rho} \right) = \delta i_{sd} + j \delta i_{sq} \tag{2.65}$$

Hence from equations (2.38), (2.58), (2.63) and (2.65)

$$\delta i_{sd} + j \delta i_{sq} = -I_s e^{j(\omega_s t + \phi)} \left(\frac{\omega_c}{\omega_s} e^{j(\omega_s t + \psi - \frac{\pi}{2})} - \frac{\delta R_s I_s}{\omega_s \Lambda_s} e^{j(\omega_s t + \phi - \frac{\pi}{2})} \right) e^{-j2(\omega_s t + \psi)}$$

$$= -\frac{\omega_c}{\omega_s} I_s e^{j(\phi - \psi - \frac{\pi}{2})} + \frac{\delta R_s I_s^2}{\omega_s \Lambda_s} e^{j(2(\phi - \psi) - \frac{\pi}{2})}$$
(2.66)

With the same observations that $\psi - \phi$ is small, we get

$$\delta i_{sd} = \frac{\omega_c}{\omega_s} I_s \sin(\psi - \phi) - \frac{\delta R_s I_s^2}{\omega_s \Lambda_s} \sin(2(\psi - \phi))$$

$$\approx \frac{\omega_c}{\omega_s} I_s (\psi - \phi) - \frac{2\delta R_s I_s^2}{\omega_s \Lambda_s} (\psi - \phi)$$

$$\delta i_{sq} = \frac{\omega_c}{\omega_s} I_s \cos(\psi - \phi) - \frac{\delta R_s I_s^2}{\omega_s \Lambda_s} \cos(2(\psi - \phi))$$

$$\approx \frac{\omega_c}{\omega_s} I_s - \frac{\delta R_s I_s^2}{\omega_s \Lambda_s}$$
(2.67)

Since $\psi-\phi$ is small the errors in i_{sq} are expected to be much higher as compared to the errors in i_{sd} . The situation is worsened by the fact that for most of the operating region of the machine i_{sq} is small. For example if $I_s=60$, $i_{sq}=6$, $\omega_c=1$ and $\omega_s=20$ then $\delta i_{sq}\approx 3$, which is 50% error. It becomes important to develop an algorithm that does not rely heavily on i_{sq} . We will see that the speed estimator developed in section 2.4 makes use of i_{sd} only.

2.2.6. Remarks on Flux Estimation

It is important to keep in mind that the above derivations are true only under certain assumptions. Even though the assumptions are made for typical steady state conditions, certain regions of operation of the machine may require more stringent assumptions and approximations. A typical example is to control the machine at very low speeds. The design parameters should therefore, be well defined in terms of requirements and operating region. The conclusion is that estimation schemes based on approximations and in presence of uncertainties impose certain restrictions on the design of the control and the region of operation.

For most of the cases, the error introduced by approximating the integrator with a filter is small and can be neglected if $\omega_s \gg \omega_c$. The only exception is the estimate \hat{i}_{sq} . However, it can be seen that the error δi_{sq} is not completely unknown. We have complete information about the filter parameters and related issues. This may help in developing some corrective measures and we could improve estimates of the desired quantities. Though we will not pursue this idea further, it may prove to be a useful tool in certain situations.

2.3. Control of Induction Machine Using Speed Measurements

It is natural and instructive to first investigate a control scheme using measurement of the mechanical speed of the rotor. After the development of the flux estimator we are in a position to implement the desired control. Once the design and related issues are clear we can move to our ultimate goal namely the encoderless control of the machine. Before proceeding any further it is important to have a discussion on certain factors. There are basically two possible configurations for the control of induction machines. One is based on current fed induction machine where as the other one is voltage fed. As far as the model of induction machine is concerned it appears that the current fed induction machine is easier to control and indeed the design and analysis of the control is somewhat simpler. This is the main reason that most of the earlier schemes of field-orientated control of machines were developed based on current-fed induction machine. Soon it was realized that practical difficulties involved in the design of a current source inverter not only complicated the situation but even restricted the

design to be useful for only a limited region of operation. These factors become significant in the field-weakening region as explained by Leonhard. On the other hand voltage source PWM inverters are very popular in numerous industrial applications. Their architecture enables reliable and high performance design of induction machine drives. Since our emphasis is not on the theory and design of PWM inverters, we would cut short this discussion by saying that for practical as well as theoretical reasoning we will restrict our design to voltage-fed induction machine where a PWM inverter will act as a three-phase voltage supply.

2.3.1. The Control Variables

One of the fundamental questions in any control problem is clear knowledge of the state variables to be controlled. In the case of stator flux orientated control of an induction machine, our goal is to control the direct and quadrature components of the stator current independently of each other. If this is possible, we would then be able to control flux and torque. The problem of speed control is basically related to the torque control problem as would become clear in the following discussion.

In the case of a voltage-fed induction machine, the voltage source inverter acts as the control effort. However, it is important to realize that we are trying to control the direct and quadrature components of the stator current. Furthermore we lack the exact knowledge of how to resolve the stator current into desired components. The best we can do is to use the estimates \hat{i}_d , \hat{i}_q instead of the actual variables.

2.3.2. Coupled Nature of Direct and Quadrature Current Components

One of the limitations of the stator flux orientated control is that the stator current components i_{sd} , i_{sq} are not completely decoupled. If the field orientation is done along the rotor flux, the corresponding current components are decoupled.

Leonhard has compared this phenomenon with armature reaction of a DC machine. He has derived steady state expressions as follows

$$i_{sd} = \frac{1 + \sigma (S\tau_r)^2}{1 + (\sigma S\tau_r)^2} \frac{i_{ms}}{1 + \sigma_s}$$

$$\approx \frac{i_{ms}}{1 + \sigma_s}$$
(2.68)

$$i_{sq} = \frac{(1-\sigma)S\tau_r}{1+(\sigma S\tau_r)^2} \frac{i_{ms}}{1+\sigma_s}$$

$$\approx (1-\sigma)S\tau_r \frac{i_{ms}}{1+\sigma_s}$$
(2.69)

If there were a change in the load, a transient would result in the stator flux. A flux controller can overcome this difficulty. However, it is known from the multivariable control theory that without proper decoupling the transient behavior of the system may be adversely effected. The remedy to this problem is given in the next section.

2.3.3. Flux Controller and Decoupling Through Feed Forward

In certain cases it is possible to do away with a flux controller. However, in our case flux control is a kind of requirement. Two natural choices are sliding mode control and proportional integral (PI) control. The first one is expected to be robust and has proved to be a reliable method in the rotor flux orientated control.

Details can be found in Strangas and Khalil [10,20]. Because of its simplicity, the second method is more widely used. The main disadvantage is that the tuning of proportional and integral gains could be a problem. Even if the gains appear to work well under certain conditions, the control may deteriorate with the change in operating conditions. In summary, the PI controller is simple to design but faces a problem of tuning of gains.

Our case is, however, different because of the decoupling requirement. It would become a harder problem to device a technique whilst using the sliding mode control. We therefore, resort to PI control. Another option to overcome the problem is to use a scheme where decoupling is achieved by a different choice of field orientated variables. However, that would be altogether a different scheme and would take us away from pursuing the stator flux orientated control. If, on the other hand, we do not use the decoupling term at all, it turns out that the transient response of the system is slowed down to an extent that may be unacceptable as far as high performance drive requirements are concerned. This would be demonstrated by simulating a control scheme without a decoupler.

In the case of voltage-fed induction machines we are trying to control i_{sd} and i_{sq} . Under the assumption that our controller is capable of doing this task, we can design a decoupling scheme in terms of a current-fed induction machine. The main incentive is the convenience in deriving such a scheme. We make use of the scheme proposed by Novotny and Lipo [15]. The current-fed induction machine model in stator frame of reference is

$$L_{s}i_{sq} + \sigma\tau_{r}L_{s}i_{sq} - S\omega_{s}\tau_{r} (\lambda_{s} - \sigma L_{s}i_{sd}) = 0$$

$$\lambda_{s} + \tau_{r}\dot{\lambda}_{s} = L_{s}i_{sd} + \sigma\tau_{r}L_{s}i_{sd} - S\omega_{s}\tau_{r}\sigma L_{s}i_{sq}$$

$$T_{d} = \frac{3p}{4}\lambda_{s}i_{sq}$$
(2.70)

In this model i_{sd} and i_{sq} act as the control inputs rather than the state variables to be controlled. A PI controller of the following form is used

$$i_{sd} = K_p \left(\lambda_{s,ref} - \hat{\lambda}_s \right) + K_i \left[\left(\lambda_{s,ref} - \hat{\lambda}_s \right) dt + i_{decoup} \right]$$
 (2.71)

where $\lambda_{sd,ref}$ is the reference to be tracked and i_{decoup} is the additional decoupling term. Substituting in second of the equations (2.70) we get

$$\lambda_{s} + \tau_{r} \dot{\lambda}_{s} = \left(1 + \sigma \tau_{r} \frac{d}{dt}\right) L_{s} \left[K_{p} \left(\lambda_{s,ref} - \hat{\lambda}_{s}\right) + K_{i} \int \left(\lambda_{s,ref} - \hat{\lambda}_{s}\right) dt\right] + \left(1 + \sigma \tau_{r} \frac{d}{dt}\right) L_{s} i_{decoup} - S\omega_{s} \tau_{r} \sigma L_{s} i_{sq}$$

$$(2.72)$$

To decouple d-axis stator flux λ_{sd} from the q-axis stator current, we require

$$\left(1 + \sigma \tau_r \frac{d}{dt}\right) L_s i_{decoup} - S \omega_s \tau_r \sigma L_s i_{sq} = 0$$
 (2.73)

 $S\omega_{\rm s}$ can be calculated from first of the equations (2.70)

$$S\omega_{s} = \frac{\left(1 + \sigma\tau_{r} \frac{d}{dt}\right) L_{s} i_{sq}}{\tau_{r} \left(\lambda_{s} - \sigma L_{s} i_{sd}\right)}$$
(2.74)

Eliminating $S\omega_s$ from equations (2.73) and (2.74) we get

$$i_{decoup} = \frac{\sigma L_s i_{sq}^2}{\lambda_c - \sigma L_s i_{sd}}$$
 (2.75)

The version of the decoupler that we can implement is based on available quantities.

$$\hat{i}_{decoup} = \frac{\sigma L_s \hat{i}_{sq}^2}{\hat{\lambda}_s - \sigma L_s \hat{i}_{sd}}$$

$$= \frac{\sigma L_s \hat{i}_{sq}^2}{L_m i_{ms} - \sigma L_s \hat{i}_{sd}}$$
(2.76)

There is a singularity in the decoupler equation when all the currents are zero. However when the machine is running, the singularity never appears. This follows from the fact that $L_m > \sigma L_s$ and $i_{ms} > \hat{i}_{sd} > 0$.

After that we have developed a decoupler for the current-fed induction machine, we now adapt it for the voltage-fed machine. With λ_s converging to zero at steady state, equation (2.30) gives

$$u_{sd} \approx R_s i_{sd}$$
or
 $u_{sd,ref} \approx R_{so} i_{dref}$
(2.77)

The proposed flux controller works well if the gains are properly tuned. However, it faces problems if there is considerable detuning and parameter variations. These facts are difficult to analyze but will be demonstrated through simulations.

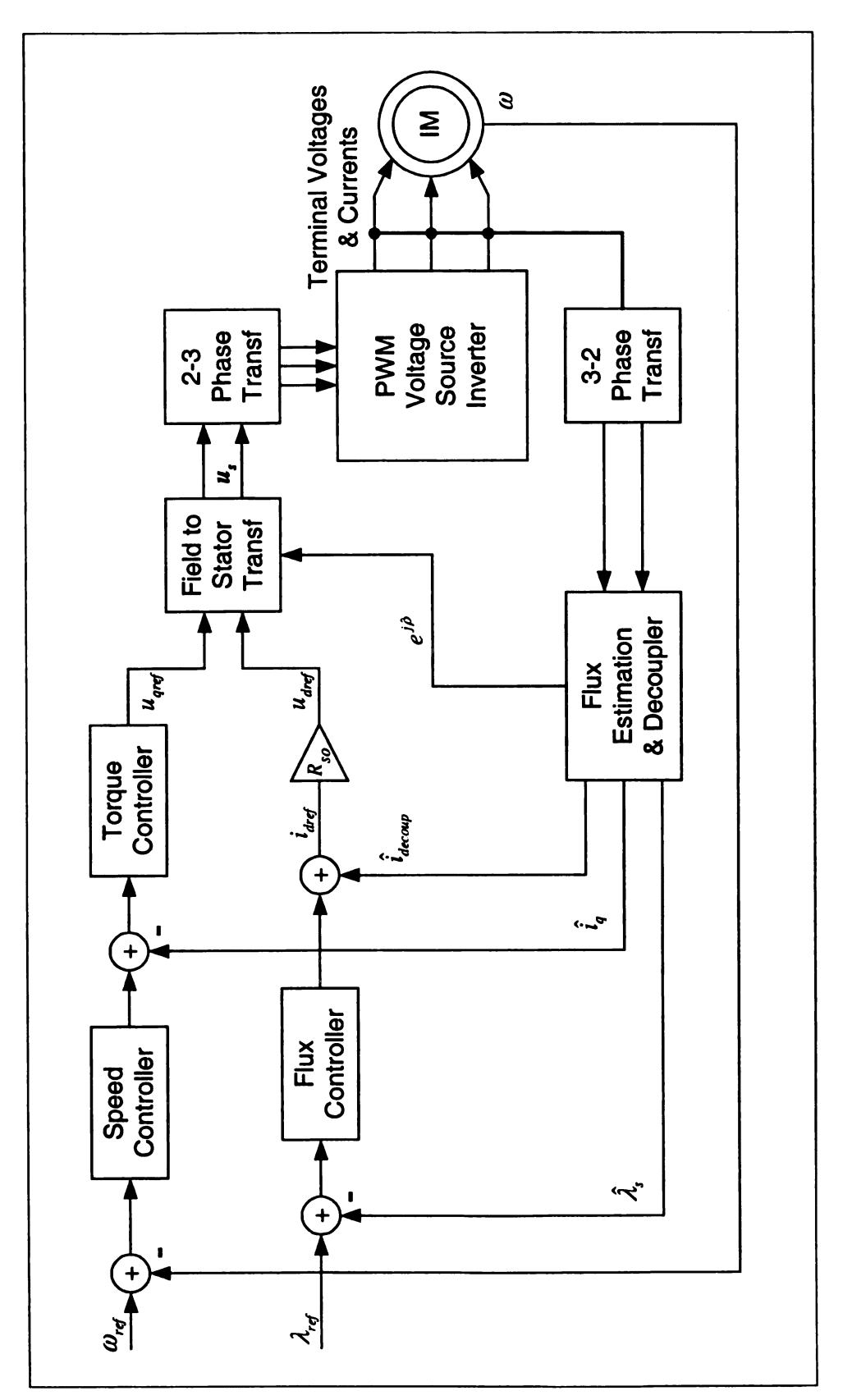


Figure 2-5. Stator field-orientated control of induction machines using speed measurements

2.3.4. Torque and Speed Controller

A combination of a PI speed controller followed by a PI i_{sq} controller proves to be a useful solution in this regard. From equation (2.16) it is clear that if the magnetizing current i_{ms} is successfully maintained at the desired level by the flux controller then the i_{sq} controller is essentially a torque controller. Because of the combinations of two PI controllers, tuning of proportional and integral gains may become tedious and time consuming. The scheme is prone to face difficulties if the load-torque or parameter variations are significant.

One may think to employ robust control methods like sliding mode control for the torque and speed controllers. It has been observed by Aloliwi [19] in his experimental work that the chattering inherent with sliding mode control becomes undesirably large. The missing link is obviously unmodeled dynamics and phenomena.

Under these considerations we restrict ourselves to the PI controllers. Simulations and experimental results with this scheme appear to be satisfactory.

2.3.5. Position Measurement

In most cases, the use of a position sensor is a preferred choice over a speed sensor. This situation, however, requires differentiation of the position to obtain speed. The use of high-gain observers reliably handles the problem. Strangas and Khalil [10,20] have in fact used high-gain observers for the same purpose in rotor flux orientated control.

2.3.6. High Gain Observers

The process of differentiation being non-causal is not realizable. The use of high gain observers not only reliably calculates the derivatives in real time but is also robust to disturbances. Consider the system

$$\dot{x}_1 = x_2$$

$$\dot{x}_2 = f(x_1, x_2)$$

$$y = x_1$$
(2.78)

Treating $f(x_1,x_2)$ as a disturbance, we can make use of the high gain observer as follows

$$\dot{\hat{x}}_{1} = \hat{x}_{2} + (a_{1}/\varepsilon)(y_{1} - \hat{x}_{1})
\dot{\hat{x}}_{2} = (a_{2}/\varepsilon^{2})(y_{1} - \hat{x}_{1})$$
(2.79)

With the change of variables

$$z_1 = (\hat{x}_1 - x_1)/\varepsilon$$

$$z_1 = \hat{x}_2 - x_2$$
(2.80)

we get

$$\varepsilon \dot{z}_1 = -a_1 z_1 + z_2$$

$$\varepsilon \dot{z}_2 = -a_2 z_1 + \varepsilon f(x_1, x_2)$$
(2.81)

It can be shown by singular perturbation theory that for bounded $f(x_1, x_2)$, z_1 and z_2 are $O(\varepsilon)$. In other words the error in differentiation is $O(\varepsilon)$.

This system is referred to as a full-order high-gain observer. There could be other variations such as reduced order observer and extended order observer. In terms of transfer functions we can represent these variations as

$$\dot{\hat{y}}_{ro} = \frac{s}{(s/\varepsilon) + a}$$

$$\dot{\hat{y}}_{fo} = \frac{s}{(s/\varepsilon)^2 + a_1(s/\varepsilon) + a_2}$$

$$\dot{\hat{y}}_{eo} = \frac{s}{(s/\varepsilon)^3 + a_1(s/\varepsilon)^2 + a_2(s/\varepsilon) + a_3}$$
(2.82)

It is apparent that in all the cases the transfer function can be thought of as a cascade of an ideal differentiator and a low pass filter. The Bode plots of the three observers are illustrates below

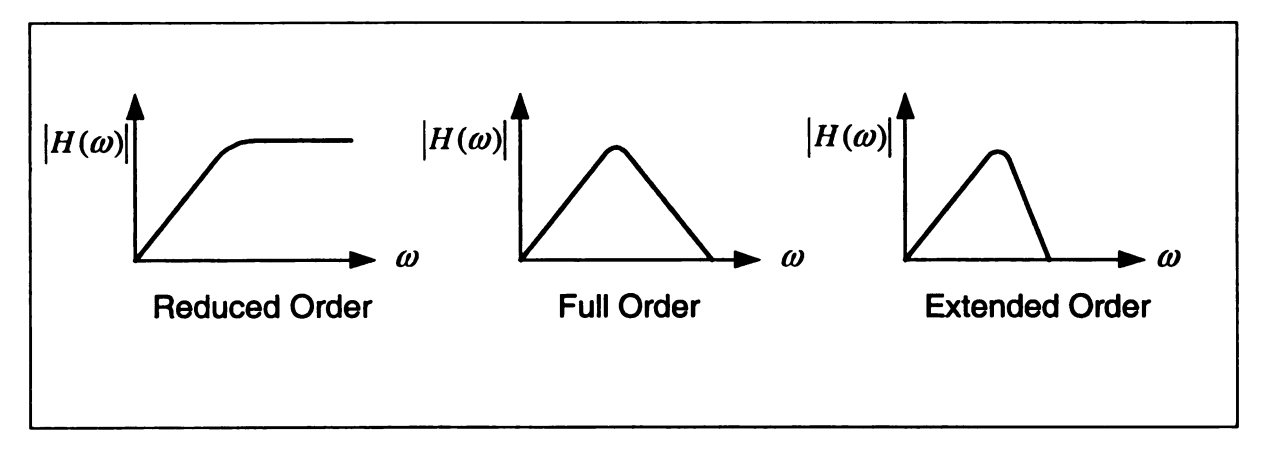


Figure 2-6. Transfer functions of different high gain observers

Whereas high gain observers appear to be sensitive to noise, they have been used in physical control systems where the noise is always present. The performance of high-gain observers in the presence of noise can be improved by observing following precautions.

- Do not choose ε to be very small. Increasing the bandwidth unnecessarily will only deteriorate performance in the presence of noise.
- Avoid using a reduced order observer. This fact is apparent from the transfer function plot where the bandwidth is infinite.

- The use of extended order observer may reduce the noise but be careful about the implementation issues of higher order filters. These issues are explored later in the chapter. Furthermore, the higher the order the poorer is the transient response. It is important to realize that as far as noise performance is concerned, the transient response is as important as the magnitude plots.
- Amongst the commonly used filters, Butterworth filter has good transient response. Bessel and Gaussian filters exhibit even better transient response but are not very frequently used. Use of a low pass filter embedded in the high gain observer that has the best transient behavior will slightly improve the noise performance. For a discussion of transient behavior of filters refer to Daniels [4] and Deliyannis [5].
- Extra precaution should be taken when a high-gain observer is used for digitized discrete-time signal. The group delay of the low pass filter should be larger than ten times the sampling period if not more. Otherwise, at each transition the high-gain observer is going to give sharp response. This behavior is definitely not desirable. We observed this fact during the use of a high-gain observer for estimating speeds from the position measurement obtained through an optical shaft encoder.

2.4. Speed Estimation and Error Bounds

Our ultimate goal is to control the speed of the induction motor without using a mechanical position or speed sensor. To be able to do this, we must develop a

reliable scheme for estimating the speed of the machine. Our emphasis would be on a scheme proposed by Leonhard. However, we will try to go into deeper details of the analysis and try to assess the error bounds of the speed estimate.

Transforming equation (2.17) into field coordinates we get

$$v_s e^{-j\rho} = v_{sd} + jv_{sq} = \frac{-R_r}{1 + \sigma_r} i_{ms} + \omega \sigma L_s i_{sq} + j\omega \left(L_m i_{ms} - \sigma L_s i_{sd} \right)$$
 (2.83)

from which we get

$$\omega = \frac{v_{sq}}{\left(L_{m}i_{ms} - \sigma L_{s}i_{sd}\right)} \tag{2.84}$$

The idea of estimating speed appears to be simple but unfortunately we do not have access to certain quantities in equations (2.83) and (2.84). We can only make use of the estimators. Equation (2.18) takes the form

$$\hat{\mathbf{v}}_{s} = \mathbf{u}_{s} - \left(R_{so} + \frac{L_{s}}{L_{r}}R_{ro}\right)\hat{\mathbf{i}}_{s} - \sigma L_{s}\hat{\hat{\mathbf{i}}}_{s}$$
 (2.85)

where R_{io} and R_{ro} are the nominal values for stator and rotor resistances. \hat{i}_{i} is the estimate of the derivative of i_{i} . We make use of high gain observer to find the derivative of i_{i} . We have the following equation

$$v_s - \hat{v}_s = \delta v_s = -\left(\delta R_s + \frac{L_s}{L_r} \delta R_r\right) i_s - \sigma L_s O(\varepsilon)$$
 (2.86)

Note that there are no dynamics associated with this equation. The equation with estimates as compared to equation (2.83) is

$$\hat{\mathbf{v}}_{s}e^{-j\hat{\rho}} = \hat{\mathbf{v}}_{sd} + j\hat{\mathbf{v}}_{sq} = \frac{-R_{ro}}{1+\sigma_{r}}\hat{\mathbf{i}}_{ms} + \hat{\omega}\sigma L_{s}\hat{\mathbf{i}}_{sq} + j\hat{\omega}\left(L_{m}\hat{\mathbf{i}}_{ms} - \sigma L_{s}\hat{\mathbf{i}}_{sd}\right)$$
(2.87)

where

$$\hat{\mathbf{v}}_s e^{-j\hat{\rho}} = (\mathbf{v}_s - \delta \mathbf{v}_s) \left(e^{-j\rho} - \delta e^{-j\rho} \right) = \mathbf{v}_s e^{-j\rho} - \delta \mathbf{v}_s e^{-j\rho} - \mathbf{v}_s \delta e^{-j\rho} - \delta \mathbf{v}_s \delta e^{-j\rho}$$
(2.88)

The first term on the right hand side is the actual expression as in equation (2.83) whereas the last term may be neglected being a second order error term. Using equation (2.58), the final error expression comes out to be

$$\delta(\mathbf{v}_{s}e^{-j\rho}) = \delta\hat{\mathbf{v}}_{sd} + j\delta\hat{\mathbf{v}}_{sq} = \delta\mathbf{v}_{s}e^{-j\rho} + \mathbf{v}_{s}\delta e^{-j\rho}$$

$$= \delta\mathbf{v}_{s}e^{-j\rho} - \mathbf{v}_{s}e^{-j2\rho}\delta e^{j\rho} = \delta\mathbf{v}_{s}e^{-j\rho} - (\mathbf{v}_{d} + j\mathbf{v}_{q})e^{-j\rho}\delta e^{j\rho}$$
(2.89)

Subtracting equation (2.87) from equation (2.83) we arrive at the following important result.

$$\delta\left(v_{s}e^{-j\rho}\right) = -\frac{\delta R_{r}i_{ms} + R_{r}\delta i_{ms} - \delta R_{r}\delta i_{ms}}{1 + \sigma_{r}} + \sigma L_{s}\left(\delta\omega i_{sq} + \omega\delta i_{sq} - \delta\omega\delta i_{sq}\right) + \\ jL_{s}\left[\omega\left(\frac{\delta i_{ms}}{1 + \sigma_{s}} - \sigma\delta i_{sd}\right) + \delta\omega\left(\frac{i_{ms}}{1 + \sigma_{s}} - \sigma i_{sd}\right) - \delta\omega\left(\frac{\delta i_{ms}}{1 + \sigma_{s}} - \sigma\delta i_{sd}\right)\right]$$
(2.90)

Neglecting small errors, the equation simplifies to

$$\delta\left(v_{s}e^{-j\rho}\right) = -\frac{\delta R_{r}i_{ms} + R_{r}\delta i_{ms}}{1 + \sigma_{r}} + \sigma L_{s}\left(\delta\omega\hat{i}_{sq} + \omega\delta i_{sq}\right) + jL_{s}\left[\omega\left(\frac{\delta i_{ms}}{1 + \sigma_{s}} - \sigma\delta i_{sd}\right) + \delta\omega\left(\frac{i_{ms}}{1 + \sigma_{s}} - \sigma i_{sd}\right)\right]$$
(2.91)

From this equation we can now move towards our actual goal of calculating error bounds on speed estimate. We get two expressions corresponding to the real and imaginary parts of the equation however we would use only one.

$$\delta\omega = \frac{\frac{\delta v_{sq}}{L_s} - \omega \left(\frac{\delta i_{ms}}{1 + \sigma_s} - \sigma \delta i_{sd}\right)}{\frac{i_{ms}}{1 + \sigma_s} - \sigma i_{sd}}$$
(2.92)

The dynamical behavior of the system is dependent on the controller. Therefore, we would delay any further discussion till the actual control is designed and analyzed.

2.5. Control of Induction Machine Using Speed Estimation

Finally we are in a position to design and implement the encoderless control of an induction machine. We will assume that any sort of mechanical speed or position measurement is not available. Hence we will have to rely on the estimate of the speed.

The fundamental estimates would be of the stator flux and rotor mechanical speed. It is interesting to note that the estimate of stator flux is independent of the rotor speed. This is one of the major differences in the estimation of rotor and stator flux. In rotor flux based schemes, the rotor flux estimator is a function of rotor speed. Details could be found in Strangas and Khalil [10,20]. All the discussion and analysis we have done in the previous section for stator flux estimation would be valid here.

The idea would again be to estimate the stator flux angle and perform field orientation with respect to it. In the process, we resolve the stator currents into direct and quadrature axes components. These current components would then be used in the estimation of the mechanical speed. The speed estimate is therefore dependent on the stator flux estimate. Any errors in estimating stator flux affect the accuracy of the rotor speed. Furthermore, we have already seen that the rotor resistance comes in as another factor in the speed estimation.

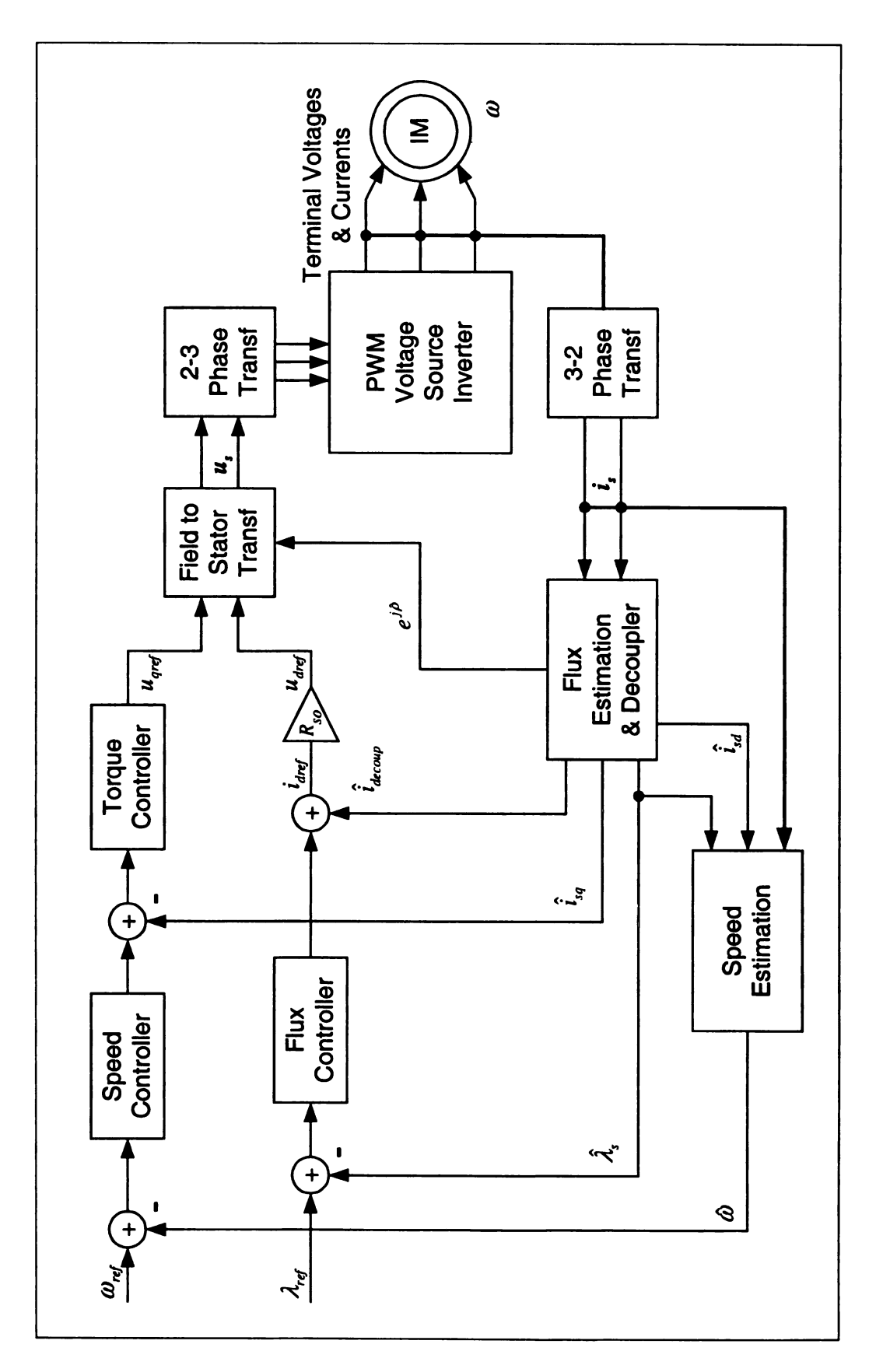


Figure 2-7. Encoderless stator field-orientated control of induction machines

The point to be emphasized is that the encoderless control schemes are always prone to different errors that may have an adverse effect. The robustness becomes an important issue. There may be situations when we are expecting an error in the tracking but the control may actually breakdown

2.5.1. Low and High Speed Operation

The encoderless schemes experience certain limitations. The most glaring is the operation of the machine at low or very low speeds. It is a well-known fact that the stator-based estimators do not behave well at low speeds. Our analysis supports this fact as ω_s appears in the denominator of error estimates. This is one of reasons that people prefer to use other methods for low speeds. However, the most important point to be noted in this context is that most of the factors determining the low frequency limitations are somewhat technology dependent. The clear implication is that by improving the methods of implementation we can get better results. This is one of the prime objectives of our work.

The stator flux and speed estimates tend to become more and more accurate as the speed increases. There are no special considerations involved in this regard except that at very high speeds we have to cater for some other issues such as field weakening.

Finally machine saturation may become an important factor for extreme operating conditions. Unfortunately the machine model with core saturation incorporated in it becomes complicated and we will restrict our discussion and analysis to linear or almost linear region of the magnetic hysteresis curve.

2.5.2. Starting of the induction machine

Any control scheme requires certain time interval before tracking of the references actually begins. The filter approximation can become a problem in this context. If the time required for the control to start tracking is greater than the group delay of the filter, the machine may not start at all. In this situation, the stator flux estimate starts to fall down after the initial transient, whereas the actual flux is present. The apparent solution is to decrease the bandwidth of the filter to the required level. It turns out that this method generally requires bandwidths that are not feasible to implement. A common technique used in this situation is to start the machine by using some other method. The controller takes over at some appropriate time. We have implemented the same approach, which is working well without any problems.

2.5.3. Speed Reversal

One of the challenges of the encoderless control of the induction machine is to achieve speed reversal. This task is in fact a difficult problem even for synchronous machines where the situation is not as complicated. The striking feature of the scheme we are working on is its capability to do speed reversal. The main problem is that while the machine is in transition from one direction of motion to the other, it passes through the generating mode. The stator flux estimator being independent of the rotor speed is robust to this transition. However, the controller faces some difficulties. A simple remedy to the problem is to use a low pass filter at the output of the speed estimator. The bandwidth of the filter should be sufficiently large so as not to disturb the stability of the

system. The filter can be thought of sensor dynamics. Besides, a saturation function should be used for the speed estimate.

2.6. Lowest Possible Speeds

Now we turn our attention to the lowest speed at which the machine can be operated using stator flux-orientated control. This problem has no definite answer because of a wide range of factors involved in the control scheme. If the analysis predicts failure in the steady-state conditions then the scheme is expected to break down. However, it is possible for the scheme to fail even if steady-state error analysis does not provide this information.

The expressions derived in section 2.2 show us that the errors in estimates depend on different parameters and conditions. In most of the cases the error is inversely proportional to the stator frequency ω_s , which is different from the rotor speed. The relation between the two involves the knowledge of load torque, which is unknown itself. However, at zero speed and no load torque we have $\omega_s = 0$. This implies that it is not possible to control the motor for these conditions even if mechanical speed is available for measurements.

Stator frequency ω_s is generated by the controller. However, exact value of ω_s may not be obvious in certain control schemes. In those cases, we can use the relation

$$\omega_{s} = \frac{d}{dt} \left[\tan^{-1} \left(\frac{i_{b}}{i_{a}} \right) \right]$$
 (2.93)

where the differentiation can be done using high-gain observers. Another useful approximation of equation (2.93) is given below

$$\omega_{\rm s} \approx \frac{d\,\hat{\rho}}{dt} \tag{2.94}$$

where $\hat{\rho}$ is the estimate of the stator flux angle as before.

In the presence of external active loads we may achieve zero speed operation. In this case we have to generate electrical torque that counters mechanical torque. The consequence is non-zero frequency of terminal voltages and currents. Considering these factors, we conclude that the limiting factor is not the rotor speed ω . Rather it is the stator frequency ω_{ϵ} .

In order to have an accurate estimate of the minimum possible speeds, we need information of quantities that are generally not available. However, error in i_{sq} gives us a rule of thumb. We have seen in section 2.2.5 that i_{sq} is vulnerable to extreme conditions when compared to other current components. Any control scheme would break down if i_{sq} and \hat{i}_{sq} have different signs. This follows from the fact that we are trying to maintain i_{sq} at a certain level based on the estimate \hat{i}_{sq} . The above discussion gives condition for failure of the scheme. Our main interest is to have an idea of the lowest speed at which the control scheme remains operational. Based on our work and experience on this scheme, we would say that a good and sound controller should able to handle the situation when

$$\left|\delta i_{sq}\right| \le \frac{1}{2} \left|i_{sq}\right| \tag{2.95}$$

For an example of this discussion refer to section 3.5.2.

2.7. Discrete-Time Implementation

Development of computers and embedded technologies has lead to better methods of implementing sophisticated and numeric intensive controllers. The controller has to work in real time so the hardware should have enough speed as required. One may think that computational speed is the main issue. However having a deeper look at the problem, it turns out that there are other matters of significance. All of these details must be kept in mind while designing a discrete-time digital control of a continuous time analog system. Following is a brief discussion of these issues.

2.7.1. Discrete-Time Control of Continuous-Time Nonlinear Systems

There can be two possible alternatives for implementing discrete-time control of a continuous-time system. We can design the control scheme completely in continuous time and then discretize the controllers and observers etc. The other method is to find a discrete-time equivalent of the plant and then work in discrete-time only. Both methods are used depending on the nature of the problem.

The situation is much complicated if we are dealing with nonlinear systems. It is generally hard to find a discrete-time equivalent of a nonlinear system. The same is true for the complex model of an induction machine. With this limitation, we have to restrict ourselves to the first option i.e. perform the design in continuous time and then find discrete-time equivalents of the controllers and observers in our design.

It is important to note that for most design applications the controller for a nonlinear system is generally linear itself. In that case, we can make use of better discretization methods such as the bilinear transform method. This is especially true for the PID or PI controllers. The trapezoidal-rule integrator (which is equivalent to bilinear transformation of a continuous-time integrator) has superior performance as compared to a simple accumulator. This may become significant if numerical problems like round off and truncation are causing undesirable results.

State observers are a part of most of the control schemes. An observer is in one way or the other a replica of a part of the plant. In many cases the observer would therefore be nonlinear. In certain situations the controller may be nonlinear as well. Forward difference methods appear to be the simplest of all if a nonlinear system is to be discretized. The difficulties associated with forward difference method can be overcome by using sufficiently high sampling rate. As the sampling rate is increased, the different discretization methods tend to become more and more similar. Unfortunately for nonlinear systems it is difficult to calculate a lower bound of the sampling rate required for satisfactory performance. In practice, some high sampling rate is chosen based on past experience. For the case of machines, a sampling rate of 10KHz is thought to be sufficiently high to implement any of the common control schemes.

2.7.2. Difficulties Associated with High Sampling Rates

One of the basic problems of implementing a discrete-time control is the choice of the sampling rate. It turns out that if this choice is too high then one may face with a different class of problems. This is significant and some designers have a tendency to overlook it. We illustrate this issue with the stator flux estimator we have employed. Let us consider the approximation in equation (2.32). The bilinear transform method corresponds to replacing *s* by

$$\frac{2}{T_d} \left(\frac{1 - z^{-1}}{1 + z^{-1}} \right) \tag{2.96}$$

which results in

$$\frac{1}{s+\omega_c} \xrightarrow{d} \frac{T_d \left(1+z^{-1}\right)}{\left(2+T_d \omega_c\right) - \left(2-T_d \omega_c\right) z^{-1}} \tag{2.97}$$

where T_d is the sampling interval. For high sampling rate and lower cutoff frequencies $T_d\omega_c$ is small. This results in a stringent requirement for the number of bits we are using for our discrete memory. This effect is called coefficient quantization and results in a displaced location of the poles from the desired. The worst case situation would arise in cases when

$$trunc(2+T_d\omega_c) = trunc(2-T_d\omega_c) = 2$$
 (2.98)

where truncation is done for the maximum number of available bits. We would end up in implementing the exact integrator rather than an approximation by a low pass filter. Leaving aside this worst case, there is yet another factor that is critical. We know that the process of quantization introduces a noise in the data being processed. An integrator accumulates information over a period of time. If the level of quantization noise is significant, we may get undesirably large errors. The integration done by trapezoidal rule or other sophisticated schemes must be

used under these circumstances. For a detailed discussion of quantization noise refer to Oppenheim [16] and Antoniou[1].

The approximation of equation (2.42) is even more sensitive to numerical problems. The discrete version is

$$\frac{s}{\left(s+\omega_{c}\right)^{2}} \xrightarrow{d} \frac{T_{d}\left(1+z^{-1}\right)\left(1-z^{-1}\right)}{\left[\left(2+T_{d}\omega_{c}\right)-\left(2-T_{d}\omega_{c}\right)z^{-1}\right]^{2}}$$
(2.99)

The denominator of the right hand side involves addition or subtraction of $(T_d \omega_c)^2$ from 4. This may require prohibitive number of bits as far as implementation is concerned. To fully appreciate the problem lets consider the situation when sampling frequency is 10KHz and the cutoff frequency is 1 rad/s. Equation (2.99) results in

$$\frac{4.9995000374975\times10^{-5}\left(1-z^{-1}\right)\left(1+z^{-1}\right)}{1-1.9998000099995z^{-1}+0.9998000199985z^{-2}}$$
(2.100)

One may be tempted to round this expression to 7 significant digits (more than the accuracy of 32 bit floating point) resulting in

$$\frac{4.9995 \times 10^{-5} \left(1 - z^{-1}\right) \left(1 + z^{-1}\right)}{1 - 1.9998 z^{-1} + 0.9998 z^{-2}}$$
(2.101)

which simplifies to

$$\frac{4.9995 \times 10^{-5} \left(1 + z^{-1}\right)}{1 - 0.9998z^{-1}} \tag{2.102}$$

This shoes that we have totally lost the second order filter and end up in basically implementing the first order approximation of the integrator.

2.7.3. Suggested Solutions

The results in the previous section may rather be surprising that even 32-bit floating point may not be sufficient to implement certain filters.

One obvious solution is not to go for very high sampling rate. It would be in fact a good idea to decrease the sampling rate as low as permissible. The other possibility is to make use of down and up samplers. The concept is illustrated as follows.

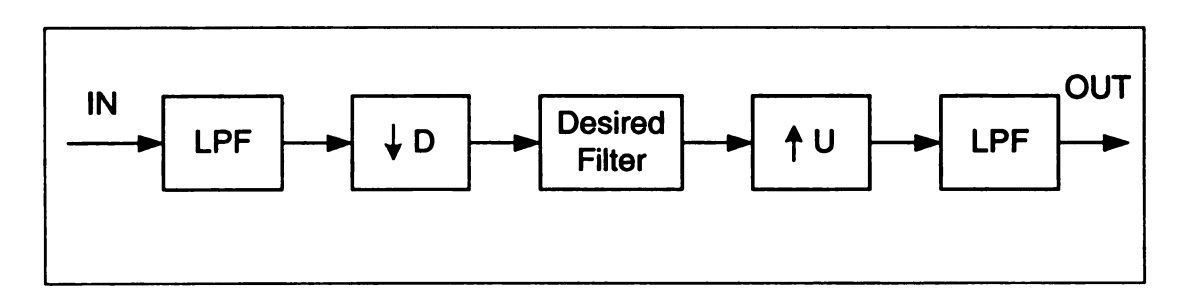


Figure 2-8. A possible scheme to handle high sampling rates

CHAPTER 3

COMPUTER SIMULATIONS

3.1. Importance of Simulations in Design

Control design is an involved task. In many cases complicated analysis is accompanied by elaborate experimental setups. Whereas analysis provides the basis of the design, it faces certain limitations. The first step is to mathematically model an actual physical system. It is generally wise to work on a simplified model, which approximates the reality with reasonable accuracy. This simplifies the control design and its analysis. However, this approach may lead to serious difficulties if the unmodeled effects play a significant role in the operation. Furthermore, for most of the practical and physical control design problems, it may be difficult to carry out exact analysis. Under such circumstances, we have to make certain assumptions or resort to approximate analysis. When we come to actual implementation, all the unmodeled effects are physically present and our assumptions and approximations may not be appropriate. To summarize, we can say that there is a gap between analysis and the experiment and it is generally not possible to fully bridge it.

The concept of simulating a control system helps reducing the distance between analysis and experiments. We can incorporate many of the unmodeled effects in the simulations. Naturally for a physical system, it is not always possible for all the state variables to be available for online measurement. Measurable variable

get corrupted by observation noise and related issues. For certain systems, the tuning of the gains may be critical as inappropriate values may have a damaging effect on the system. Some experiments may be costly to conduct or there may be certain associated hazards. Computer simulations provide a neat solution to all of these problems.

At the first look it appears that we can overcome most of our difficulties using computer simulations. It turns out that simulations themselves face certain problems. The hardest part is to develop a simulation setup. There are some intricacies of the numerical solvers and a number of parameters have to be adjusted properly. Computational speed of the computers is of prime importance. Sometimes it becomes exasperating to run a simulation even on very fast computers. The computers appear to have slowed down for simulations of moderate complexity. Sometimes we may need to modify the actual system just for the simulations to work. These changes should have a minimal effect on the system. Simulation of a physical system is a skill in itself. It requires experience, patience and definitely a sound knowledge of the mathematical model and its behavior.

On of the important points is that simulation gives an insight of the system. It is in fact a tool to learn and understand the design of the control system. Sometimes, the details obtained from a simulation may produce critical information that one has missed in analysis or even in an experimental setup.

We would say that even being an idealization of the real systems, simulations constitute an important step in the design of a control system. The extra time and

effort involved ultimately result in better results and reduce the overall time of the experiment and improve its quality.

We have done extensive simulations to demonstrate most of the facts discussed in the analysis. We have used SIMULINK as our simulator. Most of the secondary effects such as machine saturation, inverter non-linearities, sensor dynamics etc, have not been catered for. We want to concentrate on the core of the design rather than spend a lot of time on effects that either do not contribute significantly in the working of the machine or are automatically compensated for by the closed-loop nature of the control. Whenever possible we will try to simulate the part of the system we are interested in. This approach is more illustrative and logical. In certain cases we will like to simulate the machine in open loop. This would be done to demonstrate certain behavior that either becomes unclear or may actually be compensated for by closing the loop. Machine parameters that we have used in simulations are from a physical induction machine. They are listed below.

Parameter	Value
Stator Inductance, Ls	0.595 mH
Rotor Inductance, Lr	0.608 mH
Magnetizing Inductance, Lm	0.530 mH
Stator Resistance, Rs	0.032 Ω
Rotor Resistance, Rr	0.027 Ω

Table 3-1. Machine parameters used in simulations

3.2. Pure Integration

Stator flux estimation schemes based on pure integration are sensitive to disturbances, initial conditions and transient offsets. This unwanted behavior associated with pure integrators is demonstrated in the following simulations.

3.2.1. Equivalence of Open and Closed Loop Integration

According to our findings, the two methods of stator flux estimation generally referred to as open and closed-loop integration are equivalent. This fact is contrary to the idea that closed loop integrators perform better. There are two different notions in this regard. Leonhard [12] has suggested that by using the closed-loop integration, drifts are reduced to normal offsets. Whereas, Vas [21] has proposed robustness of the closed loop scheme against low frequency disturbance. We develop simulation setup for both DC drift and low frequency disturbance. The model of the estimator used is simplified and is driven by two-phase sinusoidal signal that would actually be equivalent to the voltage behind the stator resistances. Three estimators are used for each simulation. One of them is ideal and the other two are the open and closed loop schemes with a disturbance term. The principle is illustrated as follows

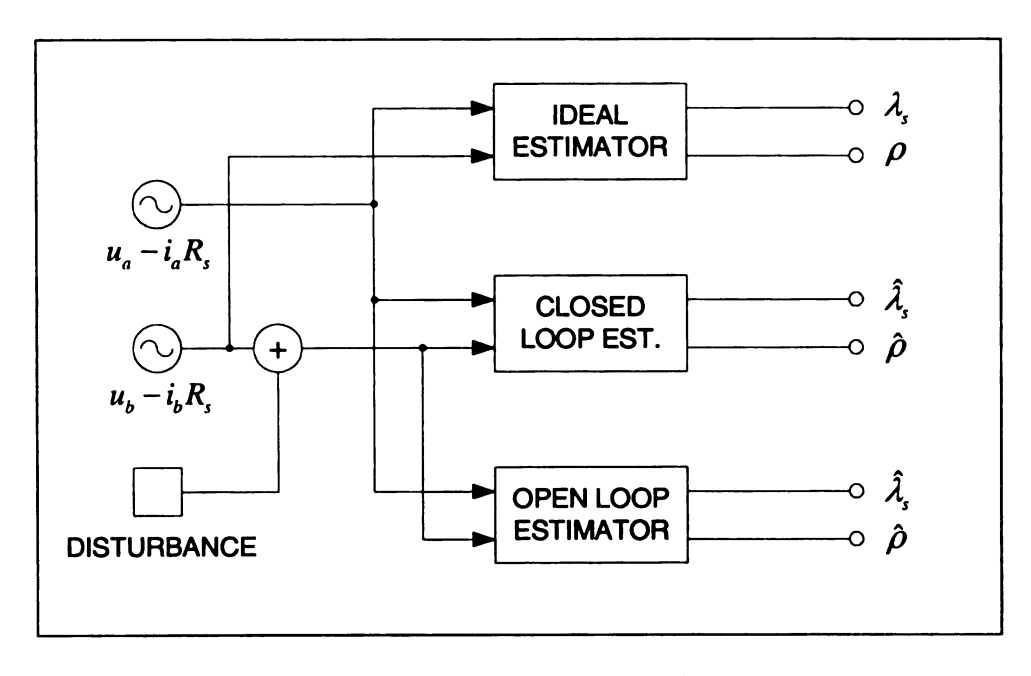


Figure 3-1. Comparison of open and closed loop estimators

The closed loop estimator has the following form.

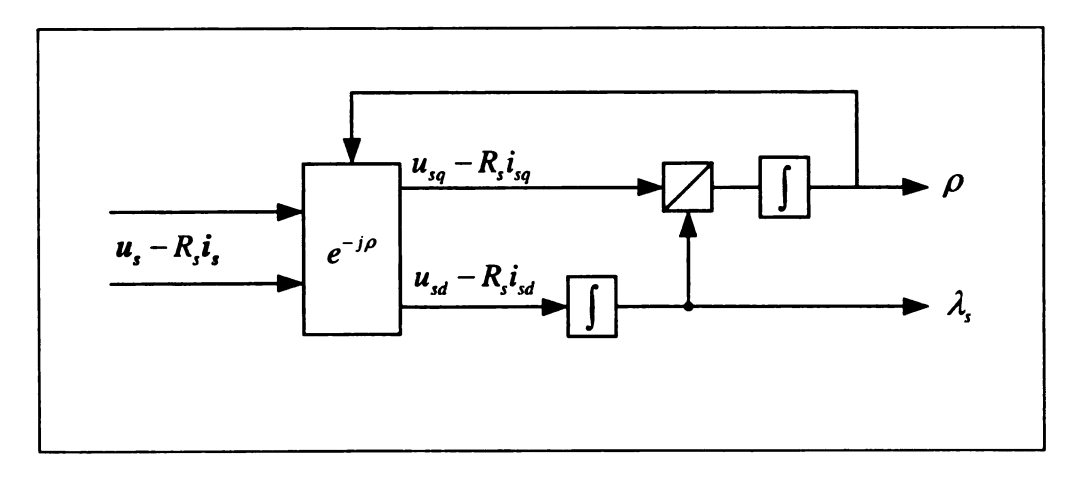


Figure 3-2. Closed loop stator flux estimation

The open loop estimator has the following form.

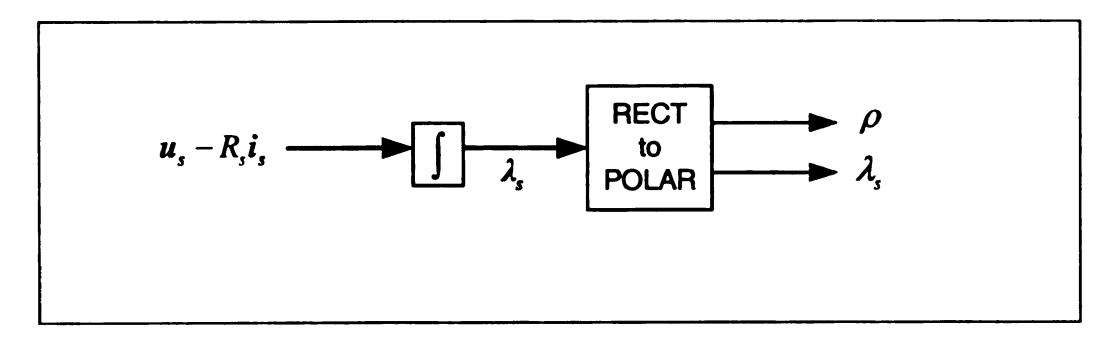


Figure 3-3. Open loop stator flux estimation

The results with DC and low frequency disturbances are illustrate in figure 3-4 and figure 3-5 respectively. The important observation is that the open and closed loop stator flux estimation schemes are behaving exactly the same way. We have demonstrated the equivalent of open and closed loop integrators.

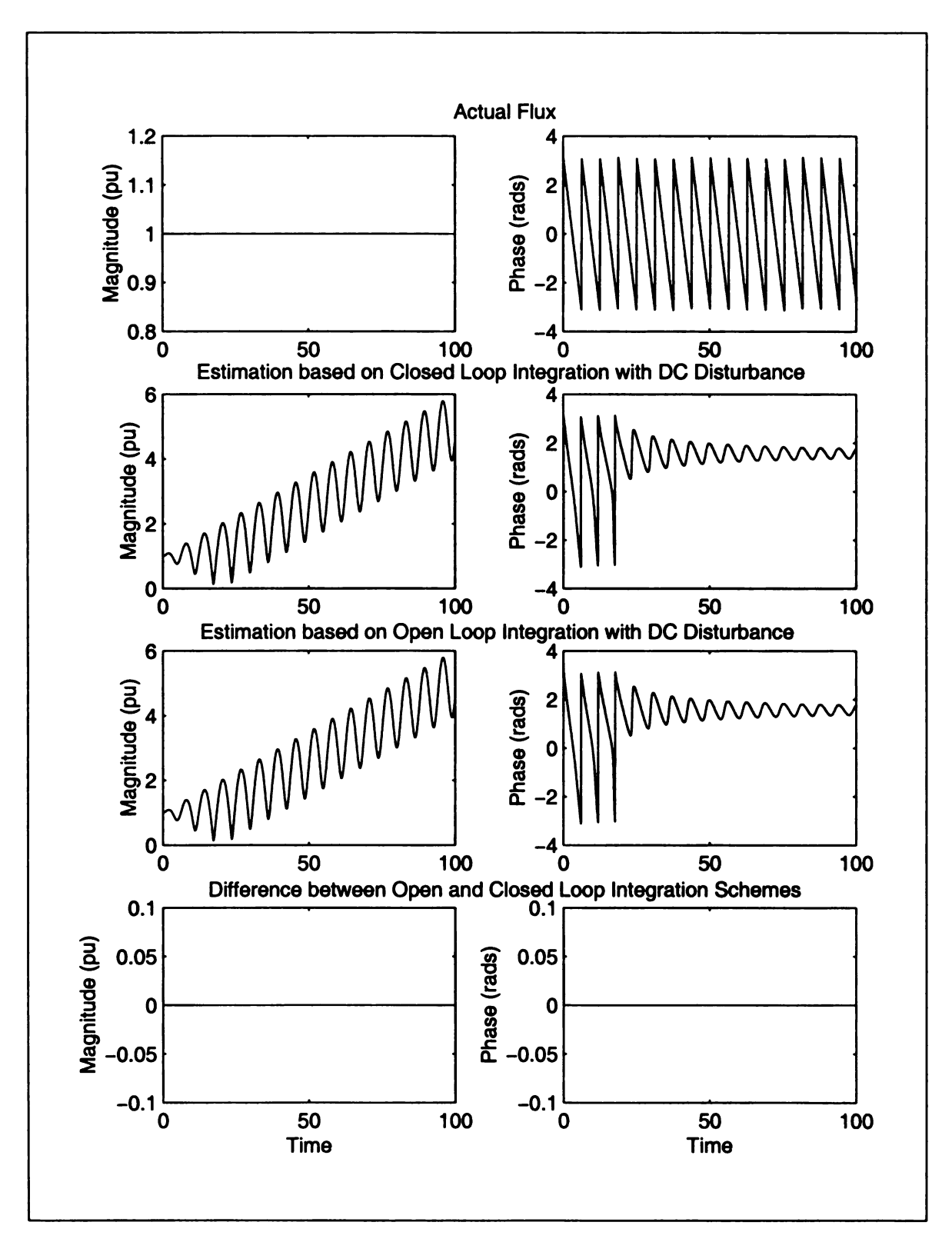


Figure 3-4. Equivalence of closed and open loop integrators for DC disturbances

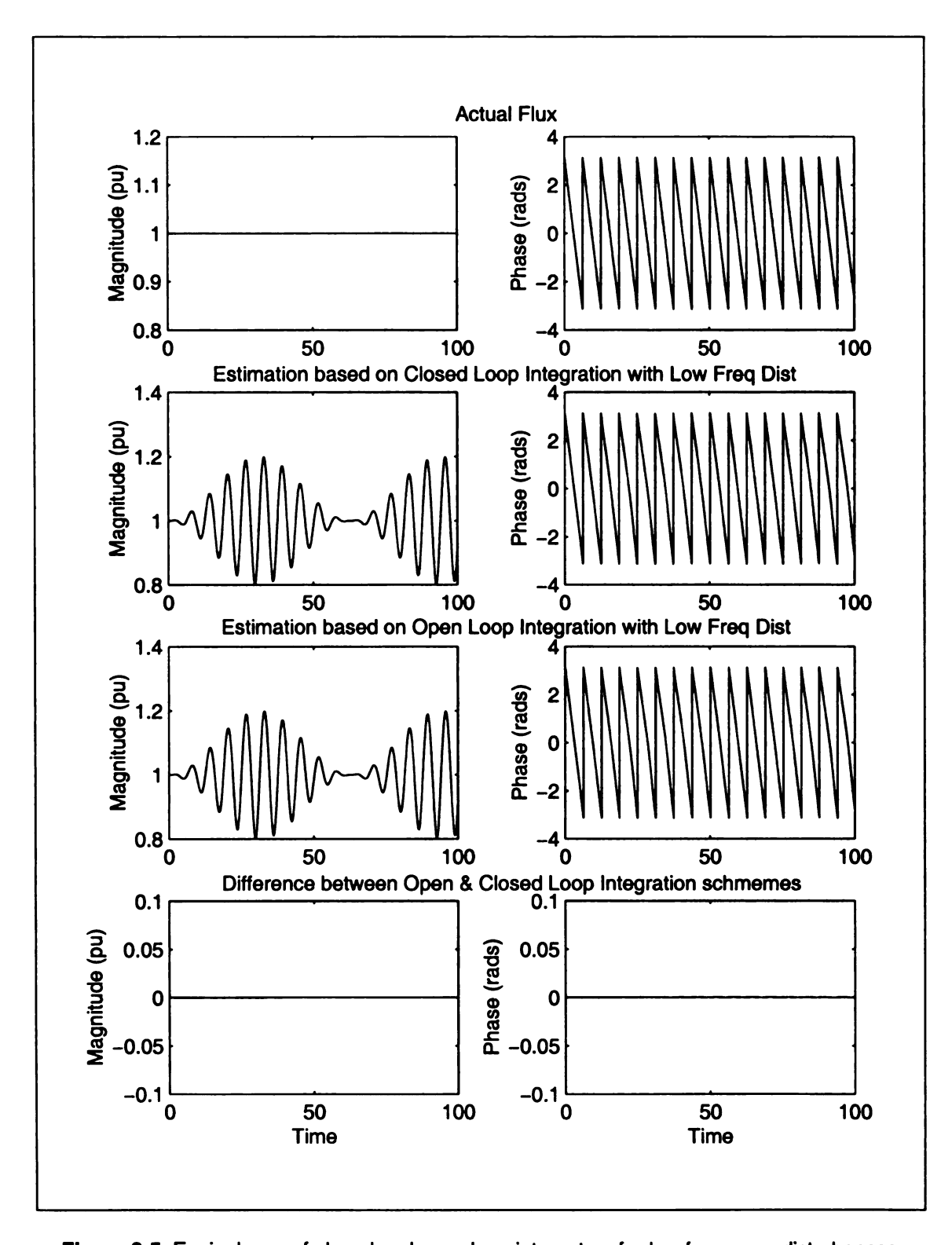


Figure 3-5. Equivalence of closed and open loop integrators for low frequency disturbances

3.2.2. Unknown Initial Conditions

It is almost impossible to have an exact knowledge of the states of the system when the system is first powered up. Pure integrators have no leakage and therefore retain any information either actual or unwanted. If this information is false, the results produced by pure integrators would certainly be wrong throughout the operation. In other words, a pure integrator lacks the ability to correct itself. The false information could be a result of error in initial conditions or some unwanted transient behavior. This behavior is demonstrated in the following setup.

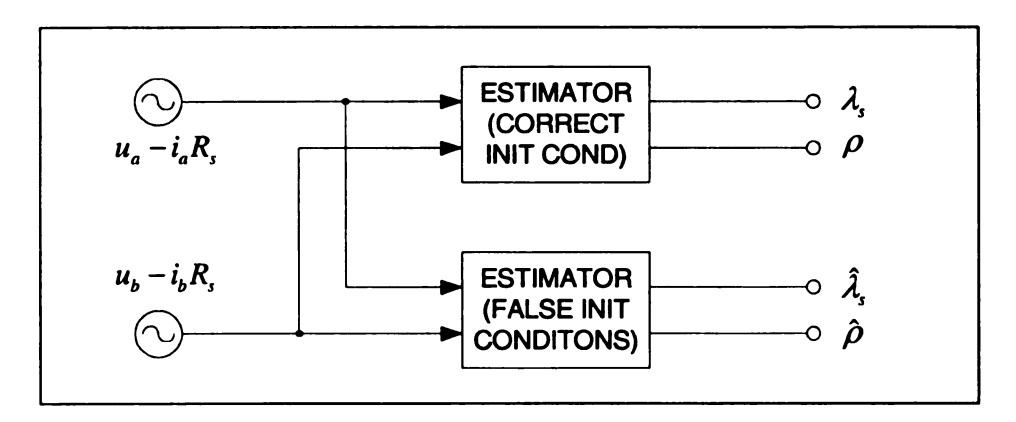


Figure 3-6. Stator flux estimation with pure integrator and false initial conditions

The error in the initial conditions is 50%. We observe that the estimator results in a 50% error. This result appears to be striking but if the zero leakage property of the integrator is kept in mind, it is not unexpected. Both the open loop and closed loop integration schemes face the same problem. The simulation results are illustrated in the figure 3-7.

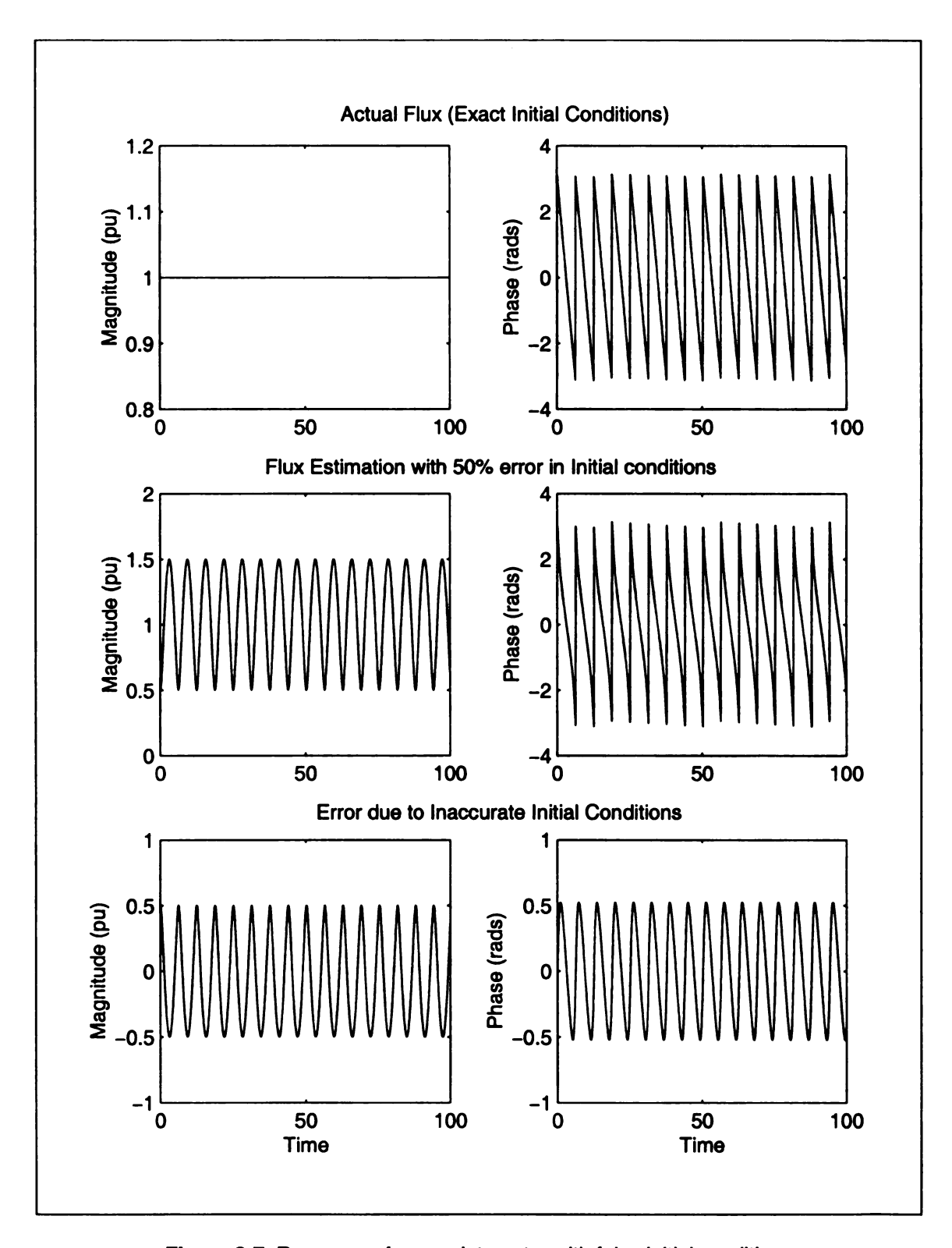


Figure 3-7. Response of a pure integrator with false initial conditions

3.2.3. Transient Behavior

Transient behavior poses another problem for a pure integrator. Even if we assume that there are no errors in the initial conditions and there are no disturbances, the estimator based on pure integrators is vulnerable to inexact knowledge of machine model. Let us consider the case if the nominal stator resistance R_{so} differs by 10% from the actual stator resistance R_{so} . The estimator would follow a different trajectory from the ideal one. If we view the estimator at some time $t_1 > t_0$ with the states of the estimator at time t_1 as the initial conditions for $t > t_1$, then it is not difficult to correlate this situation with false initial conditions. The estimator will not be able to settle down and there would be a bias as well given by equation (2.23). We investigate the behavior of the estimator using the scheme given in figure 3-8. In this case we have to simulate the complete system to have a good idea of what is happening. The results are given in figure 3-9 where the actual quantities are represented by dashed line.

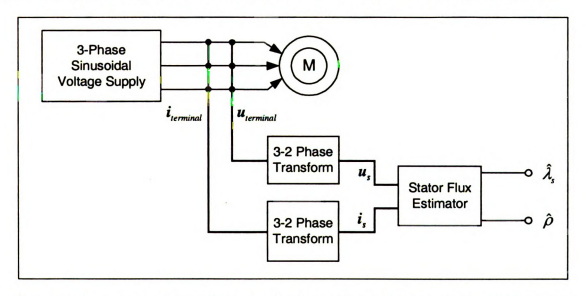


Figure 3-8. Investigation of transient behavior of stator flux estimator using pure integrators in presence of parameter uncertainty

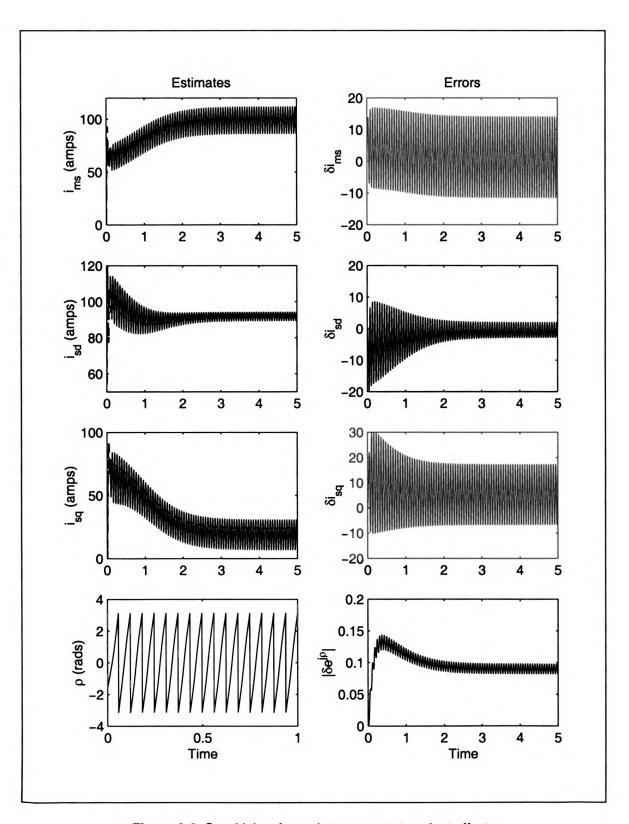


Figure 3-9. Sensitivity of pure integrators to transient offsets

3.3. Stator Flux and Speed Estimation

It may become difficult to study errors associated with an estimator if it is used in a closed-loop control system as the controller or other components can influence the estimator. If we want to concentrate purely on the behavior of an estimator, it would be a better to investigate an open-loop system with no feedback from the output of the estimator. However, since we are now investigating the behavior of the machine as a whole, we would simulate the full system rather than a part of it. The block diagram of the scheme is illustrated as follows.

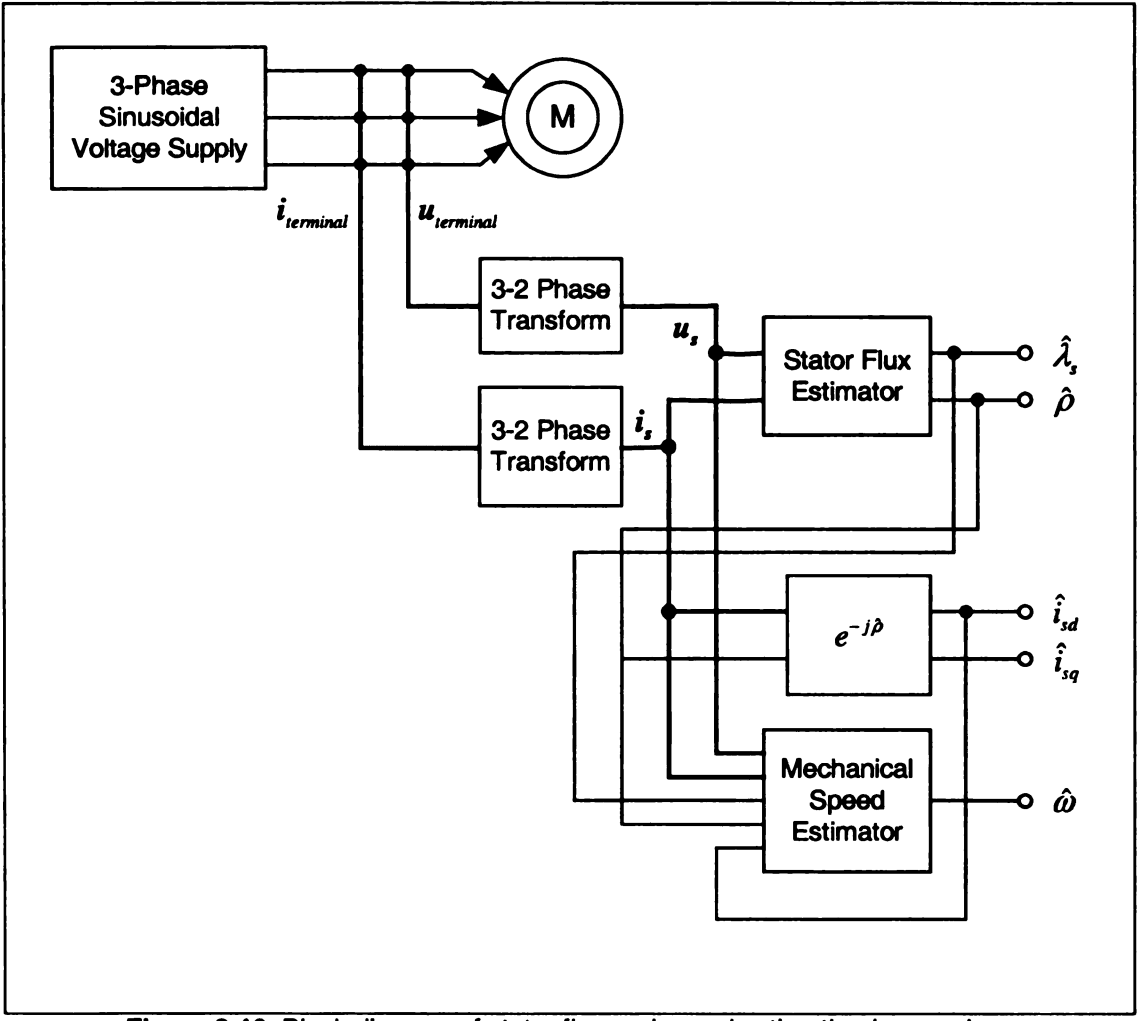


Figure 3-10. Block diagram of stator flux and speed estimation in open loop

Our eventual aim is to use the estimators in a closed-loop control system, where the estimator dynamics become part of the system. In this open-loop setup, estimator dynamics and plant dynamics are independent of each other. Therefore, the influence of the estimator on the dynamical behavior of the closed-loop system cannot be fully understood. However, we can infer about certain phenomena. One of the important things in this regard is the settling down of the estimator. The most significant information is about the steady-state errors, which remains the same if the estimator is used either in open or closed-loop. The analysis done in chapter 2 on the steady state errors can be verified in the simulation of an open-loop observer with much more convenience.

We will consider three sources of error in the operation of the machine. These are due to the approximation of the integrator with a filter and uncertainties in stator and rotor resistances. Stator flux estimation is independent of the last one. The stator flux estimator is also affected by low frequency disturbances. However, due to lack of information of the exact waveform of the disturbance we cannot have a simulation setup that will give an idea as to how the actual physical system will behave.

The estimates are given in the left column of a figure with the corresponding errors in the right column. We give two graphs in each plot corresponding to two different uncertainties in the same parameter. The estimator performance is dependent on the speed of the machine. All the results would be given separately for high ($\omega_s = 100 \, \mathrm{rads/s}$) and low ($\omega_s = 10 \, \mathrm{rads/s}$) speeds. We start off with the integrator approximated by a filter.

3.3.1. Integrator Approximation

We had considered first and second-order filter approximations of the integrator in section 2.2. The only difference between the two is the ability of the second-order filter to attenuate disturbances. Since we are not simulating disturbances, it is sufficient to restrict ourselves to the first-order filter given in equation (2.32). Our primary objective is to study the effect of the bandwidth of the filter on the accuracy of the estimated stator flux and the ability of the estimator to overcome false initial conditions or transient offsets. We investigate two different cases with $\omega_s/\omega_c=10$ and $\omega_s/\omega_c=100$, where the former is represented by the solid line and the later by dashed line. Here ω_s is the supply frequency and ω_c is the cutoff frequency of the filter that is approximating the integrator. We assume exact knowledge of the machine model. The results are given in figures 3-11 to 3-14.

Observations

The filter with larger bandwidth has faster settling time but larger steady state error as compared to the one with smaller bandwidth. The errors in i_{ms} and i_{sd} are small in all cases as predicted by equations (2.61) and (2.67). However the error in i_{sq} is much larger. In fact for low speed operation, i_{sq} and i_{sq} have different signs and we have a situation similar to the one depicted in the worst-case scenario of figure 2-4.

The error in speed estimate as given in equation (2.92), depends on certain other quantities. The plots include all the relevant details.

The results obtained through simulations verify the derivations done in chapter 2.

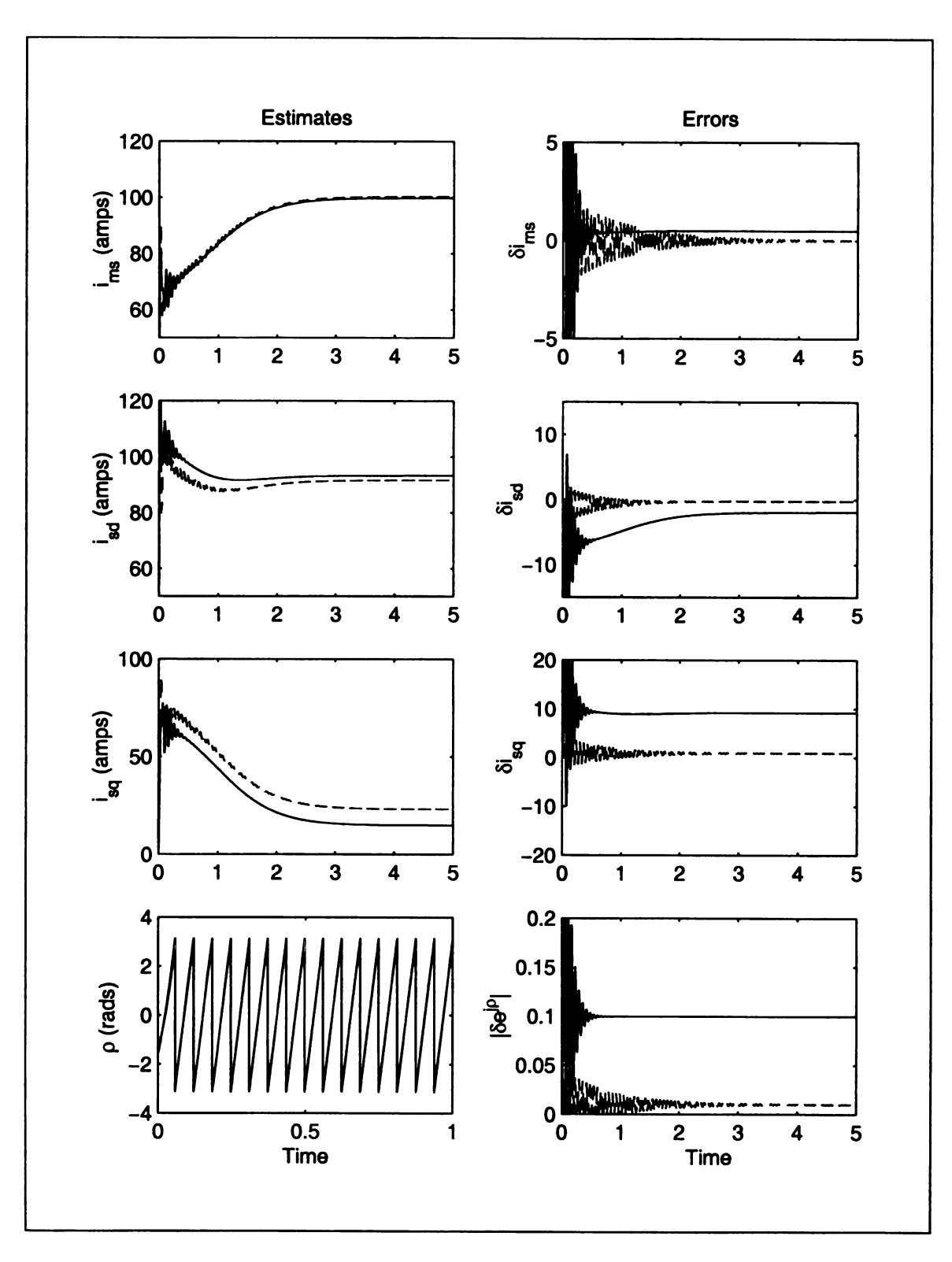


Figure 3-11. Errors due to integrator approximation at high speeds (Part I)

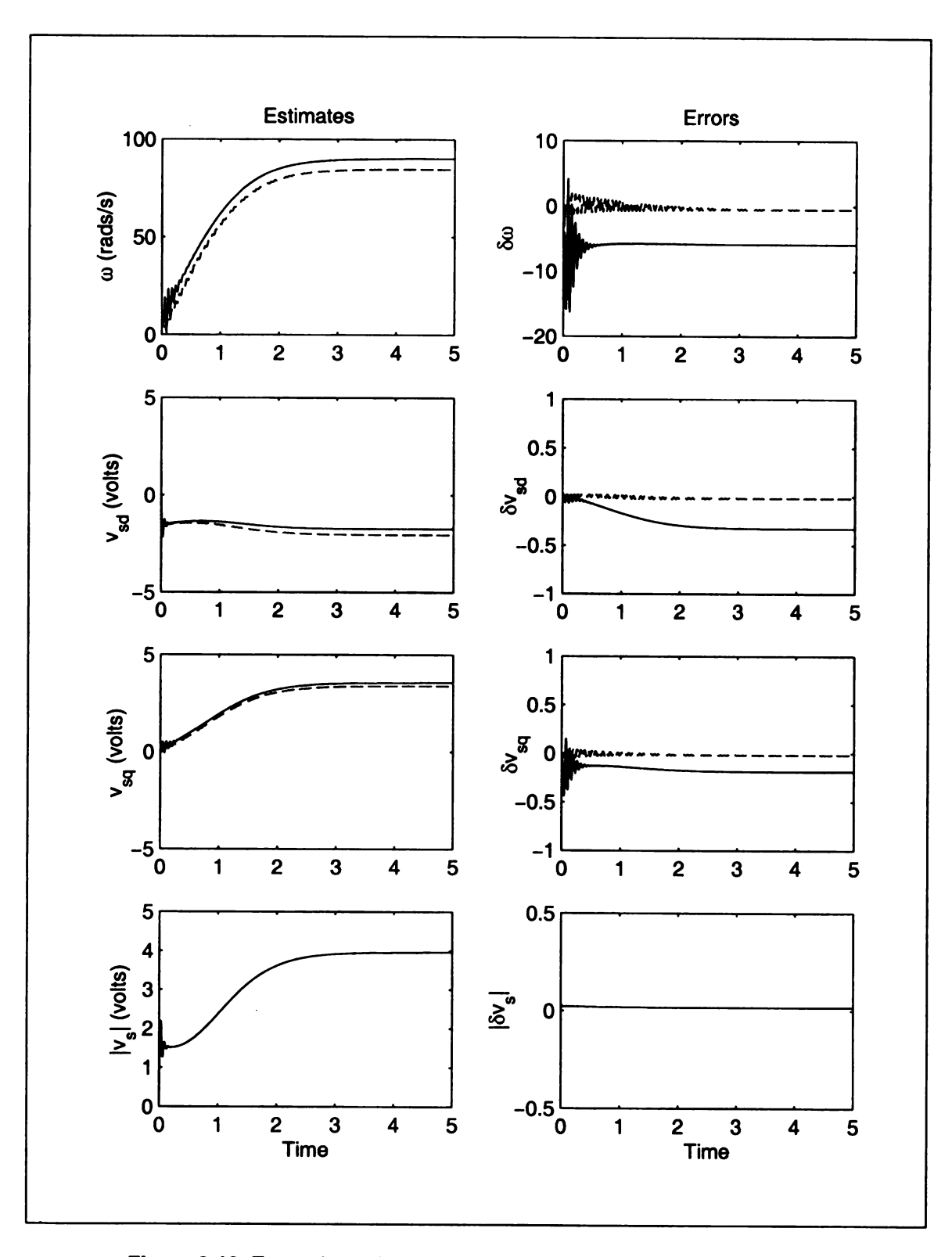


Figure 3-12. Errors due to integrator approximation at high speeds (Part II)

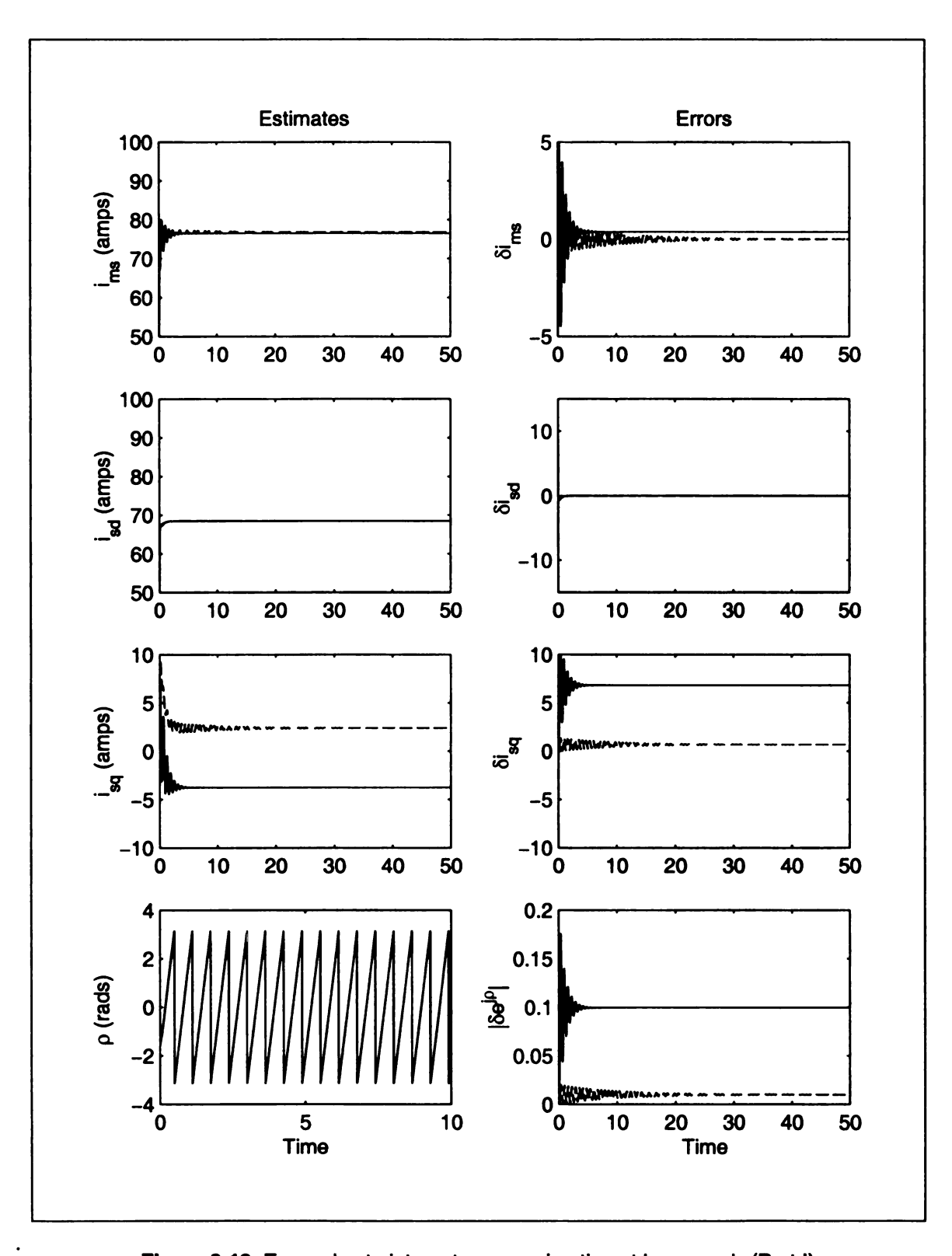


Figure 3-13. Errors due to integrator approximation at low speeds (Part I)

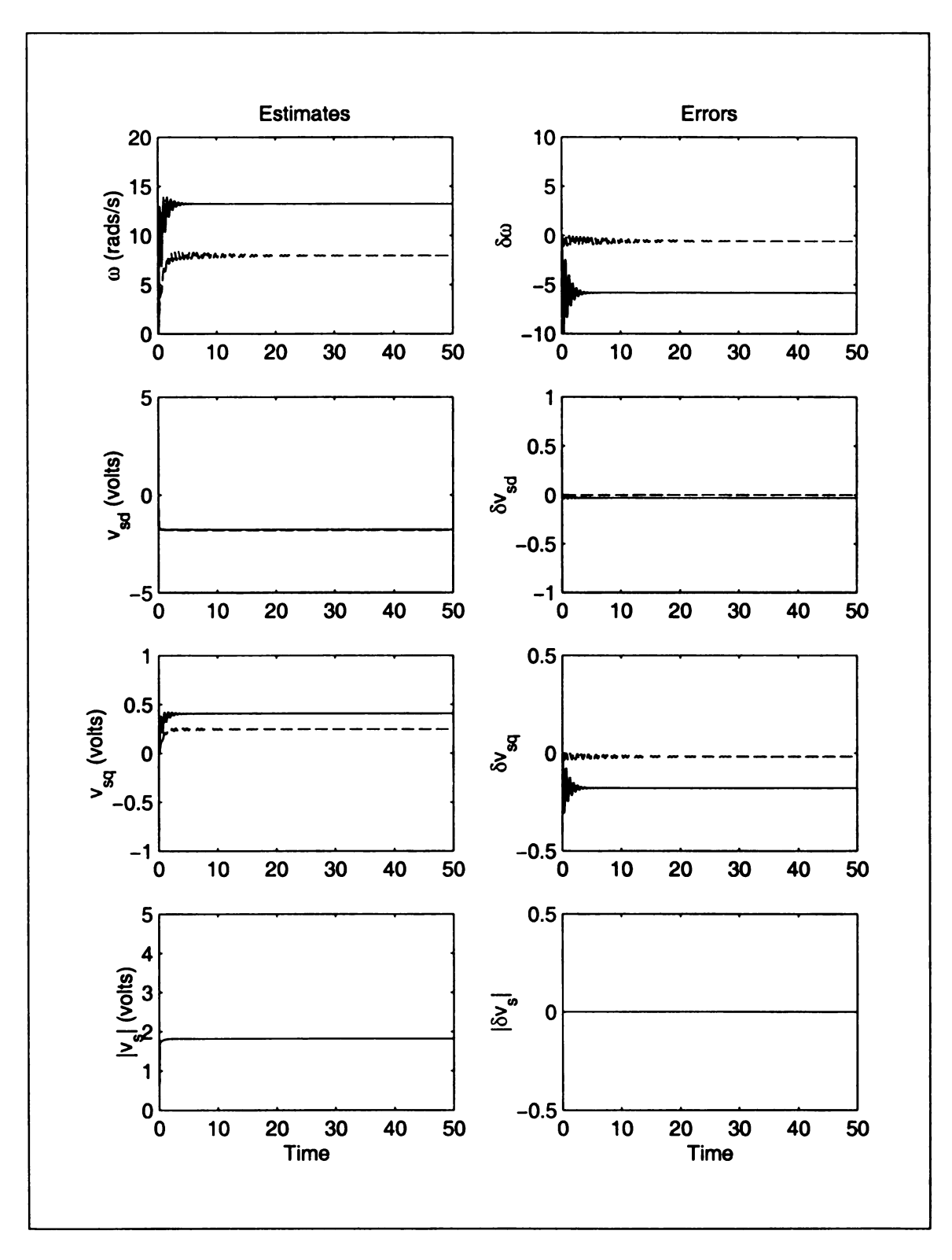


Figure 3-14. Errors due to integrator approximation at low speeds (Part II)

3.3.2. Uncertainty in Stator and Rotor Resistances

The stator resistance turns out to be an important parameter for stator based estimators. To investigate the errors in the flux and speed estimators due to uncertainty in stator or rotor resistances, we have to incorporate some approximation of the pure integrators or otherwise we will face the problem of transient offsets. In the previous section we have seen that the ratio $\omega_s/\omega_c=100$ causes small steady state errors but requires a longer settling time. We will simulate the estimator with this ratio and study the effect of uncertainty in stator and rotor resistances. We consider two cases for stator resistance with $R_{so}=1.1R_s$ and $R_{so}=1.2R_s$ and two cases for rotor resistance with $R_{ro}=1.25R_r$. The results are given in figures 3-15 through 3-20.

Observations

The errors in i_{ms} and i_{sd} are small but more pronounced as compared to the case with exact knowledge of stator and rotor resistances. The error in i_{sq} is even larger. The steady state errors are consistent with equations (2.61), (2.67) and (2.92). The results obtained through simulations verify the derivations done in chapter 2.

Since the flux estimator is independent of the rotor resistance, we do not give the results for flux errors due to uncertainty in rotor resistance.

One important observation is the dynamical behavior of the estimator, which now exhibits an overshoot before settling down to some steady state. This phenomenon could lead to instability of the closed loop system.

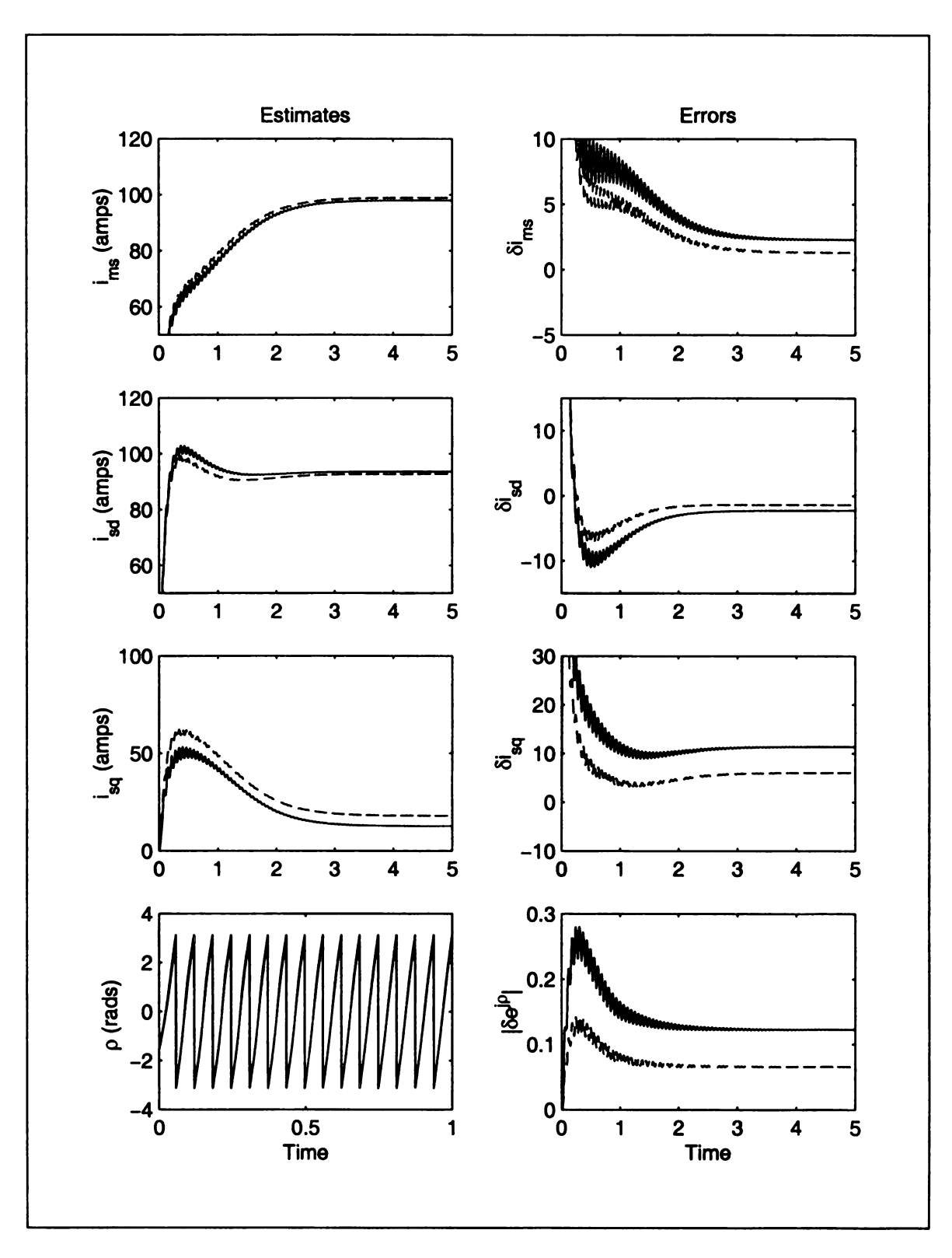


Figure 3-15. Errors due to integrator approximation and uncertainty in stator resistance at high speeds (Part I)

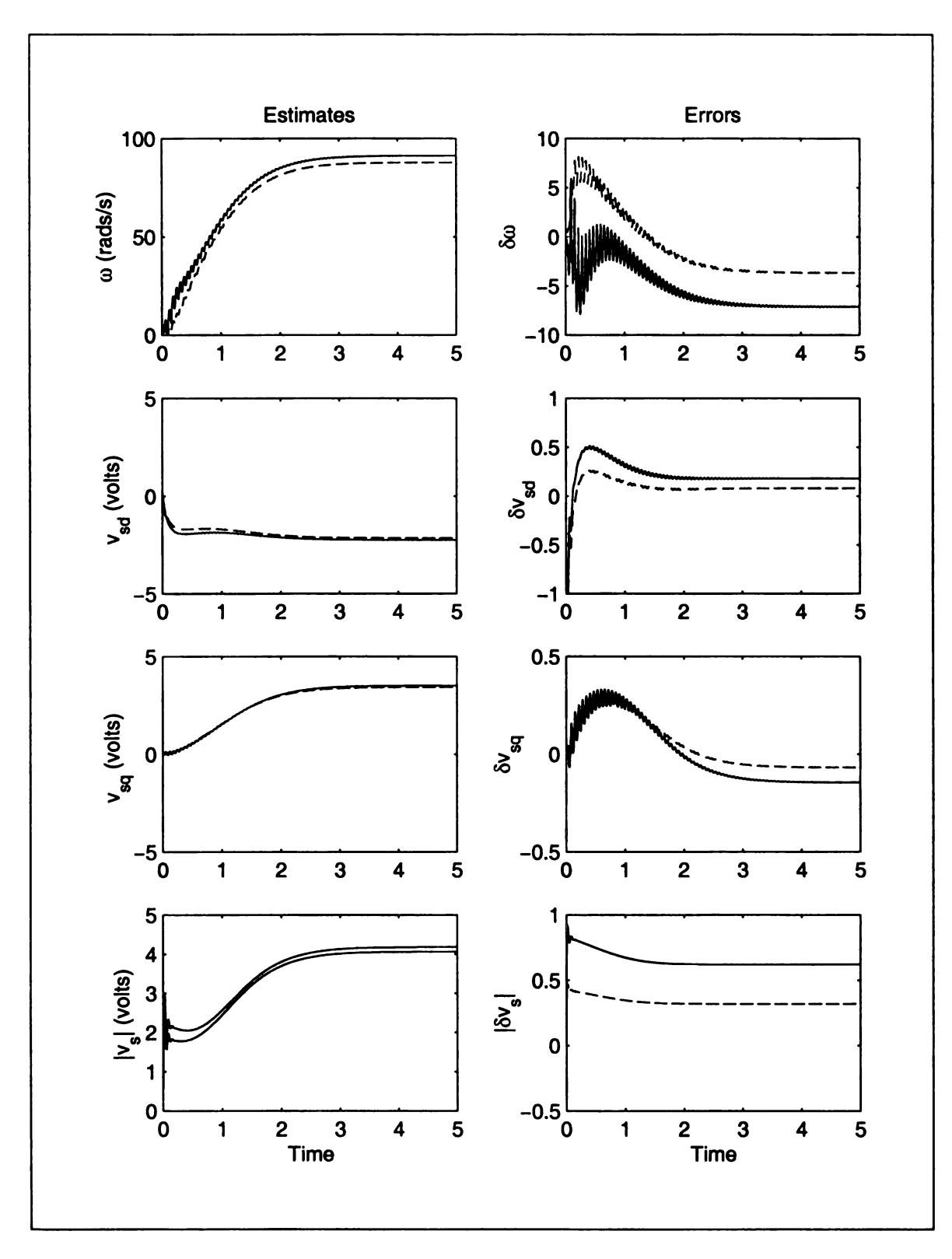


Figure 3-16. Errors due to integrator approximation and uncertainty in stator resistance at high speeds (Part II)

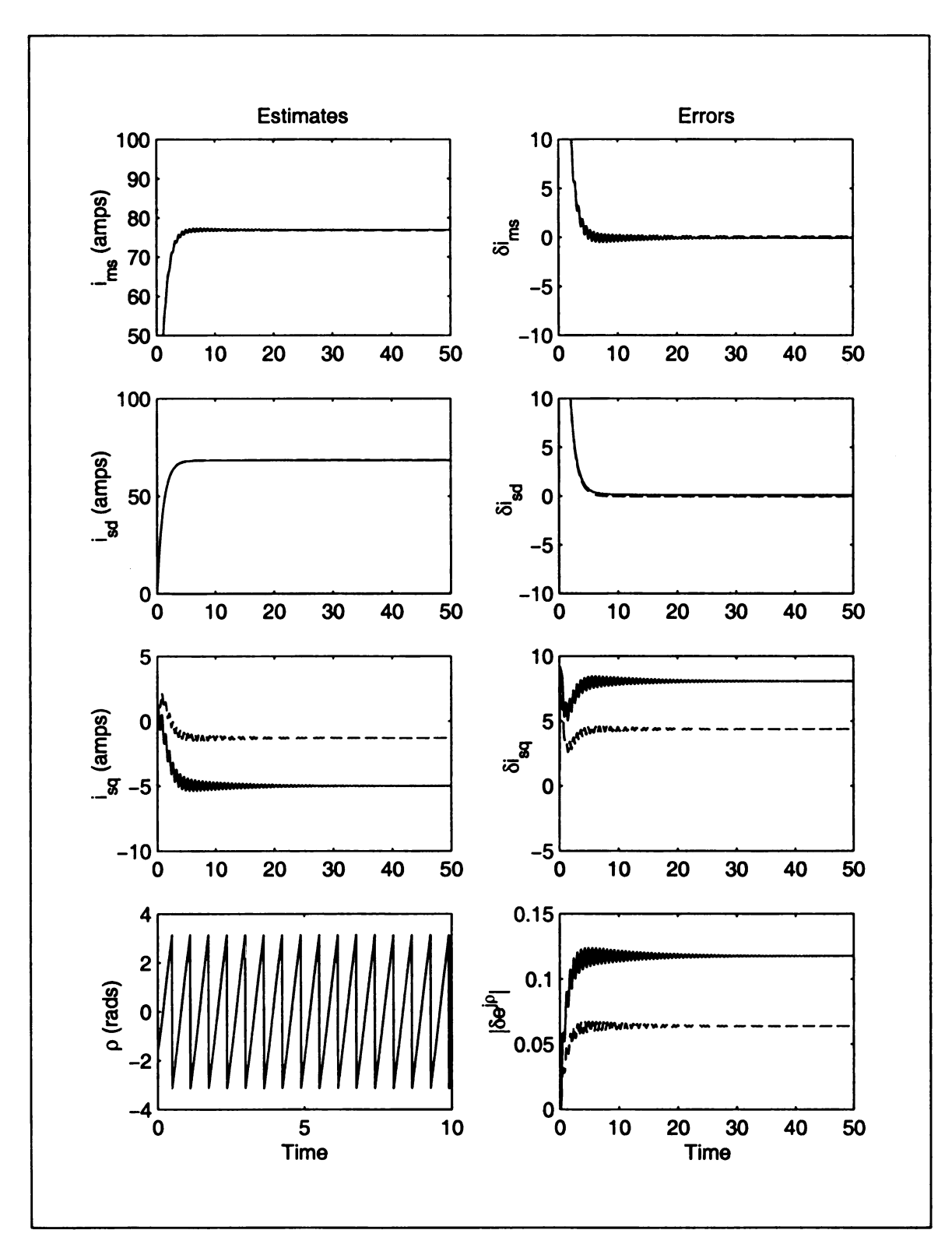


Figure 3-17. Errors due to integrator approximation and uncertainty in stator resistance at low speeds (Part I)

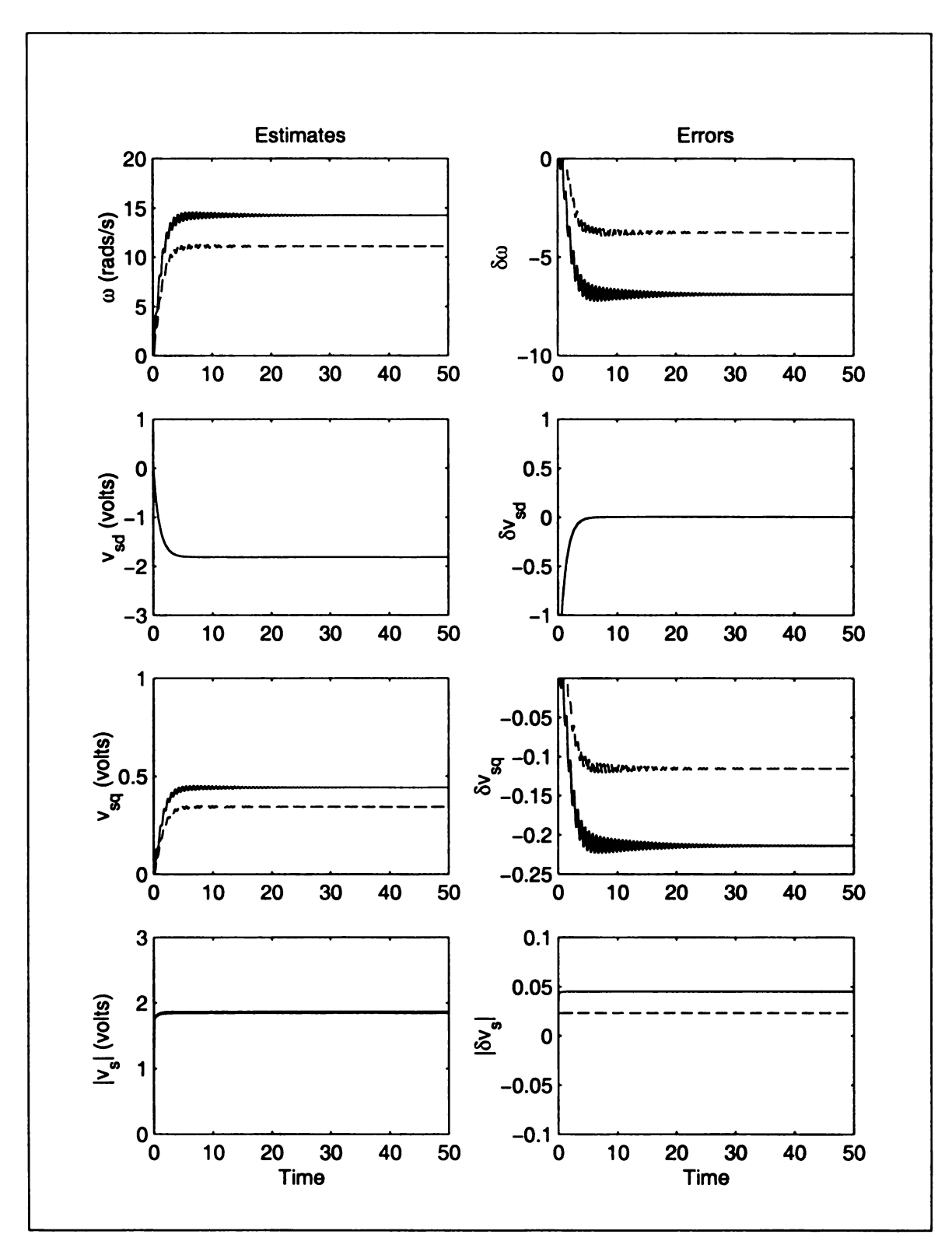


Figure 3-18. Errors due to integrator approximation and uncertainty in stator resistance at low speeds (Part II)

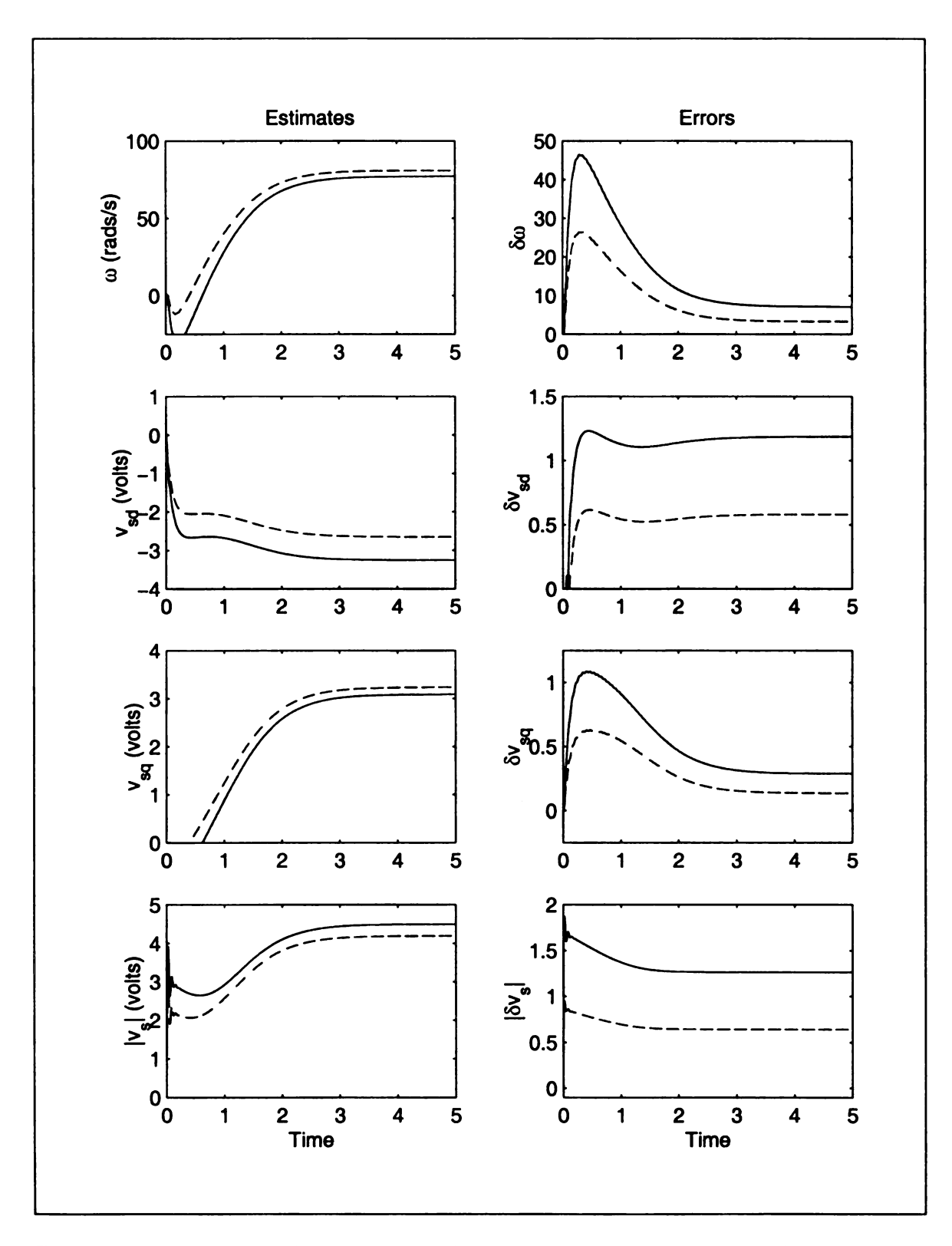


Figure 3-19. Errors due to integrator approximation and uncertainty in rotor resistance at high speeds

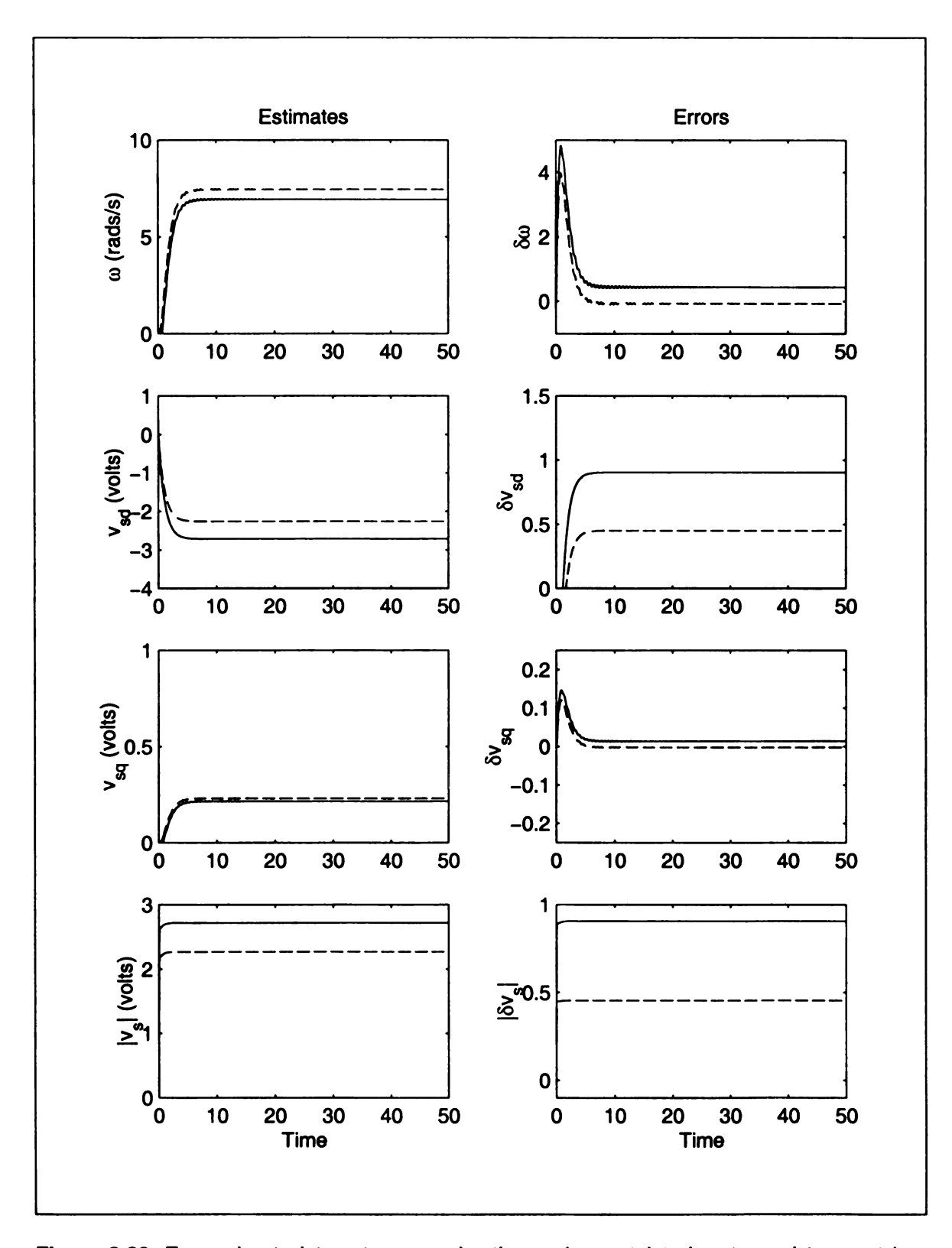


Figure 3-20. Errors due to integrator approximation and uncertainty in rotor resistance at low speeds

3.4. Closed Loop System with Feedback from Measured Speed

Now we turn our attention to the speed control of the induction machine using measured speed in the feedback loop. The block diagram is given in figure 2-5. We start with a simulation of the system under ideal conditions; there are no uncertainties or sources of errors. This simulation would serve as a standard for other cases. Since our ultimate goal is the encoderless control of the induction machine, we will give the plots for speed estimator even though it is not being used in the control loop. This will help us have some visualization of the performance of speed estimator.

The inability of the flux estimator to work at zero speed makes it necessary that the flux and speed commands be given simultaneously or within some maximum time. This is somewhat different from the rotor-based schemes where the flux command precedes the speed command. The main issues that would be demonstrated in this section would be the ability of the control system to achieve

- Starting
- Tracking of the speed reference
- Speed reversal
- Ability to handle changes in load torque

The load torque comes from both frictional losses and active loads. Whereas i_{ms} and ω are the quantities we want to control, i_{sd} and i_{sq} are fundamental to field orientated control. The plots for u_{sd} and u_{sq} are important as they serve as the control effort. We also give plots for \hat{i}_{sq} because of the large errors in it. The results are illustrated in figure 3-21.

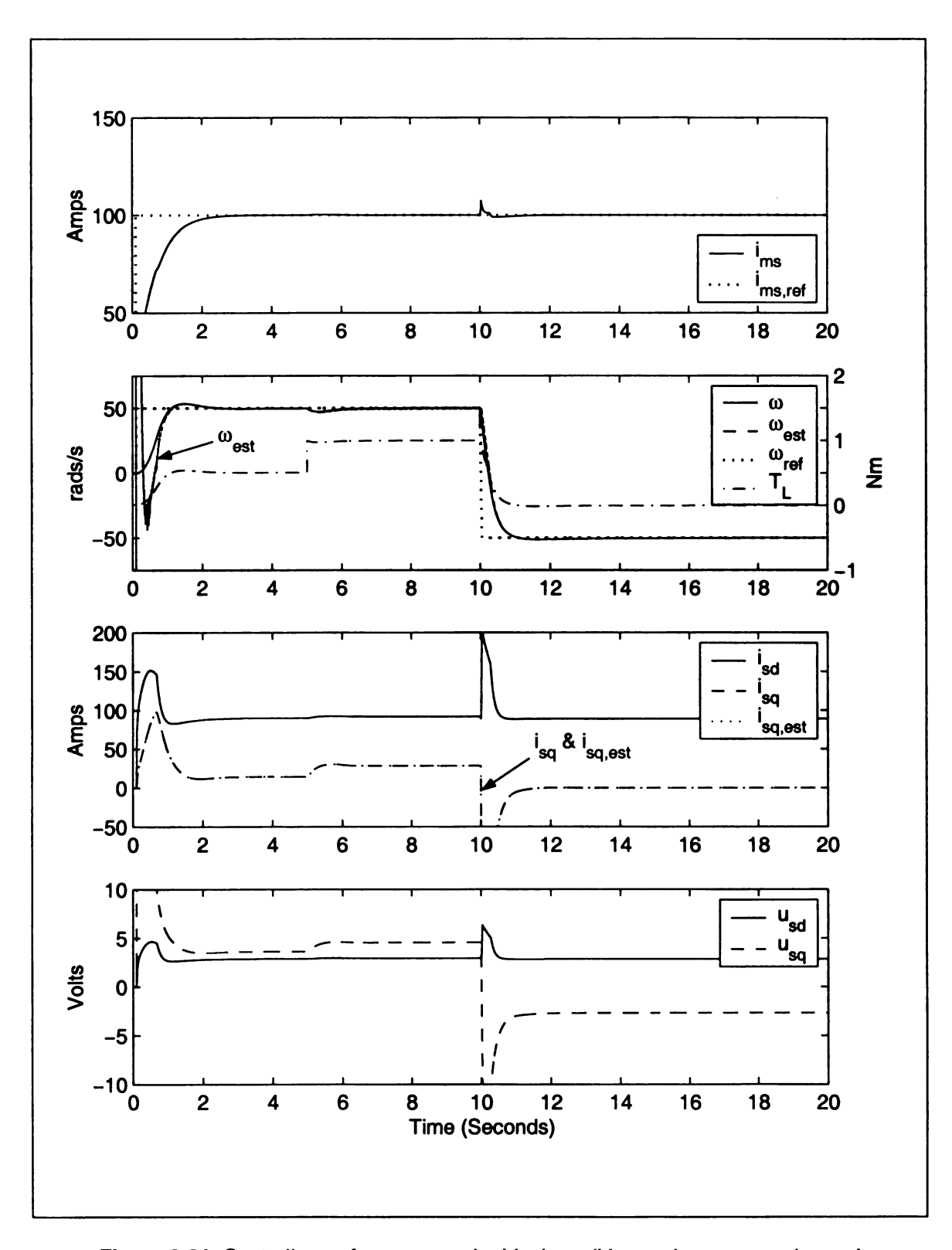


Figure 3-21. Controller performance under ideal conditions using measured speed

3.4.1. Controller Performance in Presence of Errors

The actual task and challenge to design a controller is its ability to work in an acceptable manner in the presence of disturbances and uncertainties. In this regard we study different cases. The following family of plots gives a good idea of the ability of the controller to handle errors and uncertainties.

The reference speed is tracked in almost a perfect manner. The dynamic performance of the controller however, does not remain the same as compared to the ideal case. The tracking of current components experiences errors corresponding to errors in the estimates. If the resistances are perturbed too much the control scheme breaks down. We have tried to capture the effects when the scheme is working but has started to exhibit symptoms of instability.

The results are illustrated in figures 3-22 through 3-25. The last figure combines all the sources of errors.

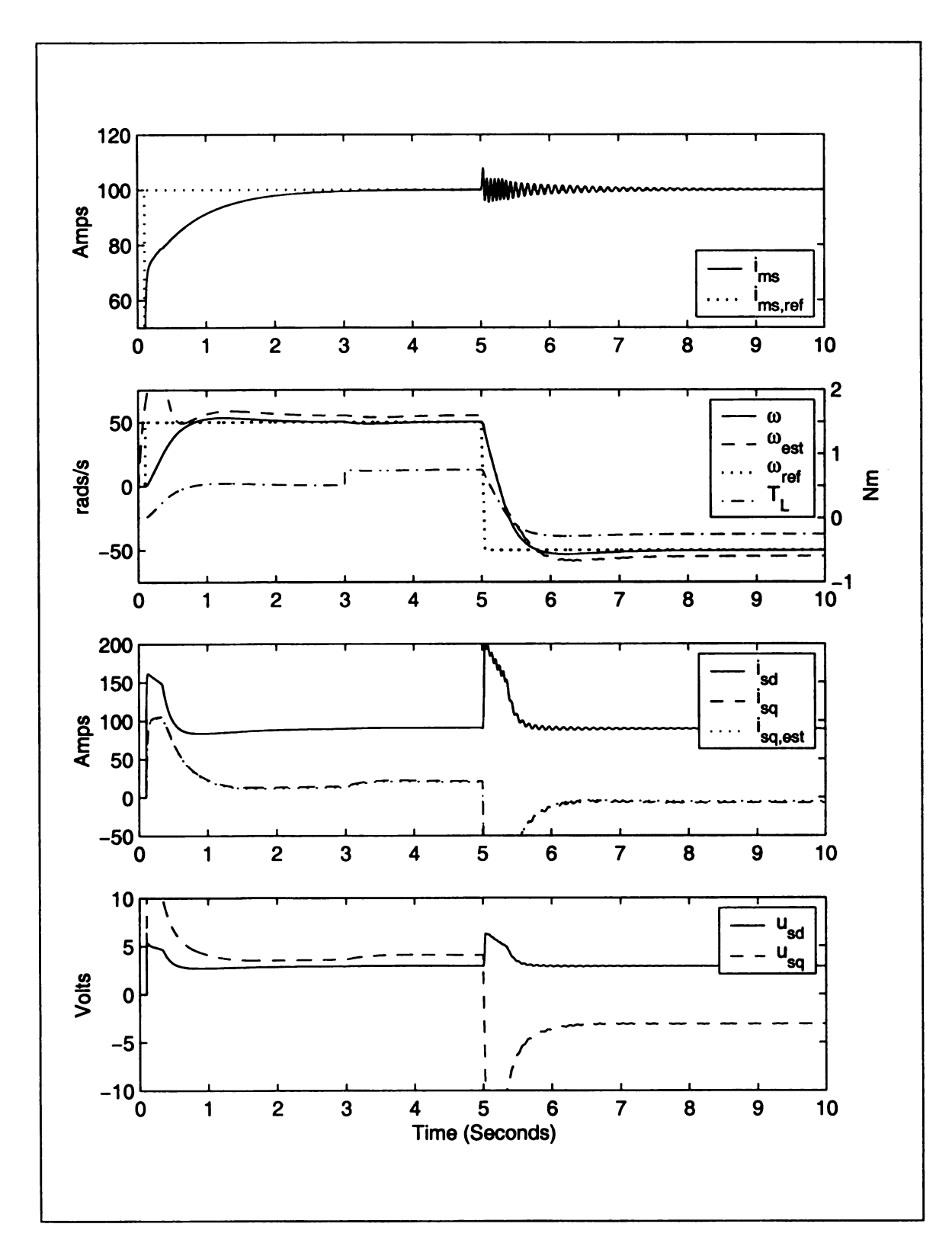


Figure 3-22. Controller performance with integrator approximation ($\omega_c=1\,\mathrm{rads/s}$) using measured speed

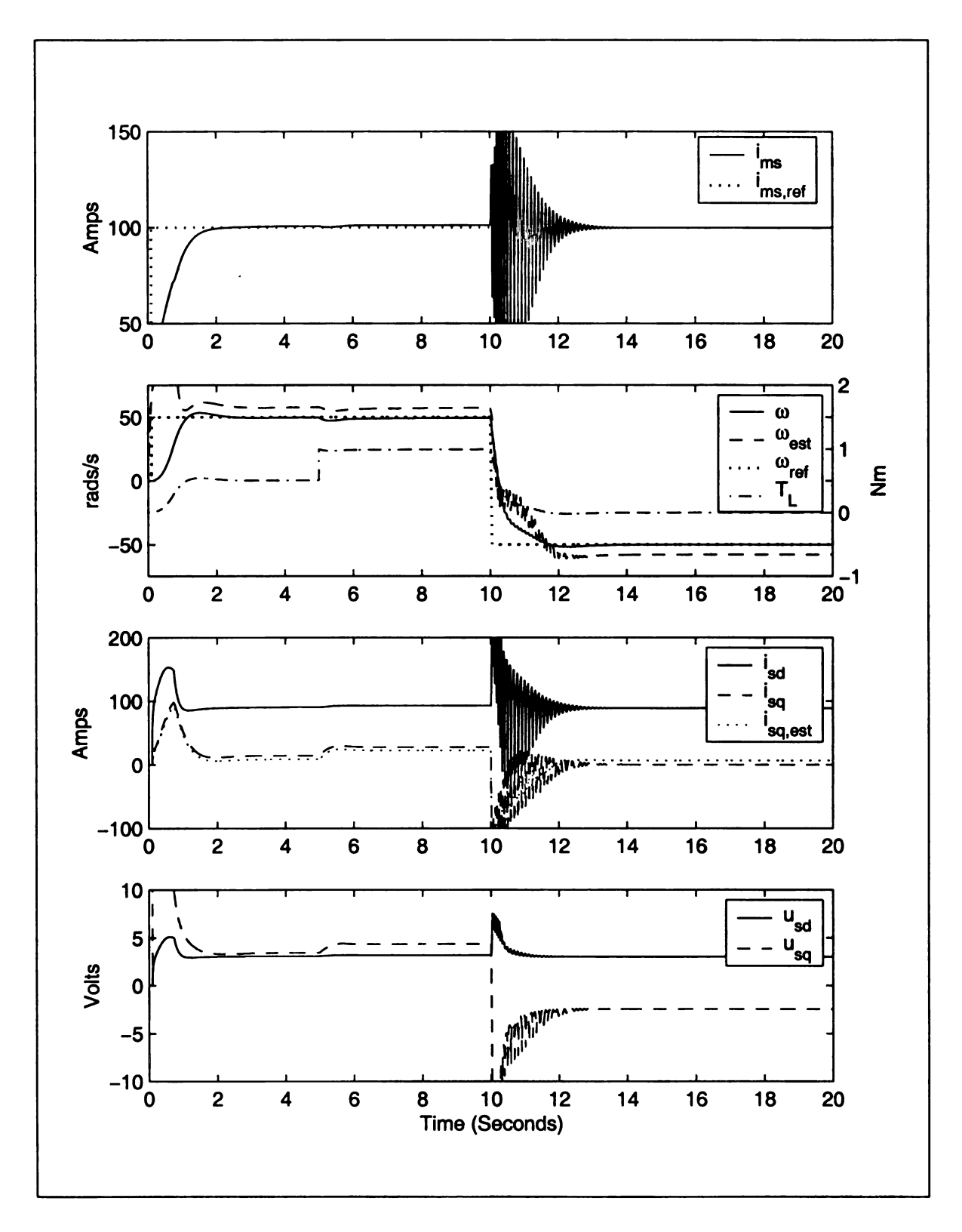


Figure 3-23. Controller performance with integrator approximation ($\omega_c = 1 \text{ rads/s}$) and $R_{so} = 1.05R_s$ as an uncertainty using measured speed.

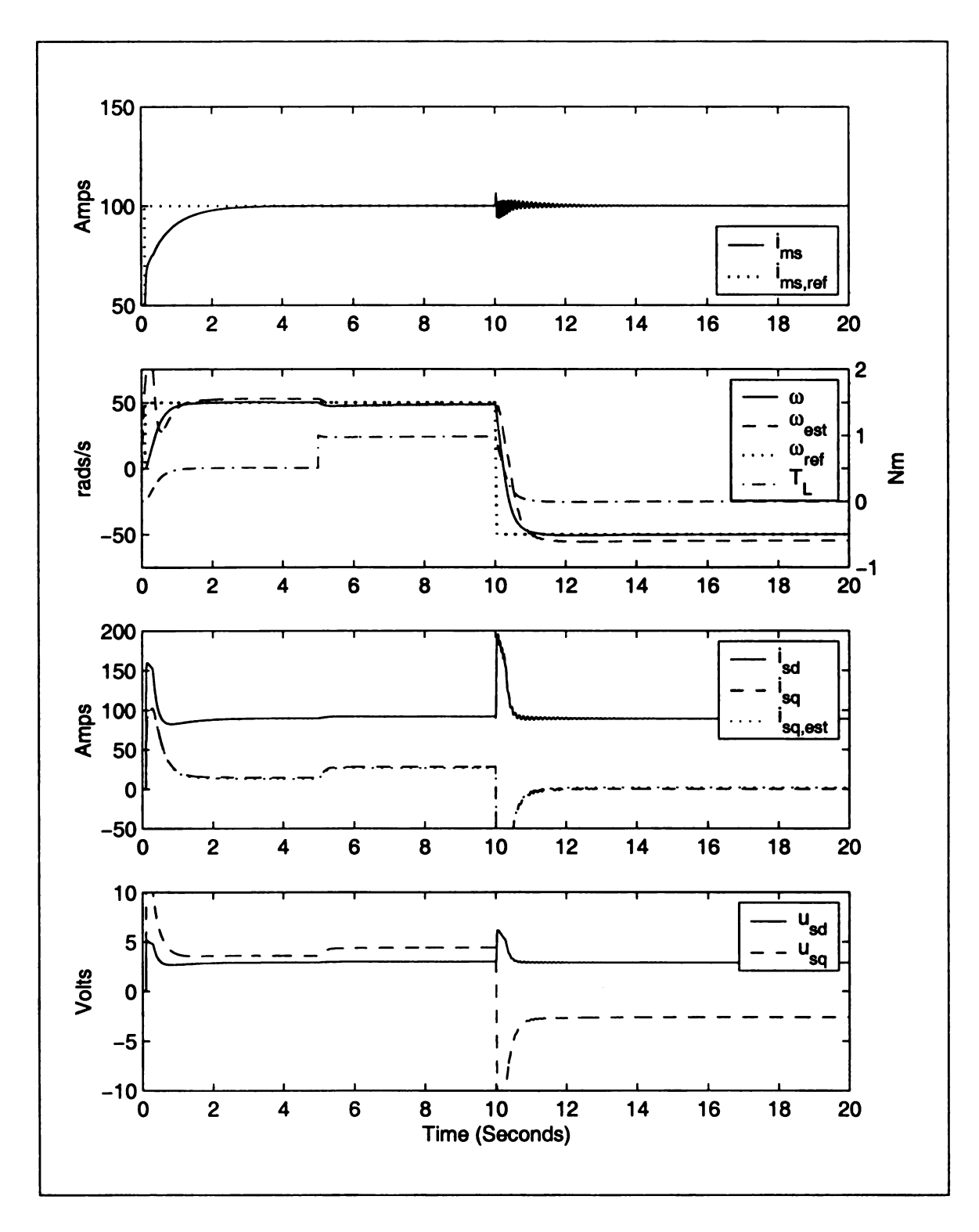


Figure 3-24. Controller performance with integrator approximation ($\omega_c = 1 \, \mathrm{rads/s}$) and $R_{ro} = 1.25 R_r$ as an uncertainty using measured speed.

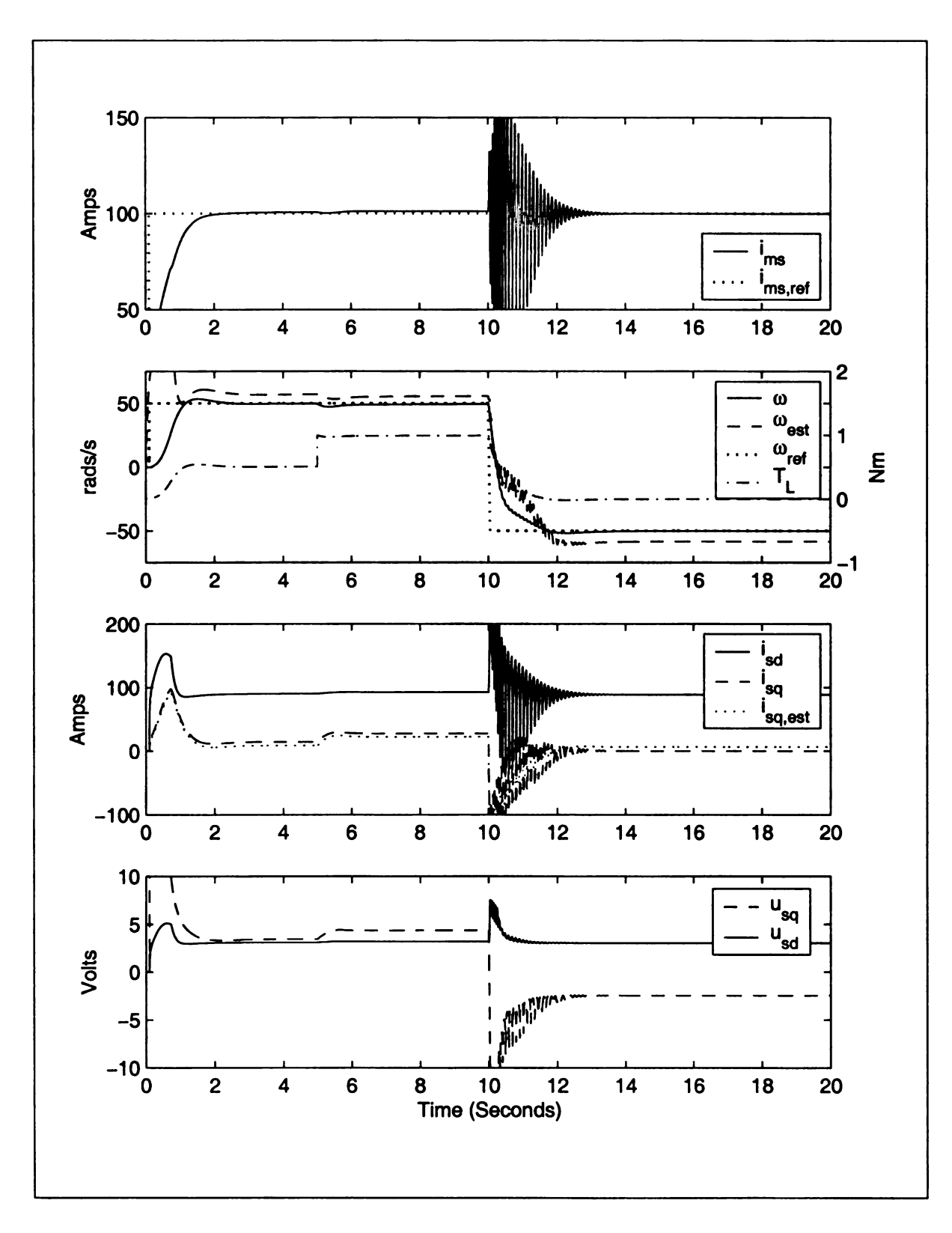


Figure 3-25. Controller performance with integrator approximation ($\omega_c=1 \, {\rm rads/s}$), $R_{so}=1.05 R_s$ and $R_{ro}=1.1 R_r$ as uncertainties using measured speed.

3.4.2. Operation at different speeds and loads

We study the operation of the system at various loads and speeds. In the first case we keep the active component of the load constant and vary the speed. The reference speed starts off with some high value and then reduces to low speed with a staircase waveform. The change in load torque is due to frictional losses. It is easily observed that the controller is working well for different speeds and the step changes in the speed reference is not a problem. The magnetizing current is maintained at the desired level except for minor transients during the speed steps.

In the other case the reference speed is kept constant and the active component of the load torque is changed. The speed tracking is once again achieved whilst maintaining the required magnetizing current.

One important observation in this regard is the change in i_{sd} with load torque.

This is caused by the decoupler and is required due to the coupled nature of the direct and quadrature currents in the stator frame of reference.

The results are illustrated in figures 3-26 and 3-27.

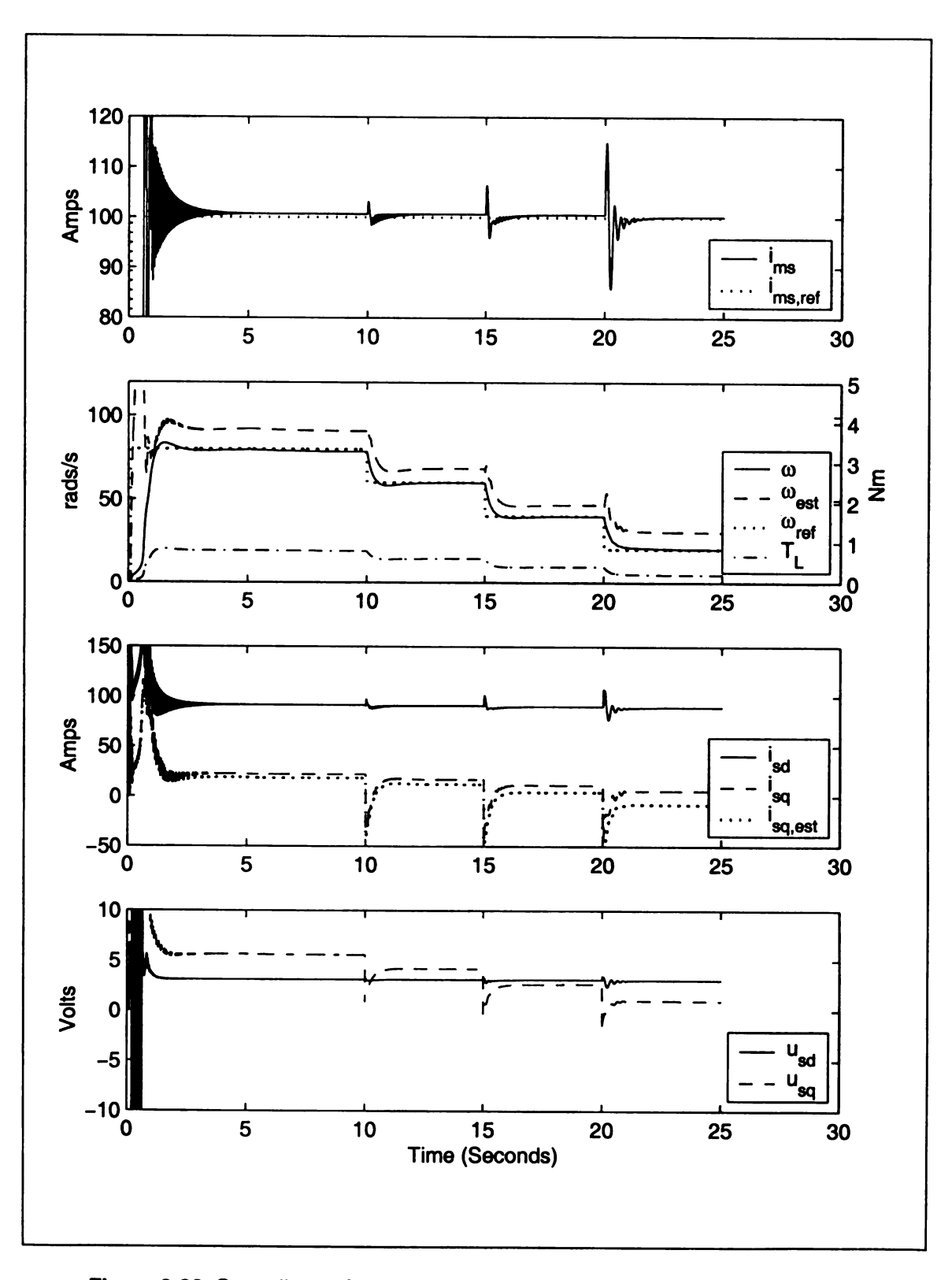


Figure 3-26. Controller performance at various speeds using speed measurements

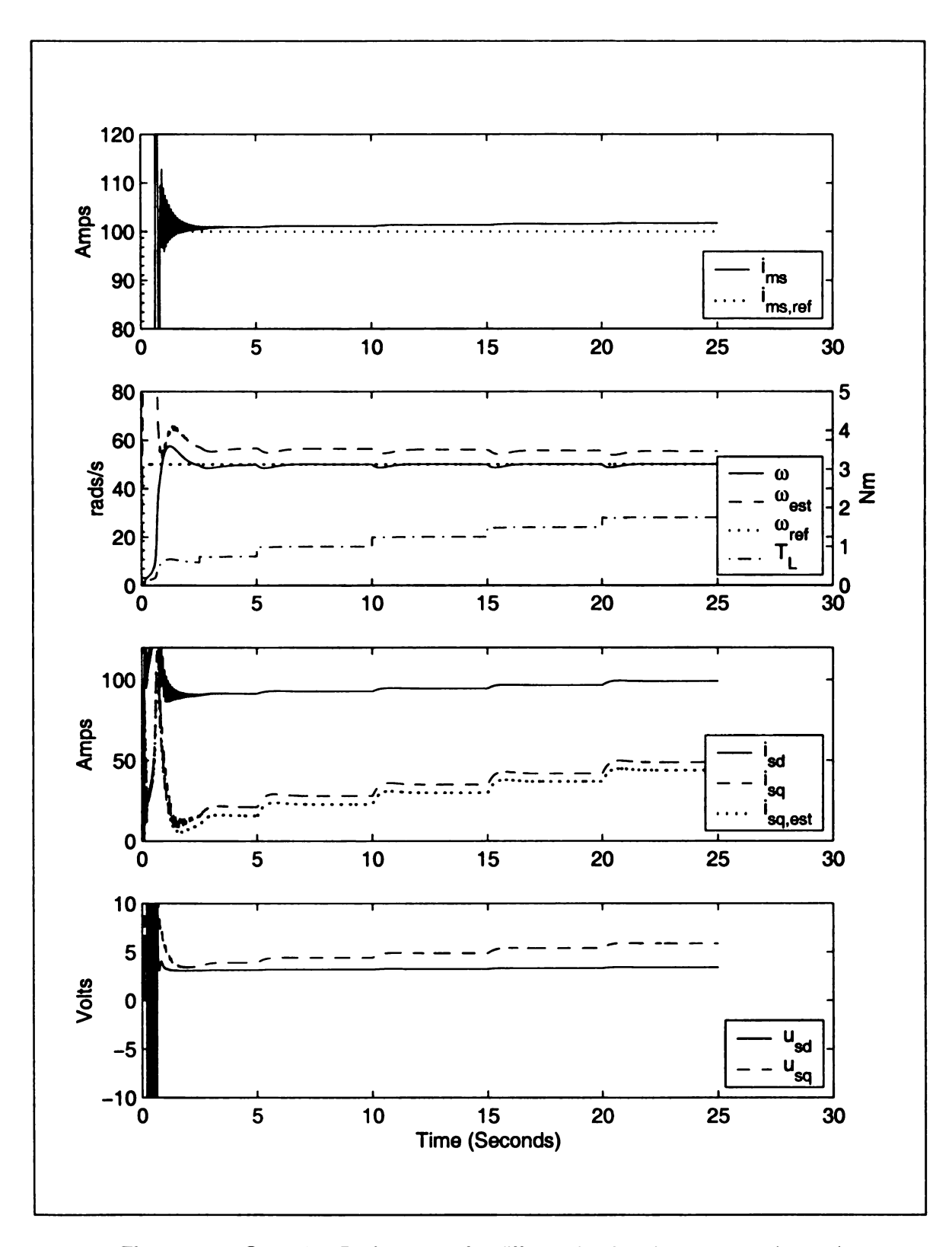


Figure 3-27. Controller Performance for different loads using measured speed

3.4.3. The Role of Decoupler

We had developed a decoupling scheme in Section 2.3.3 and used it throughout the simulations of the closed-loop system. One may be tempted to use techniques with high gain to overcome the problem of interdependence of i_{ms} and i_{sq} . It turns out that these techniques can provide a different solution than direct decoupler but at the cost of much higher control effort. The closed-loop system is simulated without the decoupler and with higher gains for the speed and flux controllers. Other than this, the system is working under ideal conditions without any errors and uncertainties.

The transient response of the system is much inferior to the case in which a decoupler is present. The settling time is longer and the flux build up is affected a lot in the region where the machine is accelerating to reach the desired value. The currents that flow during the transient period are large. The same is true with the voltages that have to be applied in order to achieve the desired results. Performance would have been worse if we had saturated the terminal voltages to ± 10 volts.

As a final comment, high gain techniques are suitable for cases where we want to overcome some uncertainty. However, if we have complete or even partial knowledge of the uncertainty, it would be better to use this information. This is exactly what the decoupler is doing. Though the decoupler is based on estimated quantities but we have seen in many simulations that it is working well even in presence of errors and uncertainties.

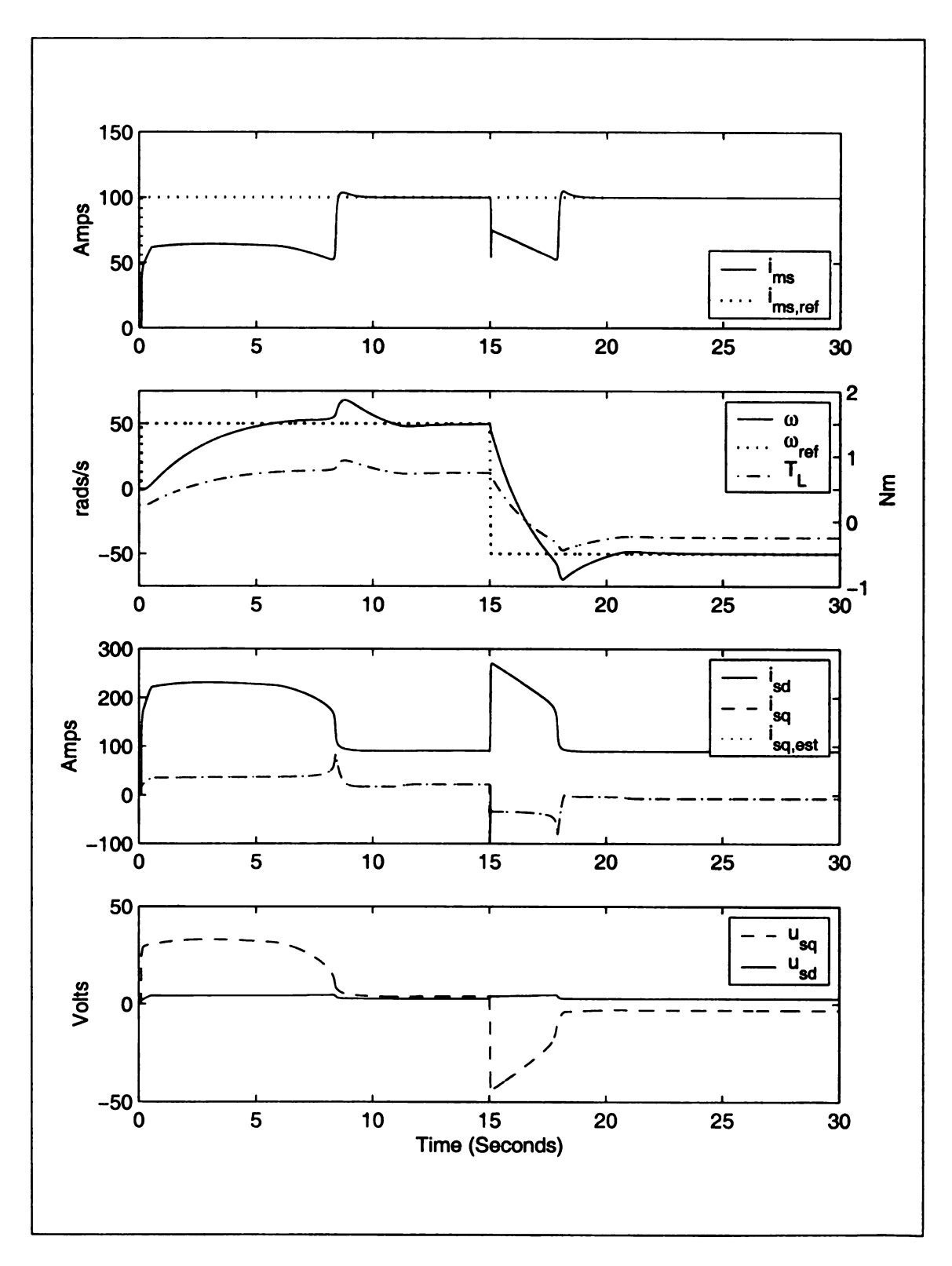


Figure 3-28. Controller performance without a decoupler

3.5. Closed Loop System with Feedback from Estimated Speed

In this section we would replace the measured speed in the feedback loop with its estimate. The scheme is illustrated in figure 2-5. It is natural to think that we may loose the accuracy in tracking the speed reference. The goal in this section would be to investigate the associated errors and effects. However, the dynamic performance of the controller with feedback from the estimated speed should be acceptable.

Once again we start with the simulation of the system under ideal circumstances with no errors and uncertainties. For this idealization, the two schemes are almost identical.

An important observation is the behavior of the estimator itself. There is an improvement in the dynamical behavior specially at the starting of the machine.

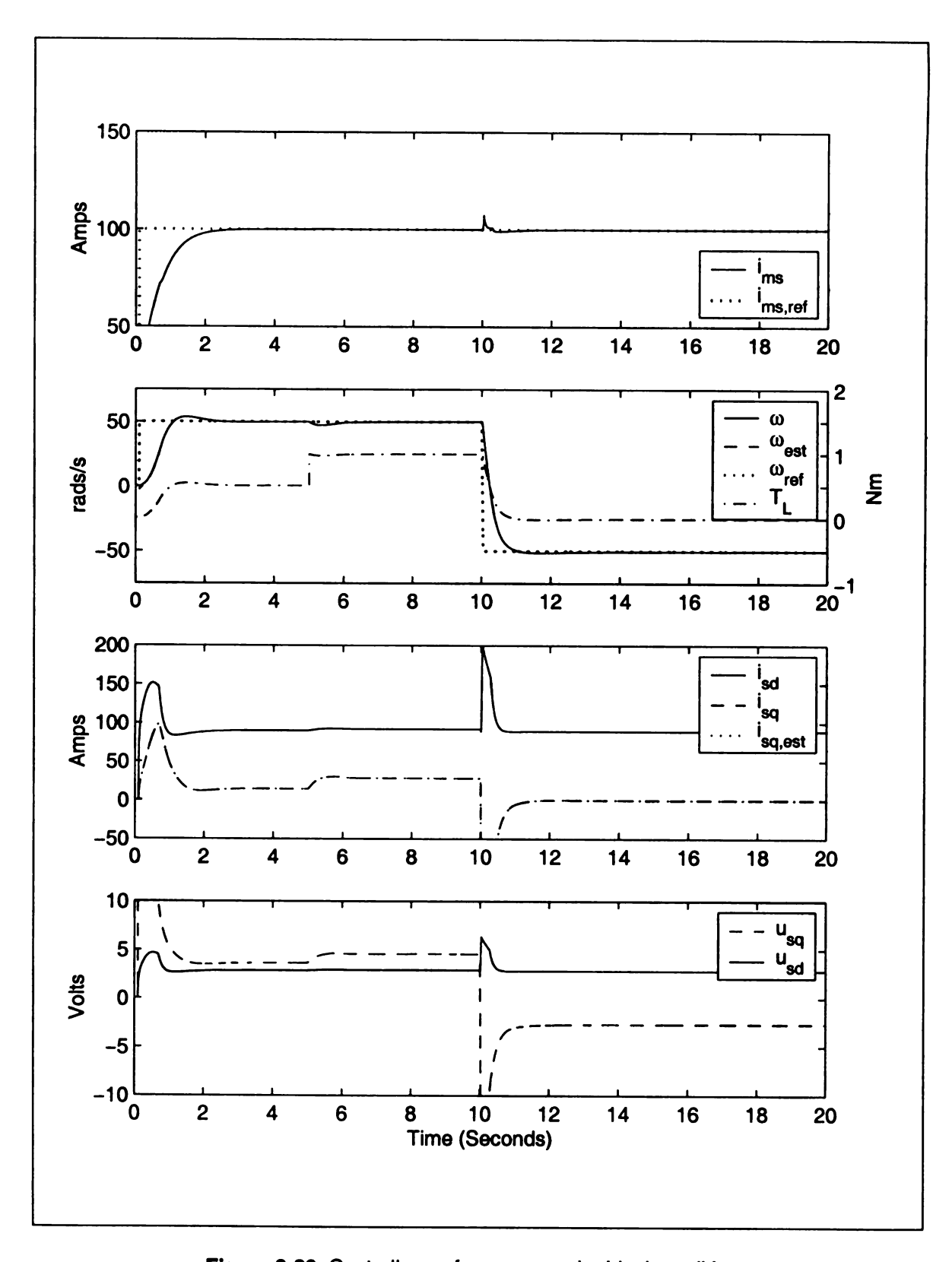


Figure 3-29. Controller performance under ideal conditions

3.5.1. Controller Performance in Presence of Errors

We are basically controlling the speed of induction machine. When the measured speed was used in the feedback loop, we could literally eliminate any steady state errors in the speed from the desired. That problem was basically the stability and robustness of the system in presence of errors. The situation in which measured speed is replaced by its estimate is however different. The accuracy and dynamics of the estimator depend on certain other factors. We have already discussed these issues at length.

Four sources of error are considered in the following simulations. These are the error in flux estimation due to integrator approximation, uncertainty in stator and rotor resistances and the influence of high-gain observer. It is more illustrative to consider one problem at a time. However, we would keep the integrator approximation in most of the cases to be as close as possible to the physical situation in which it is not possible to have a pure integrator. The results are illustrated in figures 3-30 through 3-34.

Observations

The control scheme is able to achieve its objective of encoderless control. As predicted by the analysis done in chapter 2, the actual speed settles down with a steady-state error in it. The stator resistance is seen to be the most sensitive of all parameters. On the other hand rotor resistance and high-gain observers have minimal effect on both the dynamic performance as well as the steady-state errors. Figure 3-34 combines all the effects. In this situation, the dynamic performance is worse than other cases and the steady state error is the largest.

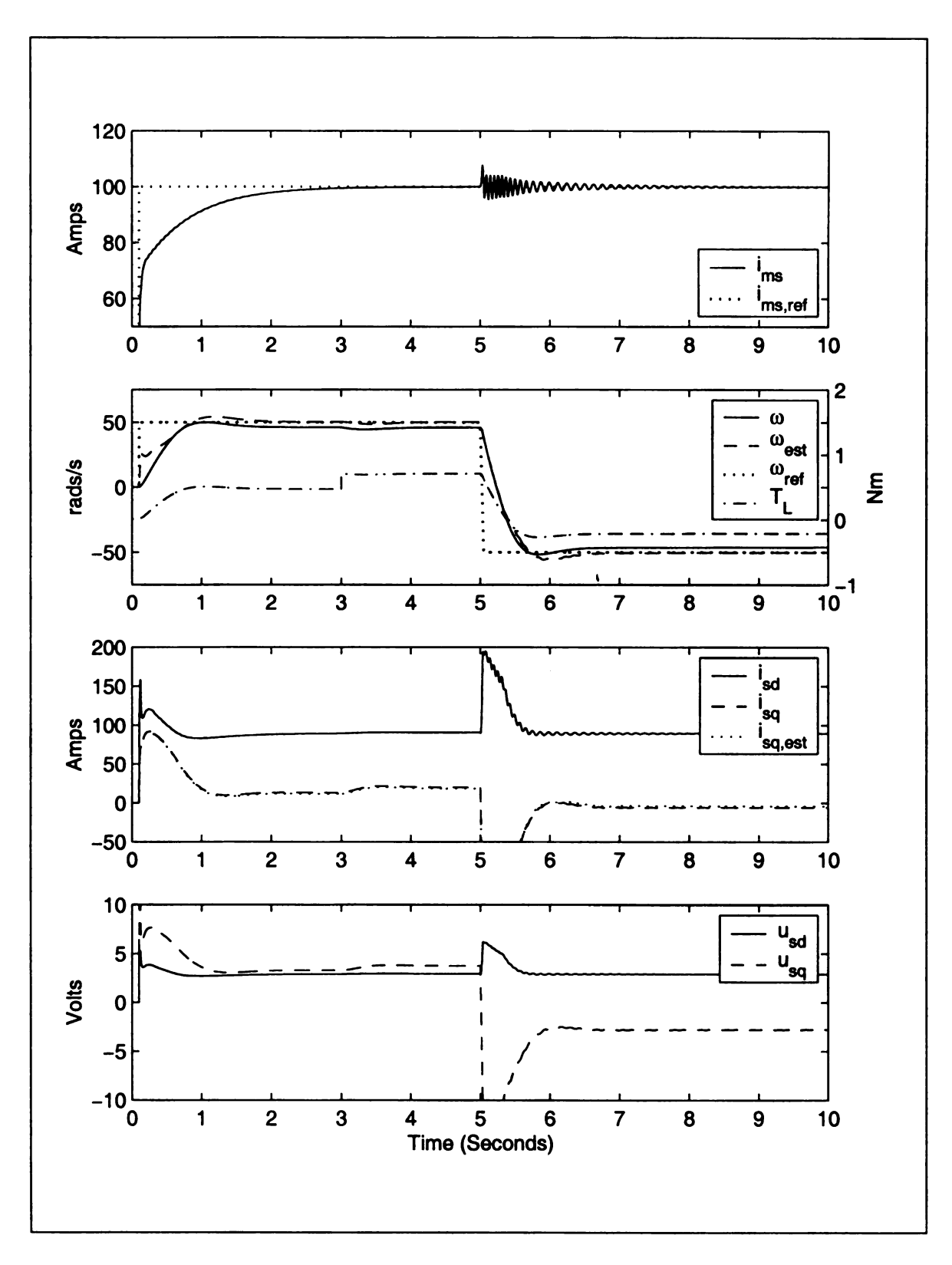


Figure 3-30. Controller performance with integrator approximation ($\omega_c=1~{
m rads/s}$)

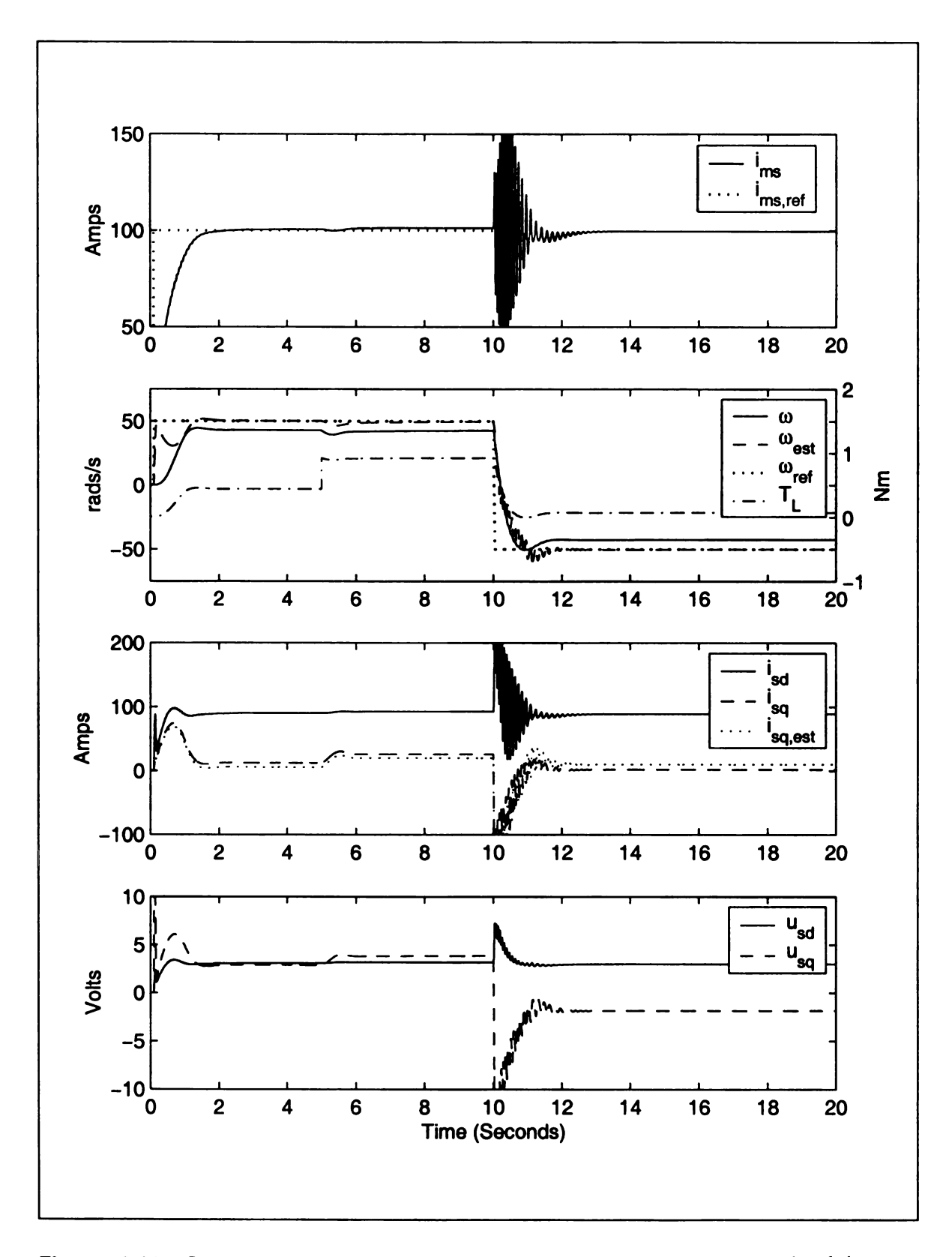


Figure 3-31. Controller performance with integrator approximation ($\omega_c=1 \, {\rm rads/s}$) and $R_{so}=1.05 R_s$ as an uncertainty

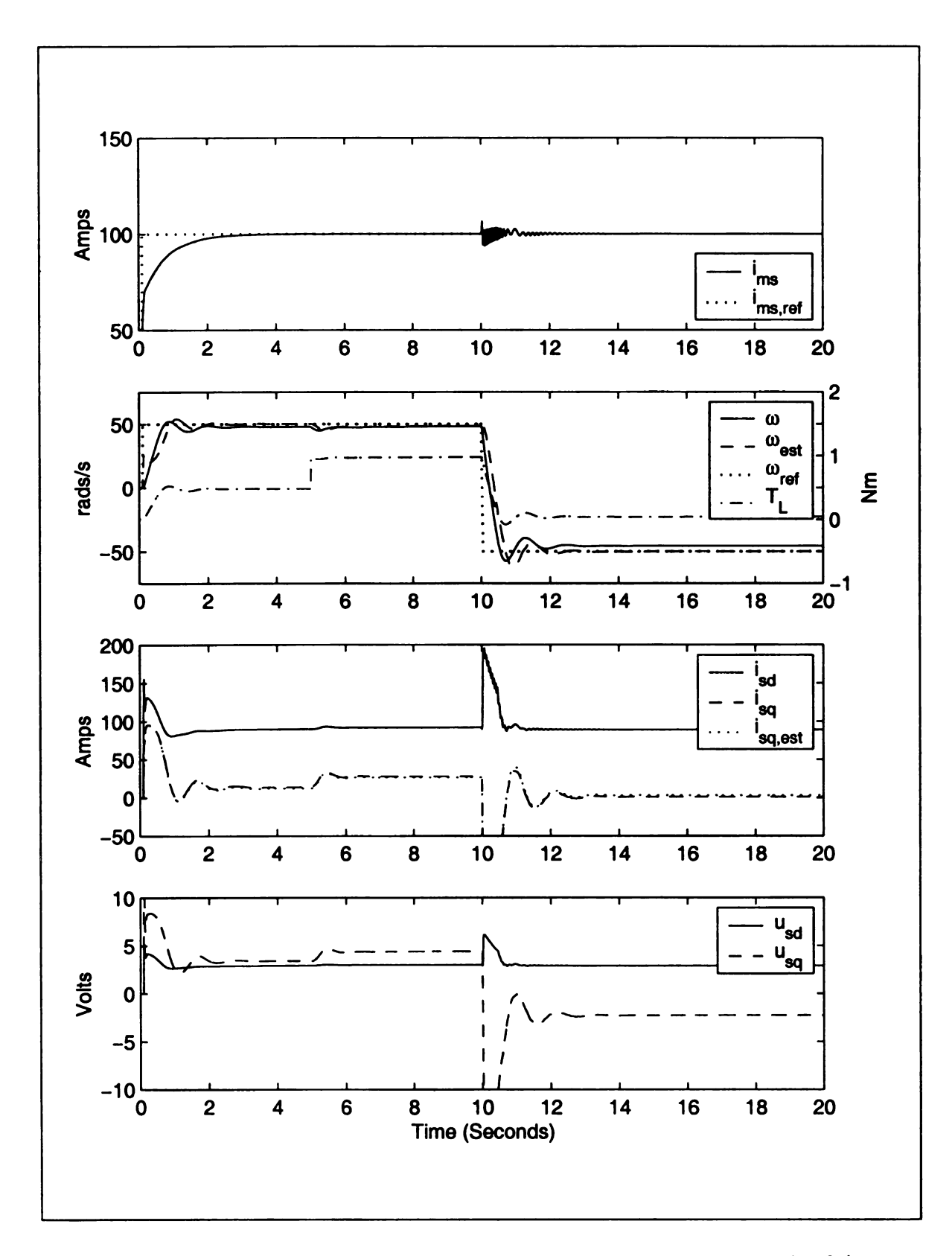


Figure 3-32. Controller performance with integrator approximation ($\omega_c=1\,\mathrm{rads/s}$) and $R_{ro}=1.25R_r\,\mathrm{as}$ an uncertainty.

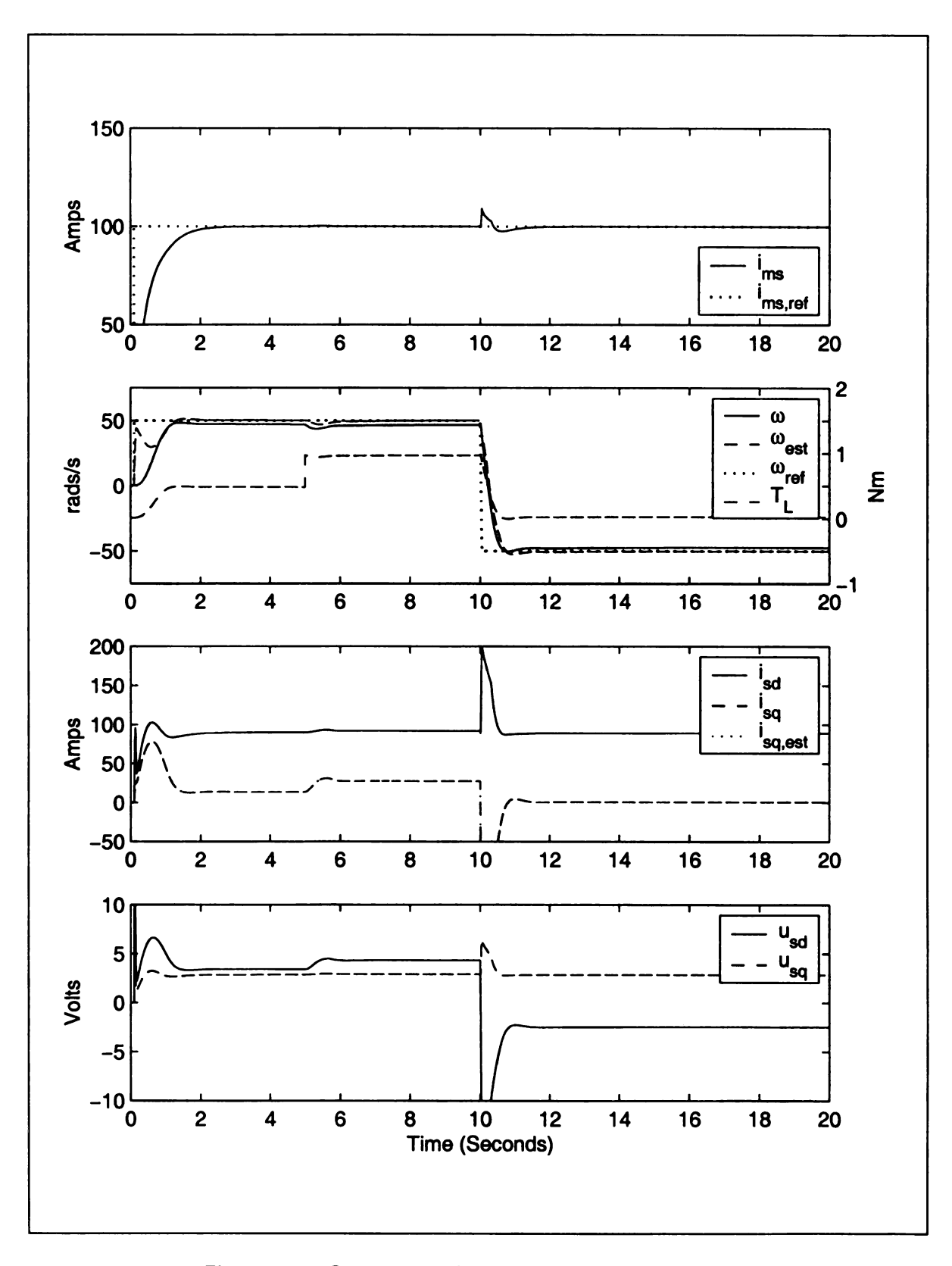


Figure 3-33. Controller performance with error due to HGO

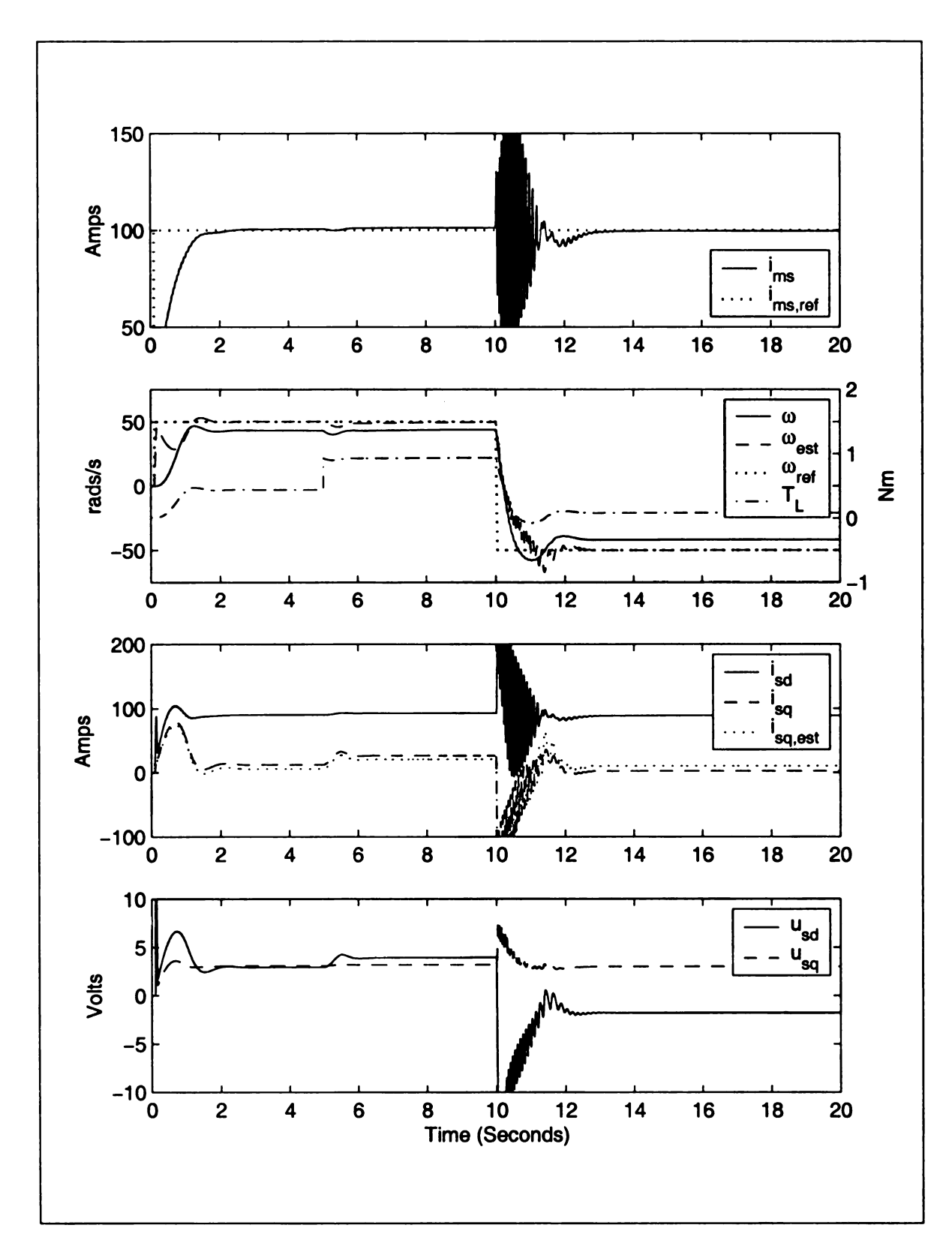


Figure 3-34. Controller performance with integrator approximation ($\omega_c=1 \, {\rm rads/s}$), $R_{so}=1.05 R_s$ and $R_{ro}=1.1 R_r$ as uncertainties and error due to HGO.

3.5.2. Operation at Different Speeds and Loads

Finally to investigate the operation of the machine under different conditions we develop a couple of simulations. The format is the same as in the case when measured speed is used in the feedback. The simulations are performed in presence of all the errors of figure 3-34.

The key observation is the breaking down of the control scheme at low speeds. This result is different from the case when measured speed is being used in the feedback. Keeping in view the analysis done in chapter 2, this result is not surprising. Assuming slip to be small we have

$$\omega_{s} \approx \omega$$

If the controller successfully tracks the references then

$$\omega \approx \omega_{ref}$$
 and $i_{ms} \approx i_{ms,ref}$

For low speed and low torque operation $i_{sd} \gg i_{sq}$ and for this simulation

$$i_{sd} \approx 90 amps \implies I_s \approx i_{sd} \approx 90 amps$$

With $i_{ms,ref} = 100 \, amps$ and above assumptions equation (2.67) gives us

$$\delta i_{sq} \approx \frac{300}{\omega_{ref}}$$

For $\omega_{ref} = 40 \, rads / \, s$, we get $\delta i_{sq} \approx 7.5 \, amps$. This result is very close to the simulation result, which gives $\delta i_{sq} \approx 7.8 \, amps$ and $i_{sq} = 15 \, amps$. The extreme conditions of i_{sq} and i_{sq} having different signs is avoided and the control if functional. Refer to section 2.6 for related details. Note that this is the case of equation (2.95).

If the reference speed is reduced further with $\omega_{ref}=20\,rads/s$ we get $\delta i_{sq}\approx 15\,amps$. By lowering the speed it is expected that $i_{sq}<15\,amps$ when compared with the previous case. This results in i_{sq} and \hat{i}_{sq} having different signs. The obvious consequence is the breakdown of the control.

This simulation is important that it not only demonstrates limitations of operating the machine at low speeds, but also validates the accuracy of analysis done in chapter 2.

Figure 3-36 illustrates the robustness of the control scheme to changes in load torques.

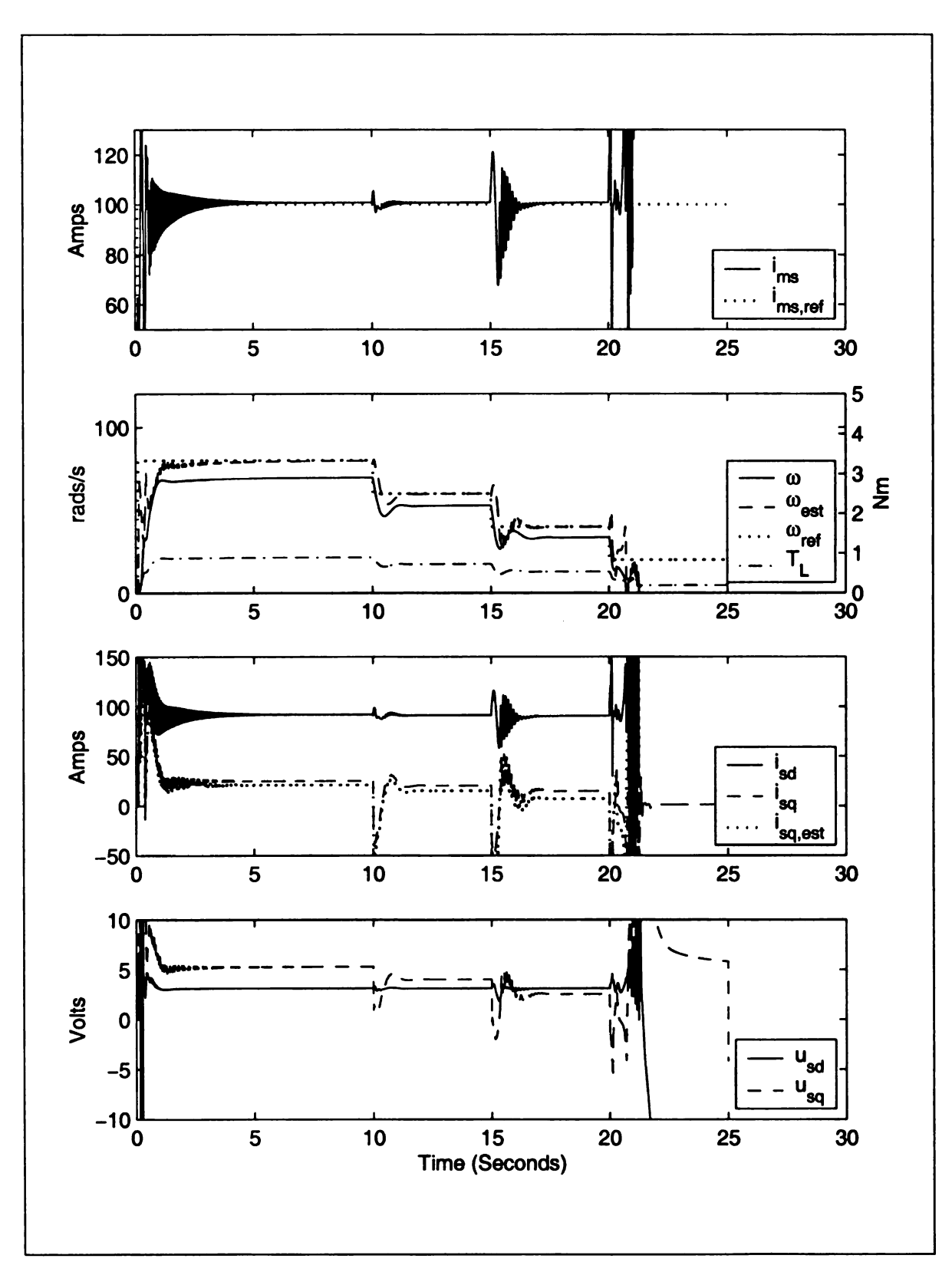


Figure 3-35. Controller performance at various speeds (Encoderless Case)

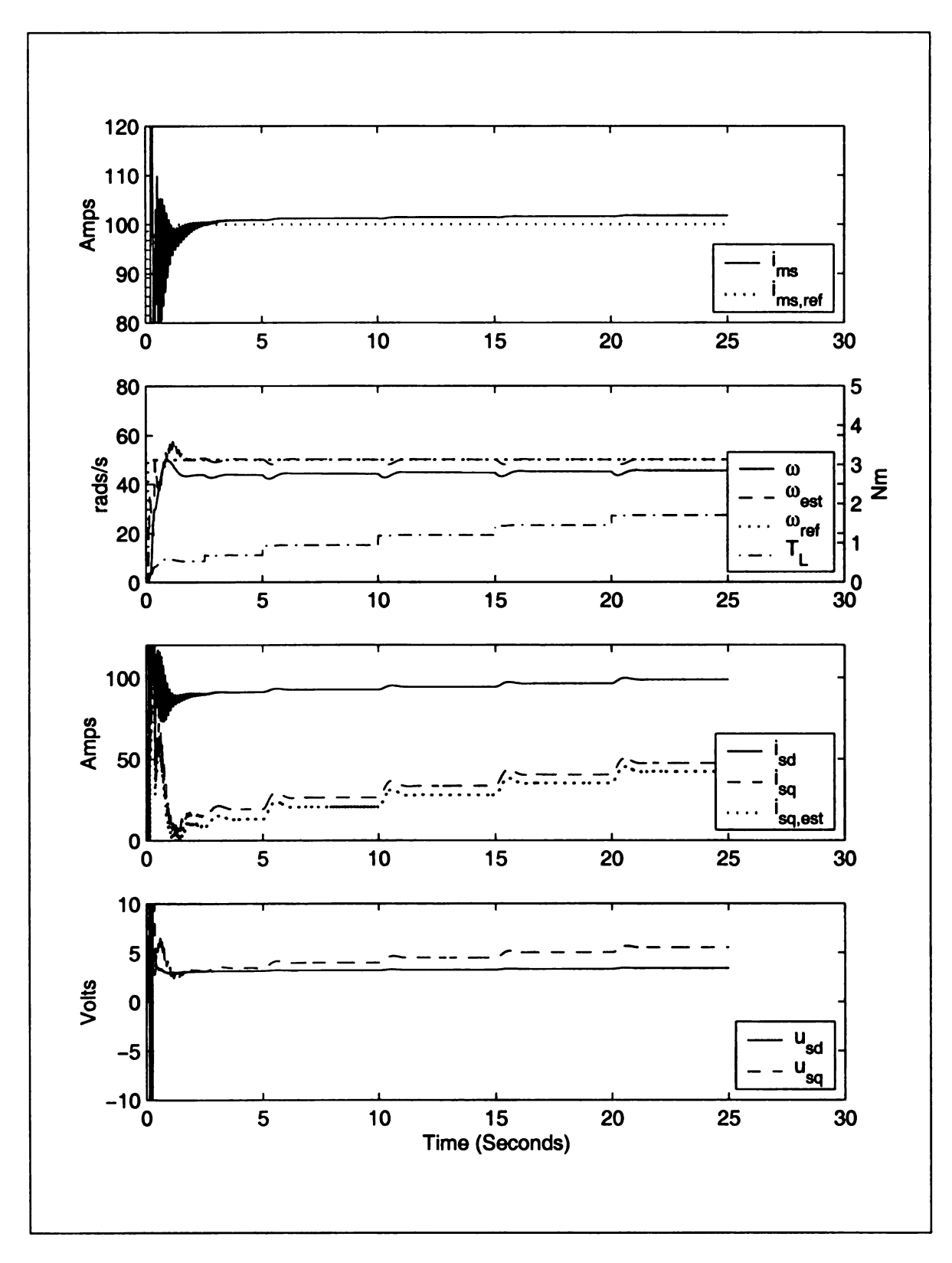


Figure 3-36. Controller performance at various loads (Encoderless Case)

CHAPTER 4

EXPERIMENTAL SETUP AND RESULTS

4.1. Introduction

Analysis and simulations are important stages in designing a control system. It is natural to think that the actual target is not accomplished unless the control scheme is physically implemented. The requirements of this final stage are radically different from the previous steps. The idealization and approximations assumed for the analysis and simulations are no longer there in a real system. All the unmodeled effects, disturbances and technology dependent issues are present. The last one of these is of prime importance in an experimental setup. The designer has to keep in mind all the basic considerations and prerequisites to work on the experiment.

The first step of design of the experimental setup is the selection of technology and methods to be used. This level is a part of project management. Decisions made at this stage play a vital role in the rest of the development. The difficultly is that the design has not even started as yet. We have to anticipate all the requirements and steps beforehand. Keeping in view all those factors, a design engineer selects from the available technologies. Other technology related issues are cost, portability and suitableness as far as personal skills are concerned. The decisions made at this stage are long lasting. Any wrong decision could result in high cost both in terms of expenses and time. The actual implementation follows.

Extra precautions have to be taken at the prototyping phase because the errors are hard to debug. We have successfully developed an experimental setup keeping in view all the design requirements.

To summarize, we have tried to give justice to all the ingredients of a control design scheme from analysis to actual experimentation. The methodical approach enabled us in completing the design with satisfactory performance.

4.2. The Experimental Setup

Our experimental setup is based on some new and novel ideas. The central theme is the use of a personal computer as an embedded microcontroller. A PCI digital input/output card has been incorporated for the personal computer to communicate with the outside world. We have developed a sophisticated machine control card. This card carries all the necessary electronics to collect data from various sensors and issue command signals to some other devices. The 3-phase power to induction machine comes from a PWM inverter. To emulate load we use a DC machine that is controlled by its own controller. This control can be manual or through the machine control card.

Voltage is directly sensed owing to the low voltage machine. Isolated current sensors provide accurate current measurements. A 1024 grating shaft encoder senses position. The stator resistance is a critical parameter. Its value however, varies with temperature. A temperature sensor helps alleviating this problem. We have also incorporated a torque sensor to accurately monitor the shaft torque.

State of the art hardware design and effective software have enabled us to perform experiments in the most elegant of manners. We are able to easily

implement the controller and all its variations. The results produced match the analysis and simulations pretty well. Block diagram of the experiment is given in Figure 4-1.

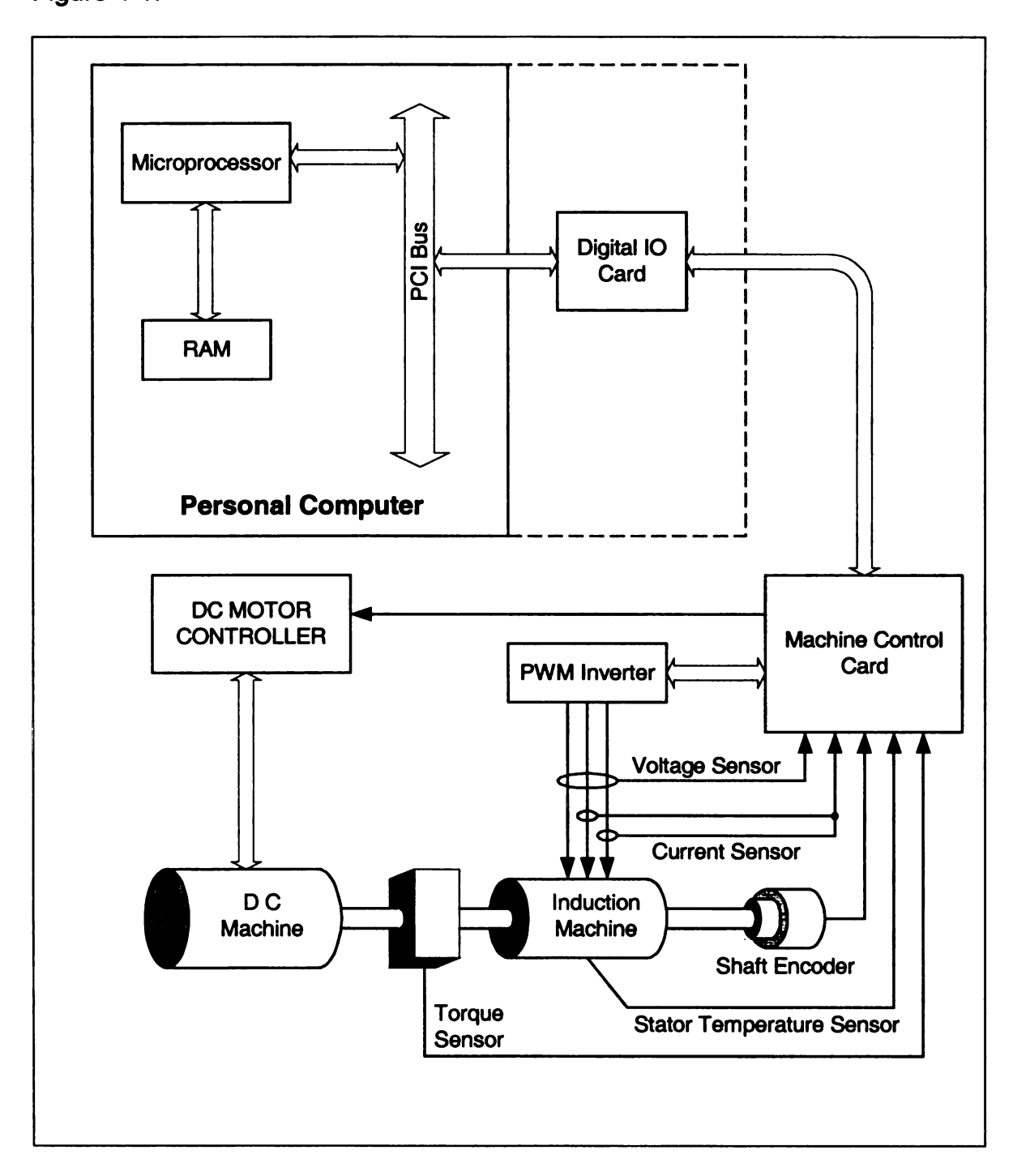


Figure 4-1. Block diagram of the experimental setup

4.3. Personal Computer as Embedded Processor

Historically personal computers and embedded technologies have been two different things with very different roles. Emerging technologies and systems have changed this concept and the boundary between the two is becoming unclear. There are many tasks that were considered to be in the domain of personal computing that are now been done by devices that are not even recognized as computers. Most common example is of the devices that can access Internet. The same is true for personal computers. However, replacing some embedded technology with personal computers is not a simple procedure. There are certain hardware as well as software requirements for accomplishing this task.

Once we are able to use personal computers we get certain benefits that are either not available in the embedded technologies or are hard to achieve. Following is a brief discussion in this regard.

4.3.1. Computational Power

The most glaring difference between commonly available micro-controllers and personal computers is the computational power of the later. The computational power of a personal computer may exceed its counterpart by orders of magnitude. The difference arises from high frequency of operation, superpipelining, parallel and multi-processing and other advanced features that are common in microprocessors of today. This helped us in implementing the most sophisticated and involved control schemes without much difficulty.

4.3.2. Memory Resources

In most of the controller applications, memory requirements are not stringent. However, during the phase of development we generally require to collect data related to state variables, controller or estimators. With high sampling rates, these data become enormous even for a short period of operation. Large memory of personal computers can handle this situation. This task is hard to implement using embedded technologies.

4.3.3. Available Data Types

We have already seen in section 2.6 that 32-bit floating points may become insufficient to handle certain common problems faced by a control scheme. On the other hand 32-bit floating points is a standard for most microcontrollers. Naturally there are ways to handle this situation but during the development phase, one would like to concentrate more on the control scheme rather than implementation issues. Personal computers use 64-bit or 80-bit floating points as a standard. This precision exceeds the requirements for most sophisticated and advanced control schemes. We have used 64-bit floating points for our implementation.

4.3.4. Mass Data Storage

This is also one of the requirements that become redundant once the control scheme is mature. However, to keep a record of development phases we require mass data storage facility. Personal computers have large hard disks and this is

not a problem. On the other hand, developing a similar facility for embedded technologies is difficult and expensive.

4.3.5. Simulating Real Data

If a design engineer is running simulations using the data collected from real experiments, then programs like MATLAB help a lot. He is able to do all of these tasks from the same computer.

4.3.6. Development Environment

Advanced and user-friendly environment of personal computers makes the task of developing a control scheme much easier. High-level programming languages like C and C++ are much more stable on personal computers as compared to other platforms. Sophisticated debugging and related facilities are common in personal computers. All of these factors have a big impact on the development time of a control scheme.

4.3.7. Flexibility

A design undergoes considerable changes before it reaches a final stage. In certain cases, we may have to change the hardware of the setup for applications implemented through embedded technologies. This alteration is tedious and time consuming. If the same work is being done on a personal computer, it is expected that most of the changes would be at the level of software. The development environment for the software on personal computers is suitable for making change in short time. This is a very important factor that has no parallel in embedded technologies.

4.3.8. **Summary**

Personal computers offer facilities and convenience that greatly help a design engineer in developing a control scheme. Both the cost and development time are considerably reduced. General awareness and user-friendliness of computers make it easy to train new people on an experimental setup. Well-set standards for personal computers reduce the problems of portability and compatibility.

The requirements of final product may however, exclude the possibility of using a personal computer. Transferring a fully developed scheme from an experimental setup based on personal computers to some other platform is a much easier task than developing the whole scheme on that platform.

4.4. RTLinux Philosophy

If a personal computer were so suitable for implementing real-time schemes then what is the reason that this idea has not been utilized until recent past? A computer is just a piece of remarkable hardware. The usefulness of the computer, however, depends on the software that is running on it. The most conspicuous reason that forbade the personal computer as an embedded processor has been the unavailability of real-time operating systems (RTOS). A realization of the powers of personal computers amongst the designers have led to the emergence of new RTOS's. RTLinux is one of them and inherits all the benefits from the well-known Linux operating system.

An operating system has to take care of controlling the hardware of the computer including all the peripherals. Some tasks are given higher priority than others.

The solution is not simple and the result is complex architecture of the operating system. If the same operating system is used for handling real time tasks, it is almost certain to miss some events that may be critical. RTLinux provides an interesting solution to this problem. It takes control of the whole machine and executes Linux as one of its low priority tasks. This makes it possible for the real time tasks not to be disturbed by any other event.

The real time tasks may be interrupt-driven or time scheduled. The later is more suitable for fixed sampling time applications and we have done the same. The details of the operating system can be found from the RTLinux web site http://www.rtlinux.org.

4.5. Software Planning

RTLinux provides facilities to develop real time programs. However, a real time task has all the system level privileges. The simple implication of this status is extreme sensitivity of the real time program to programming errors. The simplest of errors result in a system crash, whereas more serious situations may result in hardware damage. This calls for a very good high-level plan for the development of the software. This issue becomes even important for our case where we have to implement a control scheme of considerable complexity.

The real time task runs in an infinite time scheduled loop. It communicates with the machine control card via the digital IO card and has all the necessary software for controlling the induction machine. This software includes controller and estimators. The relevant data is stored in a memory buffer that is shared by a Linux task that acts as the user interface. Depending on the nature of

experiment this buffer has a size of tens of megabytes. A small portion of this memory is used for commands from the user to initiate or stop the controller. The user interface does not interfere with the real time task because of its being non-real time. Once the experiment is done, the user has the option to store the data to the hard disk. Figure 4-2 illustrates the software plan.

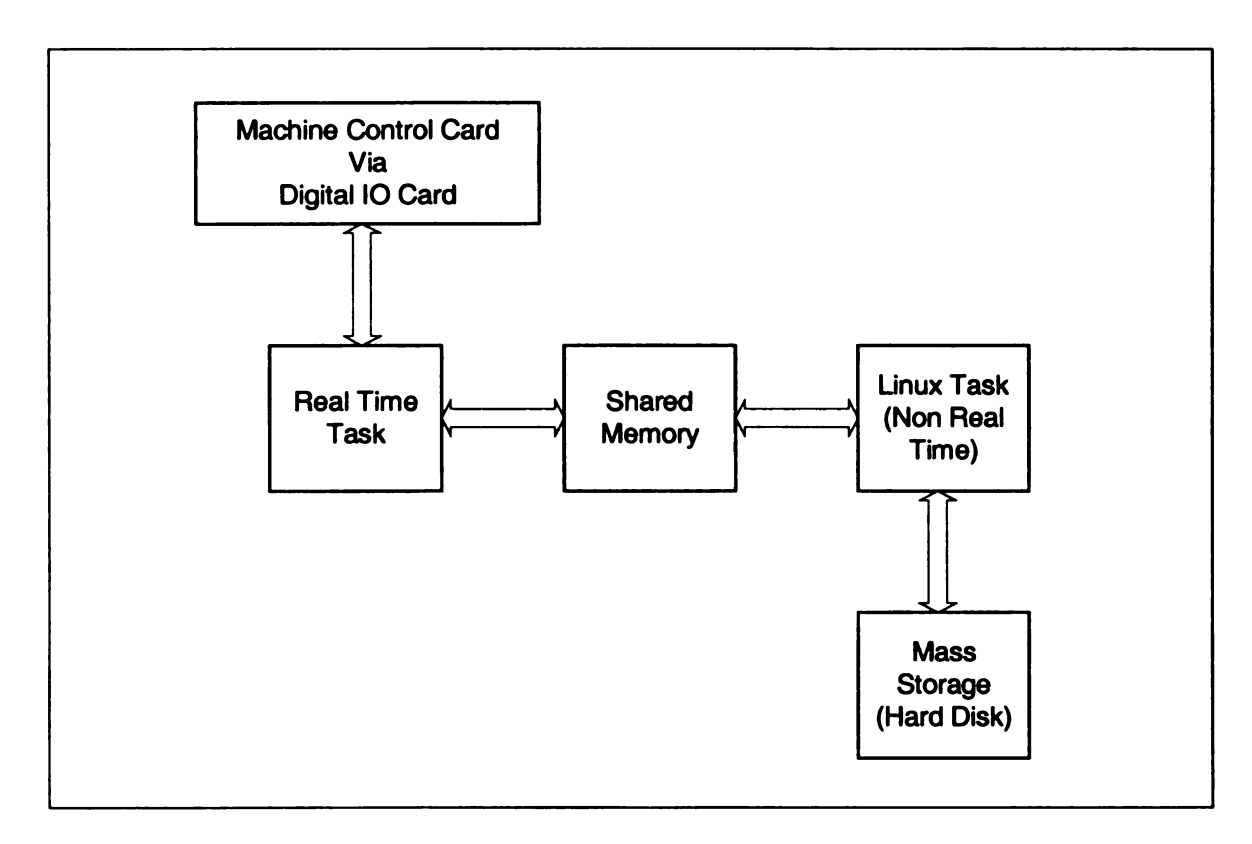


Figure 4-2. Software plan

4.5.1. Hierarchy of the real time task

The complexity of the real time task demands for modular programming. It turns out that we can go a step further for our software. We can also create a hierarchy in the modules. Figure 4-3 illustrates the complete scheme. This sort of architecture gives maximum flexibility. For example if we want to change the

machine control card at some stage, we only have to change one block of figure 4-3. There may be minor changes in higher levels as well. The highest level is basically RTLinux part of the real time task.

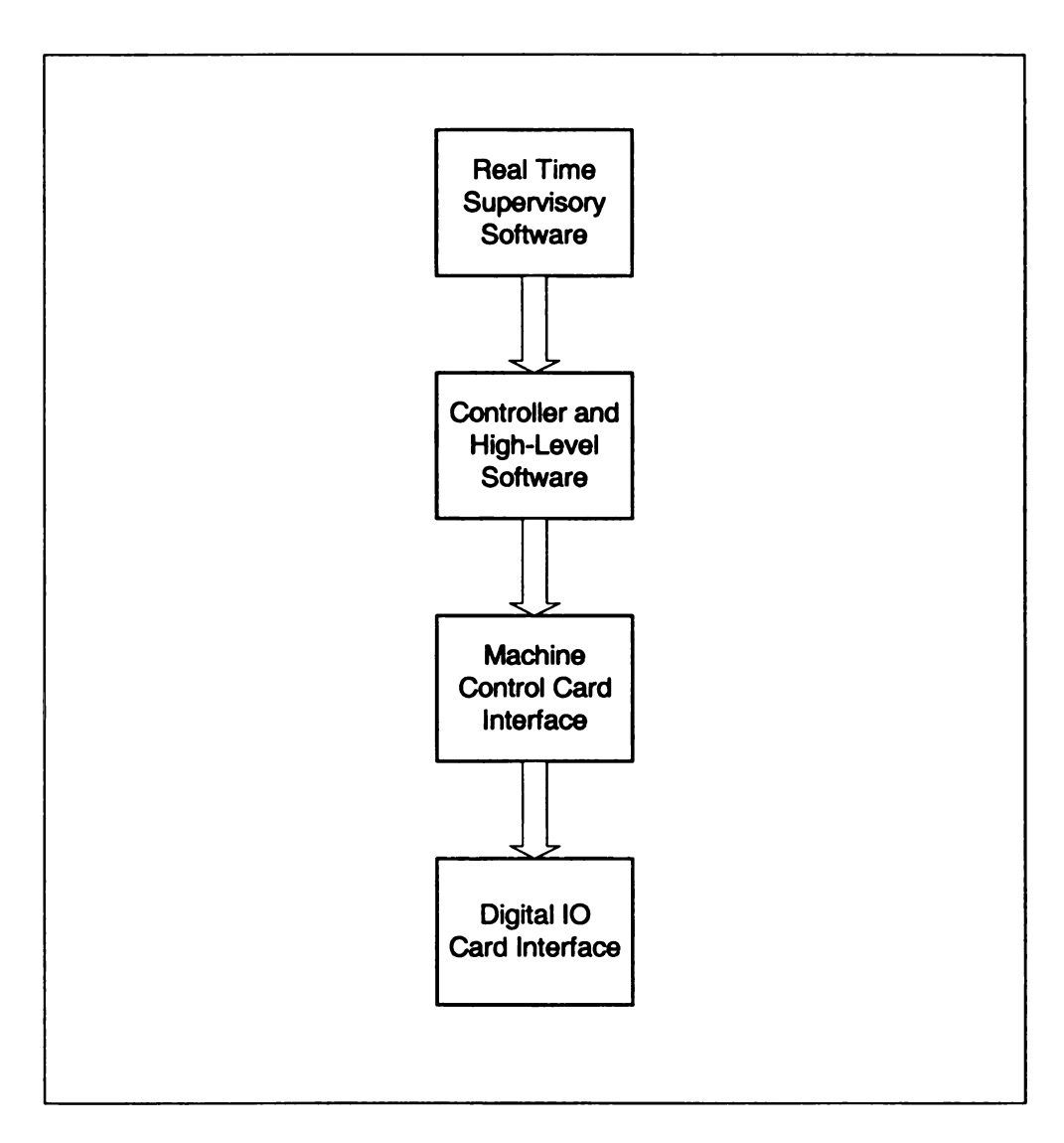


Figure 4-3. Hierarchy of real-time task

4.6. Digital IO Card

We have selected National Instruments PCI-DIO-96 card. It has 96 digital input/output lines. The card does not provide the fastest of the interfaces but satisfies our requirements. In fact using a very high-speed card may become problematic from the point of cross talk and noise immunity. The details of the card are available from National Instruments web site http://www.ni.com.

4.7. Machine Control Card

This card plays a fundamental role in the actual interface with the induction machine. Figure 4-4 illustrates the facilities available on the card. There is a 24-bit local data bus on the card. Because the number of devices is limited, we use the concept of address lines rather than the usual address bus. A data transfer protocol is required for the bi-directional nature of the data bus. Control lines are dedicated for this purpose. For clarity sake, the control lines have not been shown in the figure. This protocol is not the same for all the blocks shown in the figure. However, it is important that there are no conflicts. A brief account of the blocks follows.

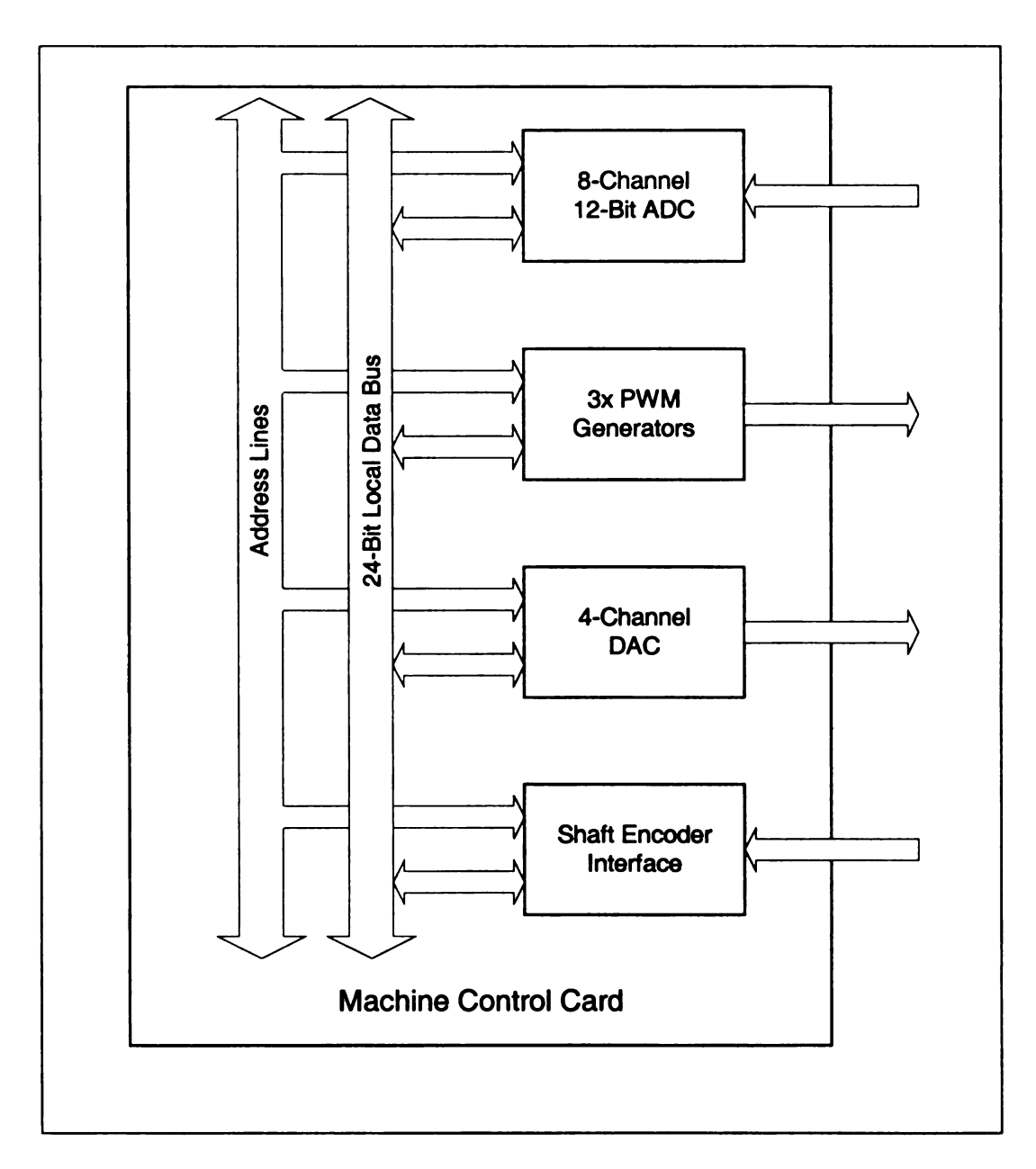


Figure 4-4. Block diagram of machine control card

4.7.1. Analog to Digital Conversion

As depicted in figure 4-1, we require 7-channels of analog to digital conversion. To improve transmission time, we use two analog to digital converter chips in parallel. Besides, anti-aliasing filters are used which play an important role in sampled data systems. Figure 4-5 illustrates the implementation.

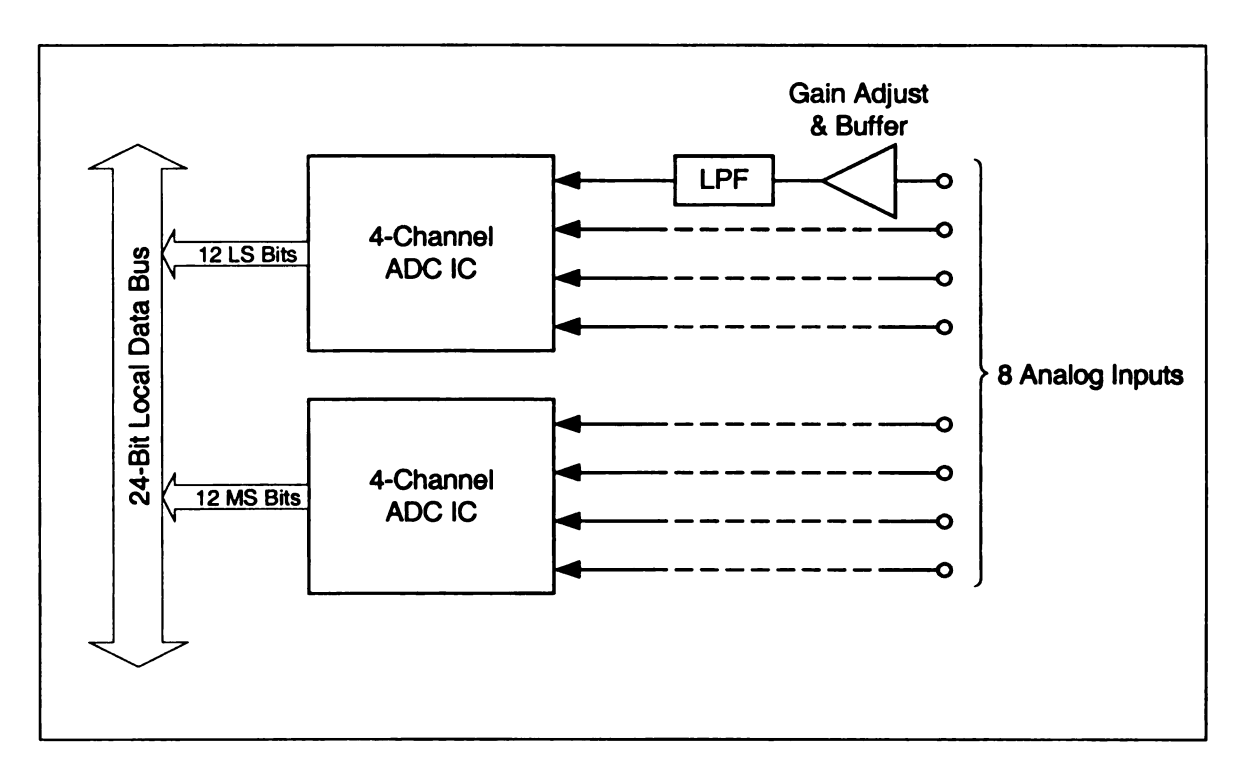


Figure 4-5. Analog to digital conversion

We use third order Butterworth filter for anti-aliasing. Sampling rate of 10KHz corresponds to Nyquist frequency of 5Khz. The transfer function of the filter is given as

$$H(s) = \frac{1}{(s/\omega_o)^3 + 2(s/\omega_o)^2 + 2(s/\omega_o) + 1}$$
(4.1)

The magnitude response is

$$|H(\omega)| = \frac{1}{\sqrt{1 + \left(\frac{\omega}{\omega_o}\right)^6}} \tag{4.2}$$

With a cutoff frequency of 500Hz, the Nyquist frequency of 5Khz undergoes attenuation of 1000 times which is sufficient for our design requirements. The circuit diagram for the filter is given in figure 4-6. Refer to Millman [14] for details.

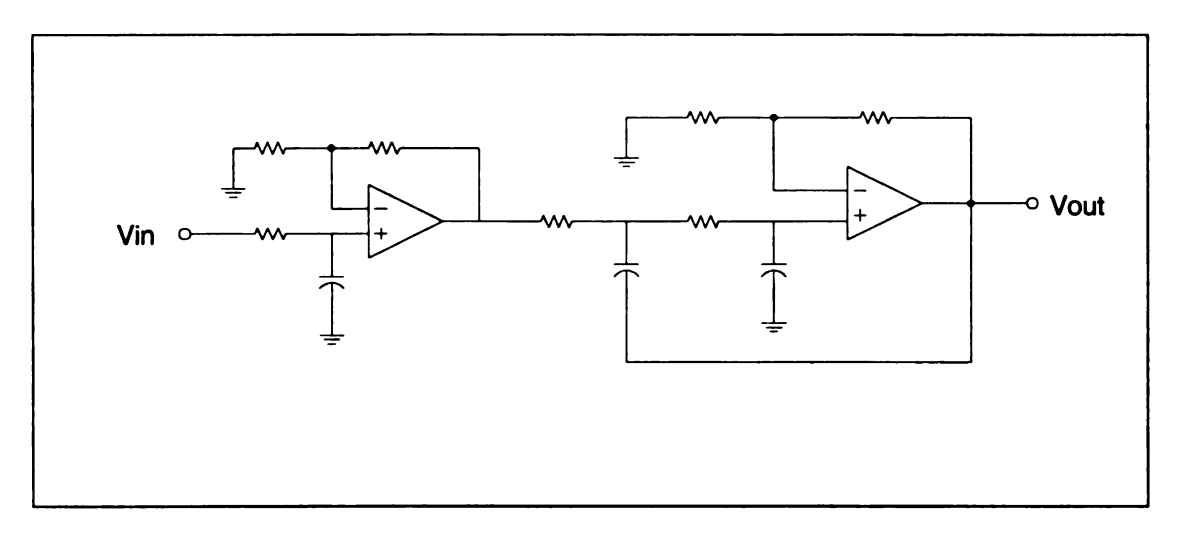


Figure 4-6. Anti-aliasing filter (3rd order low pass Butterworth)

4.7.2. 4-Channel Digital to Analog Converter

A digital to analog converter is required in transmitting signals to the DC motor controller. This is a useful facility to have on the card. Figure 4-7 illustrates the DAC.

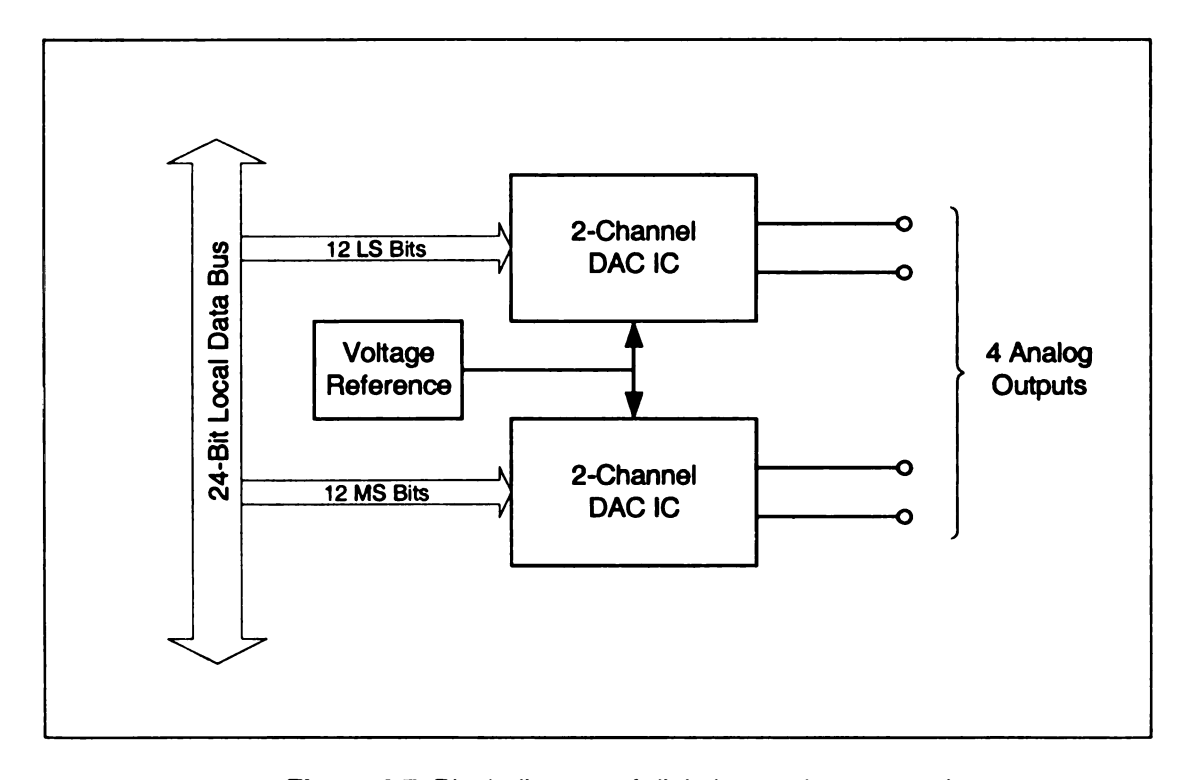


Figure 4-7. Block diagram of digital to analog conversion

4.7.3. PWM Generation

We have used PIC16F877 microcontroller for generating PWM signals. The microcontroller has two PWM modules built-in the chip hardware. Since for 3-phase systems we require a third PWM signal. This signal is created in software. The program makes use of 8-bit timer and is interrupt driven. The soft PWM can give a duty cycle of 0-100% and is synchronized with its hardware counter part. The interface is via 24-bit data latch, which is required to prevent data being corrupted.

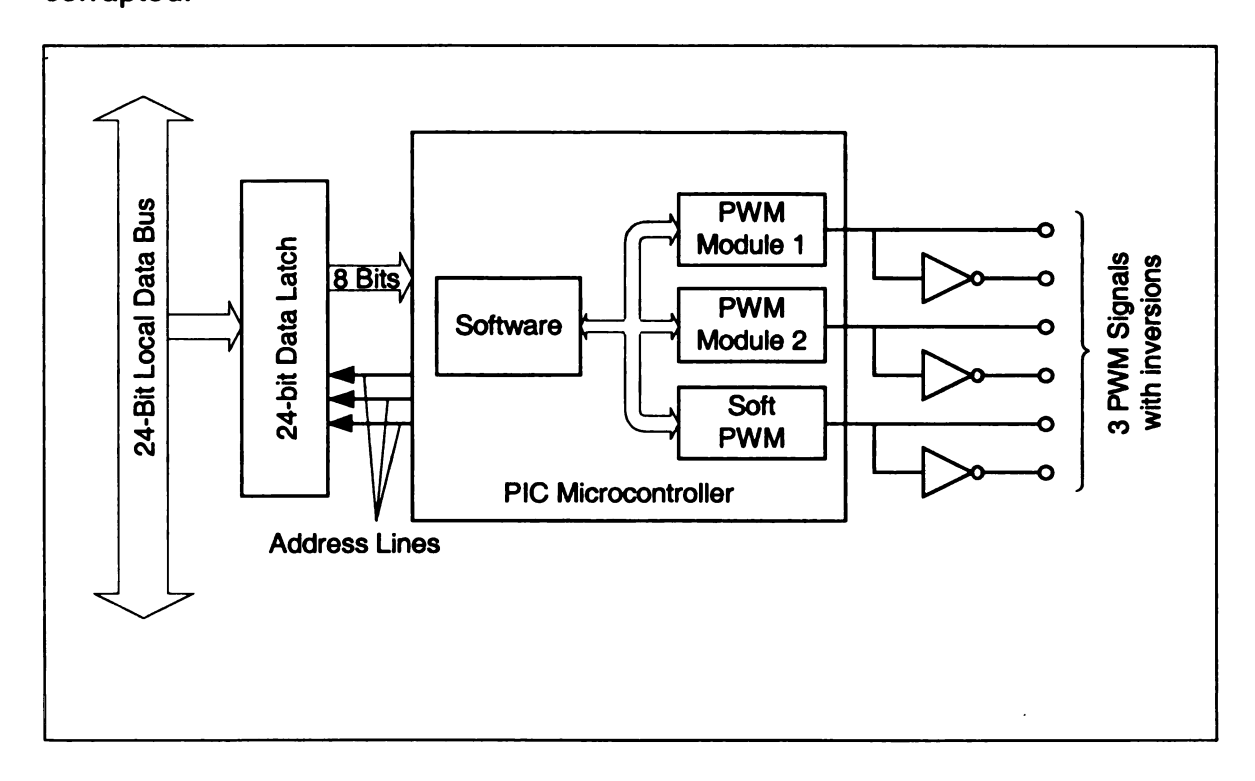


Figure 4-8. Block diagram of PWM generation

4.7.4. Shaft Encoder Interface

We have used HCTL2020 for receiving the quadrature inputs of the shaft encoder. This IC provides 8-bit bus interface.

4.8. Open Loop Experiment

We run the experiment in open loop to study the estimator performance. The basic idea is similar to the concept of figure 3-10. However, now the machine is physically run instead of being simulated. We do not have access to physical quantities like magnetizing current etc. The position of the rotor is measured and speed is obtained through the use of high-gain observer. A large voltage signal is given in the first second to facilitate the start of the motor. For the next four seconds, a signal of reduced amplitude is given. The amplitude of the signal is further reduced for the rest of the run. The frequency of the signal is kept constant throughout the experiment at 25Hz. Data are collected in real time. These data are then ported into MATLAB/SIMULINK. The estimators are run in the simulator. The results are given in the Figure 4-9 and Figure 4-10.

The accuracy of the speed estimate is the key observation. Since we do not have access to many of the physical quantities and the system is operating in open loop, it is not possible to quantitatively evaluate the estimators other than the case of speed. We can still infer that the behavior of all the estimated quantities is not different from what is expected i.e. the waveforms are logical.

The actual speed ω is estimated by passing position measurements through a high-gain observer. Equation 2.84 is used to get the speed estimate ω_{est} . We have used low-pass filters to filter out high frequency noise in estimated quantities. This noise appears primarily due to dead-time nonlinearity of PWM inverters.

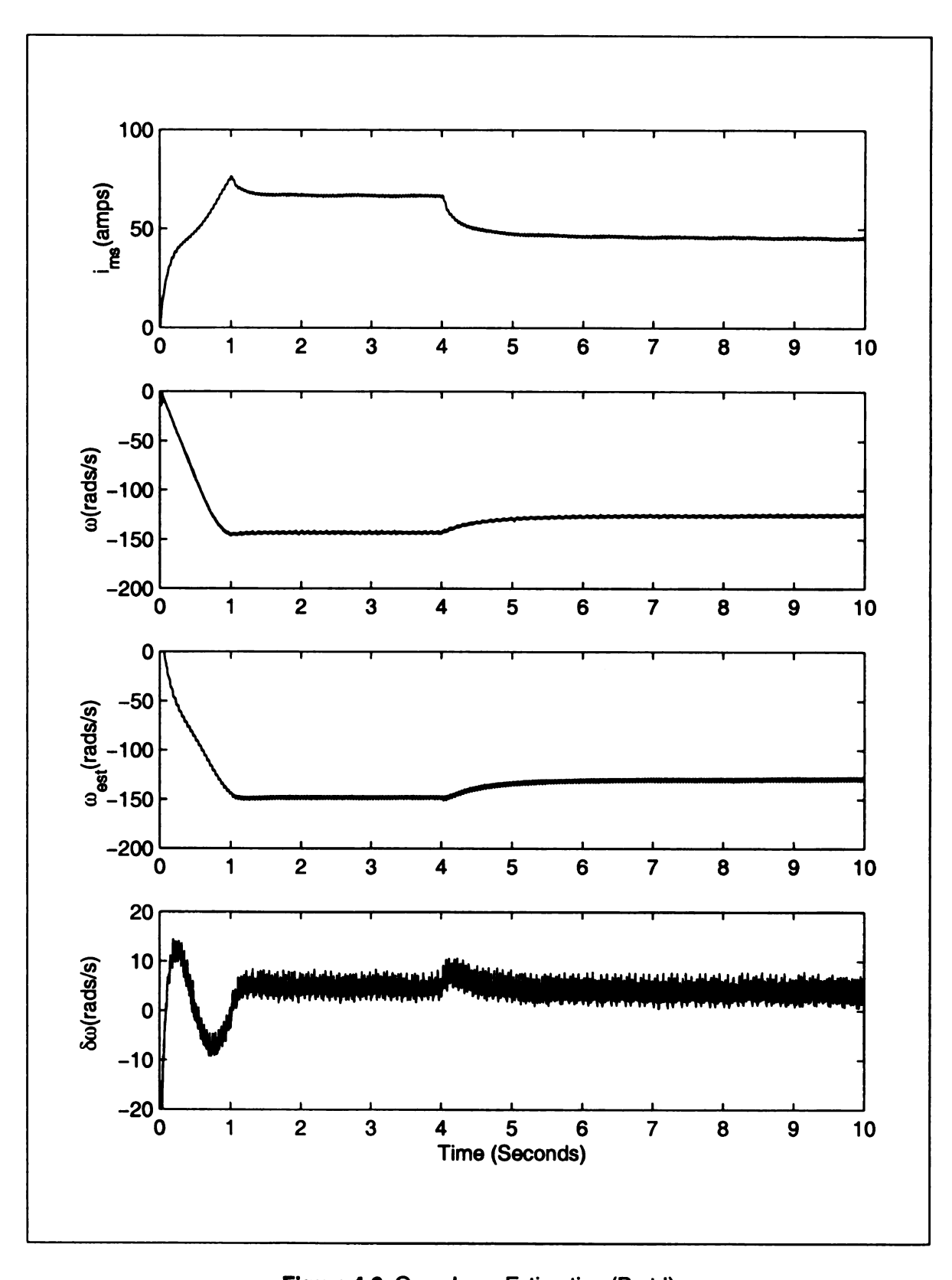


Figure 4-9. Open Loop Estimation (Part I)

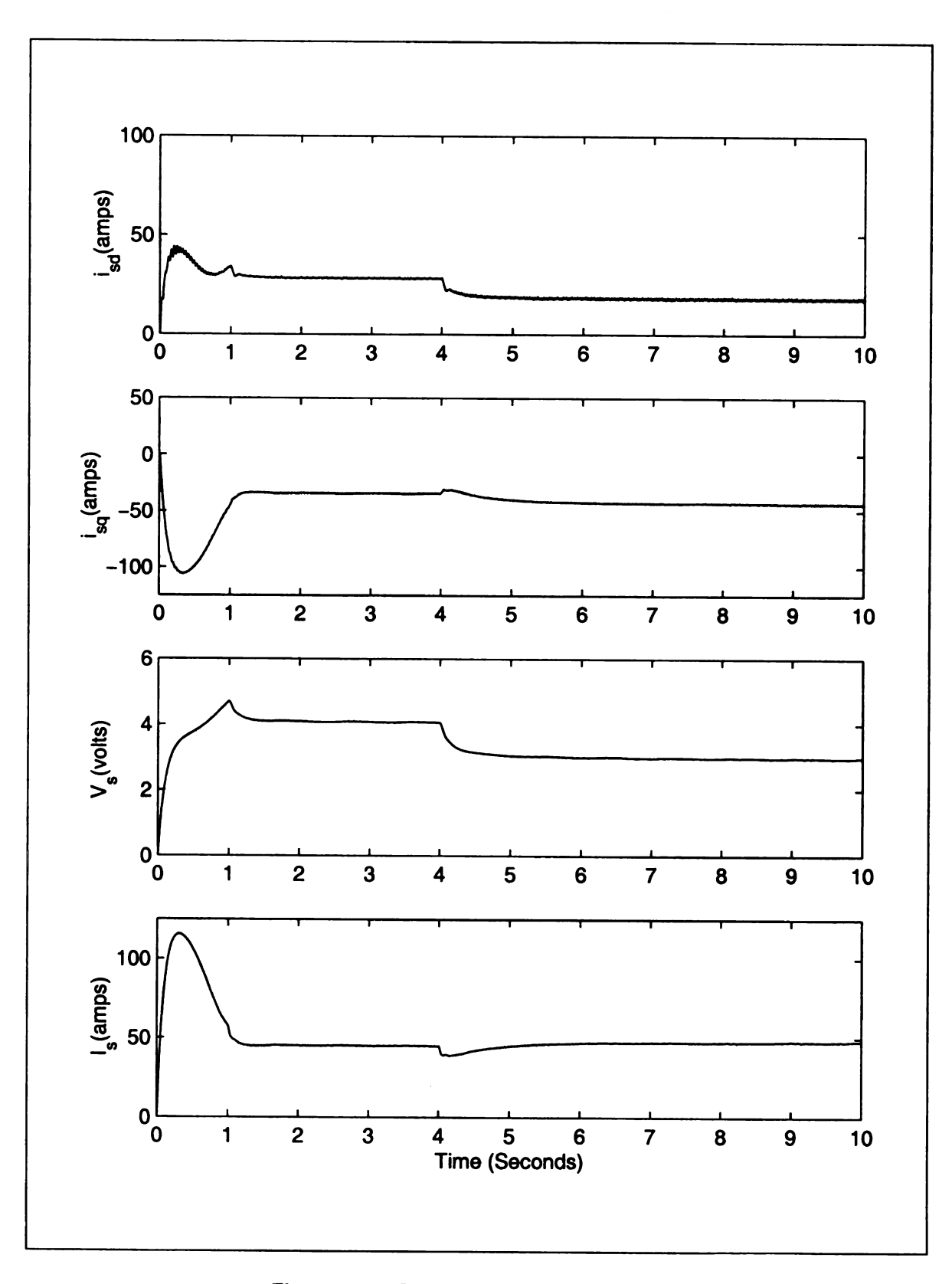


Figure 4-10. Open Loop Estimation (Part II)

4.9. Encoderless Speed Control of Induction Machine

We now conclude our chapter by presenting our ultimate goal of controlling the induction machine without any position or speed sensors. The complete scheme of Figure 2-7 comes into play. The machine is started by 3-phase sinusoidal signal. This is done to overcome the difficulties of initialization as discussed in section 2.5.2. The control scheme takes over at time t=2s with $i_{ms,ref}=40amps$ and $\omega_{ref}=100rads/s$. Command for speed reversal is given at t=6s.

We use the second-order filter of equation (2.42) with $\omega_c = 1 \, rads/s$ to approximate the integrator in stator-flux estimator. The sampling rate is 10KHz. For discrete-time implementation we have used bilinear transformation without frequency pre-warping.

We have used the exact machine parameters as given by the manufacturer.

These parameters are summarized as follows.

Parameter	Value
Stator Inductance, Ls	0.373 mH
Rotor Inductance, <i>Lr</i>	0.383 mH
Magnetizing Inductance, Lm	0.352 mH
Stator Resistance, Rs	0.0105 Ω
Rotor Resistance, Rr	0.0138 Ω

Table 4-1. Parameters of machine used in actual experiment

The sensitivity of estimators on R_s makes it important to update its value online. Accurate temperature sensor provides stator-winding temperature. We use the relation as given by Aloliwi [19].

$$R_s(T) = R_{so} \frac{T + 235}{T_o + 235}$$

where T is the stator-winding temperature in ${}^{\circ}C$ and R_{so} is the value of stator resistance at temperature T_{a} .

Currents are measured using LEM isolated hall-effect current transducers.

Voltages are measured directly by the machine control card.

Observations

The results are given in figure 4-11. The most important observation is the successful tracking of both the magnetizing current and speed references. It is important to note that the stator and rotor resistances are now true uncertainties. We cannot use the expressions of error bounds derived in chapter 2. We do not have access to actual flux but the speed ω can be calculated by passing the position measurements through a high-gain observer. The estimated speed ω_{est} is obtained by using equation (2.84). We see that error in speed tracking is small. Another observation is the successful speed reversal.

Excessive noise in estimated quantities results from dead-time non-linearity of the inverter. This noise is improved slightly as soon as the closed loop control becomes active at t = 2s. Note that the high frequency noise appears in

estimated quantities only. The machine has its own time constants, which filter out high frequency component of the input. The result is apparent in the case of speed. We observe that there is virtually no high frequency disturbance in actual speed ω .

One final remark is that this result is achieved in the presence of all unmodeled and certain unwanted factors that are not possible to eliminate from a physical system.

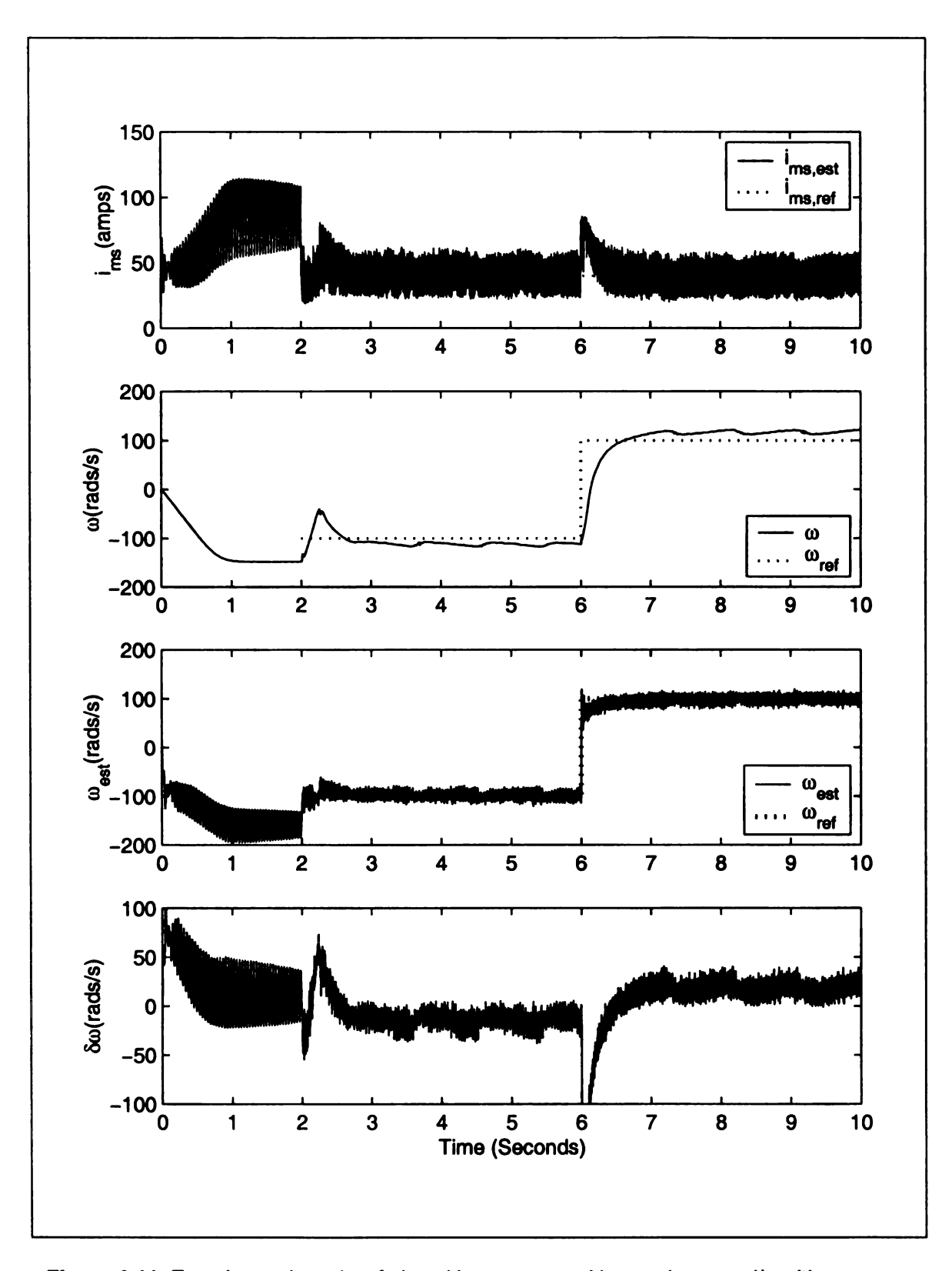


Figure 4-11. Experimental results of closed loop system without using speed/position sensors

CHAPTER 5

CONCLUSIONS AND RECOMMENDATIONS

5.1. Conclusions

The knowledge of capabilities and limitations is fundamental to successful implementation of a control scheme. The stator flux-orientated control offers faculties not available in other methods. Based on the analysis, simulations and experiments, we are now in a position to make precise and more informative statements. A brief account follows.

- We can have a quantitative estimate of the operational range of the machine.
 This requires certain information like bounds on the load torque. Section 2.6 gives a guidline in this regard.
- The error analysis in chapter 2 shows that stator based schemes rely heavily on accurate knowledge of stator resistance. This apparent demerit is actually not as big a problem. In fact if we keep in mind that the stator quantities are available for online measurement, it is possible to track changes in stator resistance. Stator temperature plays an important role in this regard. We expect minimization of errors due to uncertainty in stator resistance if some suitable scheme updates the stator resistance in real time.
- Stator flux estimation is totally independent of rotor resistance whereas the error in estimated speed is small due to uncertainty in rotor resistance. Rotor quantities are inaccessible. The temperature of rotor resistance undergoes

large variations owing to rotor losses. The obvious consequence is a greater uncertainty in rotor resistance. Under these circumstances, stator flux-orientated control appears to be a good choice.

- Stator flux estimation is independent of rotor speed. The stator flux estimator, therefore, remains the same for both measured and estimated schemes. It is also reasonable to think that this independence would also contribute to overall robustness.
- The errors in estimated quantities are reduced at higher stator frequencies.
 This makes stator flux orientated control to be well suited when the machine is to be operated at considerably high speeds.

On the other hand the stator flux orientated control faces certain limitations and difficulties.

- The properties of pure integrators rule out a possibility of using them in open loop. Therefore, stator flux estimator has to be implemented using some approximation of the pure integrator. This affects the dynamic performance and a steady state error is introduced as well. Section 2.2 deals with analysis of these errors.
- The stator flux estimator lacks the ability to operate at zero frequency. Under such conditions stator flux-orientated control is impossible to use even if the mechanical speed is available for online measurement. The simplest example is the operation of the machine at zero speed and zero load torque. These issues are discussed in section 2.6.

• Owing to increased errors at lower speeds, the stator flux orientation is not suitable for low speed operation of the machine.

5.2. Recommendations

There are many options available for the control of induction machines. All of these techniques work well under certain conditions and face difficulties otherwise. Rather than making a decision that is biased towards a particular approach, it is wise to keep in mind the actual objective of designing a control scheme. Therefore, we would not insist that the stator flux orientated control is the best choice under all conditions. However, there are certain advantages associated with it. Our findings relating to stator flux-orientated control are not different from the common understanding of this scheme. A summary of recommendations in this context follows.

- Stator flux orientated control is most suited at high-speed operation. The
 experimental results of figure 4-11 illustrate this important fact. Speed
 estimation is accurate and the scheme has a capability of speed reversal,
 which is considered a difficult proposition in encoderless control of machines.
 We would suggest using this scheme under these requirements and
 conditions.
- For low speed operation of induction machine, either a different scheme should be used or stator-flux orientated control can be combined with some other suitable scheme. The former will be the dominant controller at high speeds and the later will take charge at low speeds. The switching between

the two controls can cause a problem. Leonhard [12] has proposed a method of performing this task in a soft manner.

 If a comparison based on mathematical analysis is made between different schemes, there is a possibility of combining their advantages and getting rid of difficulties.

BIBLIOGRAPHY

- [1] Andreas Antoniou. *Digital Filters: Analysis and Design.* McGraw-Hill, 1979.
- [2] F. Blaschke. The principal of field-orientation as applied to the new Tranvektor closed-loop control system for rotating-field machines. Siemens Review 34, 217-20.
- [3] Chi-Tsong Chen. *Linear Systems: Theory and Design.* Saunders College Publishing, second edition, 1984.
- [4] R.W. Daniels. *Approximation Methods for Electronic Filter Design*. McGraw-Hill Book Company, 1974.
- [5] T. Deiyannis, Yichuang Sun and J.K. Fidler. *Continuous-Time Active Filter Design*. CRC Press, 1999.
- [6] Richard C. Dorf and Robert H. Bishop. *Modern Control Systems*. Addison-Wesley, 8th edition, 1998.
- [7] G.F. Franklin, D. Powell and M.L. Workman. *Digital Control of Dynamical Systems*. Addison-Wesley, 1996.
- [8] A. Isidori. Nonlinear Control Systems. Springer-Verlag, 1999.
- [9] H.K. Khalil. *Nonlinear Systems*. Prentice Hall, second edition, 1996.
- [10] H.K. Khalil and E. Strangas. Robust speed control of induction motors using position and current Measurements. *IEEE Trans Autom. Cont.*,1996.
- [11] H.K. Khalil and Ahmed M. Dabroom. Discrete-Time implementation of high-gain observers.
- [12] W. Leonhard. Control of Electrical Drives. Springer-Verlag, 1995.
- [13] W. Leonhard. Field-Oriented Control of a Standard AC Motor Using Microprocessors. *IEEE Trans. Ind. Applications*, 1980.
- [14] Jacob Millman and C.C. Halkias. *Integrated Electronics: Analog and Digital Circuits and Systems*. McGraw-Hill, 1971.
- [15] D.W. Novotony and T.A. Lipo. *Vector Control and Dynamics of AC Drives.* Oxford University Press, 1996.

- [16] Alan V. Oppenheim and R.W. Schafer. *Discrete-Time Signal Processing*. Prentice-Hall, 1989.
- [17] Wilson J. Rugh. *Linear Systems Theory.* Prentice Hall, second edition, 1996.
- [18] Gordon R. Slemon. *Electric Machines and Drives*. Addison-Wesley, 1992.
- [19] E. Strangas, H.K. Khalil and Bader Aloliwi. Comparison of Three Torque Controllers for Induction Motors Without Rotor and Position Sensors. Electrical Machines and Drives Laboratory, Department of Electrical and Computer Engineering, Michigan State University, 1998.
- [20] E. Strangas, H.K. Khalil, Bader Aloliwi, L. Laubinger and J.M. Miller. A Robust Torque Controller for Induction Maotors Without Rotor Position Sensor: Analysis ans Experimental Results, *IEEE Trans. Ind. Appl,* 1998.
- [21] Peter Vas. Sensorless Vector and Direct Torque Control. Oxford University Press, 1998.

